INSIDE TRACK with Lorne Graves, Mercury Systems | 32

Attenuators Reach 120 dB | 76

microwaves&rf

FEBRUARY 2015 TRUSTED ENGINEERING RESOURCE FOR OVER 50 YEARS www.mwrf.com

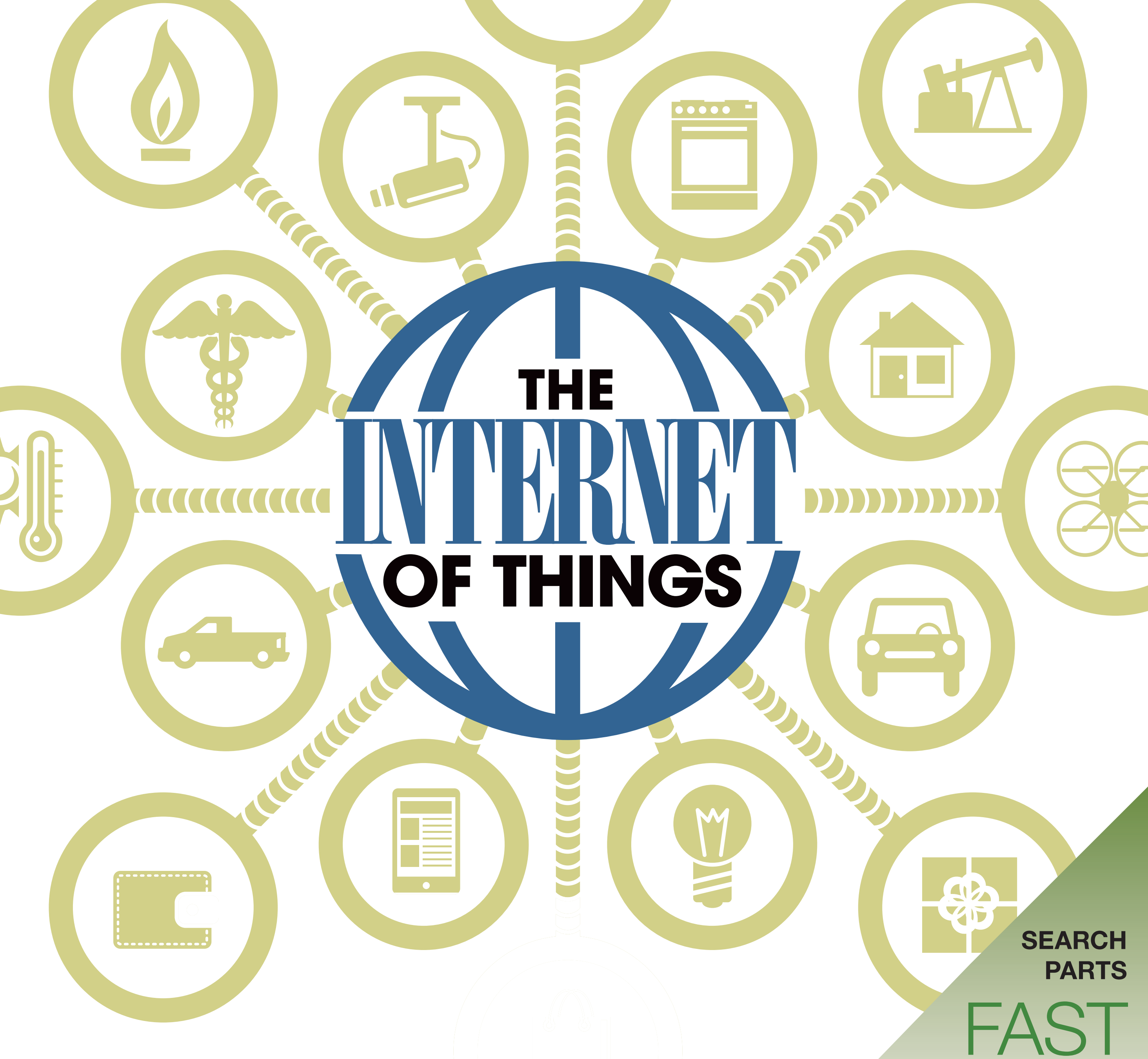

Powered by Penton®

- Amplifiers
- Attenuators - Variable
- DLVA & ERDLVA & SDLVA's
- DTO's & Frequency Synthesizers
- Filters
- Form, Fit & Function Products
- IFM's & Frequency Discriminators
- Integrated MIC/MMIC Modules
- I/Q Vector Modulators
- Limiters & Detectors
- Log Amplifiers
- Pulse & Bi-Phase Modulators
- Phase Shifters
- Rack & Chassis Mount Products
- Receiver Front Ends & Transceivers
- Single Sideband Modulators
- SMT & QFN Products
- Solid-State Switches
- Switch Matrices
- Switch Filter Banks
- Threshold Detectors
- USB Products

Planar Monolithics Industries, Inc.

Offering State-Of-The-Art RF and Microwave Components & Integrated Assemblies From DC to 40GHz

BREAKTHROUGH IN MILLIMETER WAVE FILTER TECHNOLOGY

MINIATURE, CONNECTORIZED, 18GHz to 40GHz DIPLEXER

PMI MODEL No: DPX-18G26R5G40G

Plot of K & Ka Band Crossover

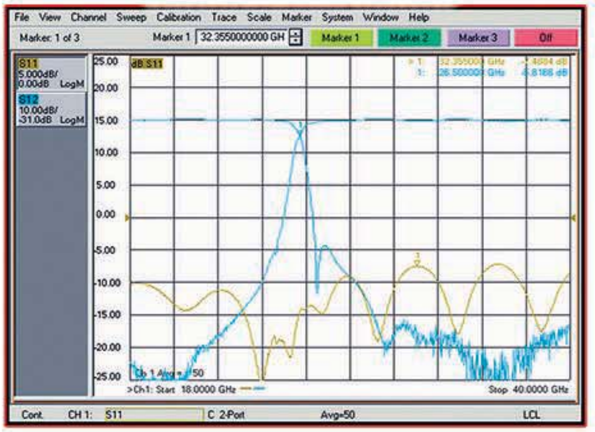

INSERTION LOSS	2.0dB
VSWR	2.5:1
K BAND PASSBAND	18GHz Min., 25GHz Max
Ka BAND PASSBAND	28GHz Min., 40GHz Max
K BAND REJECTION	32 to 46GHz, >60dBc
Ka BAND REJECTION	DC to 22GHz, >60dBc
SIZE	0.80" X 0.60" X 0.38"

20 to 40GHz High Pass Filter

INSERTION LOSS	1.5dB
VSWR in PASSBAND	2.0:1
1dB CUTOFF	20GHz
REJECTION	DC to 14.5GHz, >54dBc
SIZE	0.614" X 0.50" X 0.56"

18 to 26.5GHz High Pass Filter

INSERTION LOSS	1.5dB
PASSBAND	18 to 26.5GHz
VSWR in PASSBAND	2.0:1
REJECTION	DC to 15GHz, >60dBc
SIZE	0.64" X 0.58" X 0.38"

26.5 to 40GHz High Pass Filter

INSERTION LOSS	2.0dB
VSWR in PASSBAND	2.0:1
1dB CUTOFF	26.5GHz
REJECTION	DC to 20GHz, >54dBc
SIZE	0.65" X 0.65" X 0.50"

DC to 26.5GHz Low Pass Filter

INSERTION LOSS	1.5dB
PASSBAND	DC to 26.5GHz
VSWR in PASSBAND	2.2:1
RIPPLE	+/-0.75dB Max
REJECTION	28.5 to 40GHz, >25dBc
SIZE	0.45" X 0.38" X 0.50"

West Coast Operation:
4921 Robert J. Mathews Pkwy, Suite 1
El Dorado Hills, CA 95762 USA
Tel: 916-542-1401 Fax: 916-265-2597
ISO9001:2008 REGISTERED
Email: sales@pmi-rf.com

East Coast Operation:
7311-F Grove Road
Frederick, MD 21704 USA
Tel: 301-662-5019 Fax: 301-662-1731
ISO9001:2008 REGISTERED
Website: www.pmi-rf.com

Hermetic Sealing, High Reliability to Mil-Std-883, Small Quantity Requirements accepted & we offer Custom Designs too.


CEL
INTRODUCING
TOKYO KEIKI
CUSTOM RF PRODUCTS
Delivering High Quality & Performance
5 CLEANROOMS
JIS-Q9100 CERTIFIED FACTORY
AS9100 U.S. EQUIVALENT
Bring us your challenging specs
X-Band
100 W
GaN Power AMP
Best in Class
Lumped Element Filter
High Power Amplifier
Directional Coupler
Broadband Amplifier
PIN Diode Switch
VCO/Synthesizer
Power Divider
Cavity Filter/Duplexer
Low Noise Amplifier
Balanced Mixer
Filter
Amp
Mixer
HPA
Divider
Monitor
CEL
TOKYO KEIKI
Scan code to learn more or visit:
www.cel.com/TK-MWRF

VOLUME 54, ISSUE 2

In This Issue

FEATURES

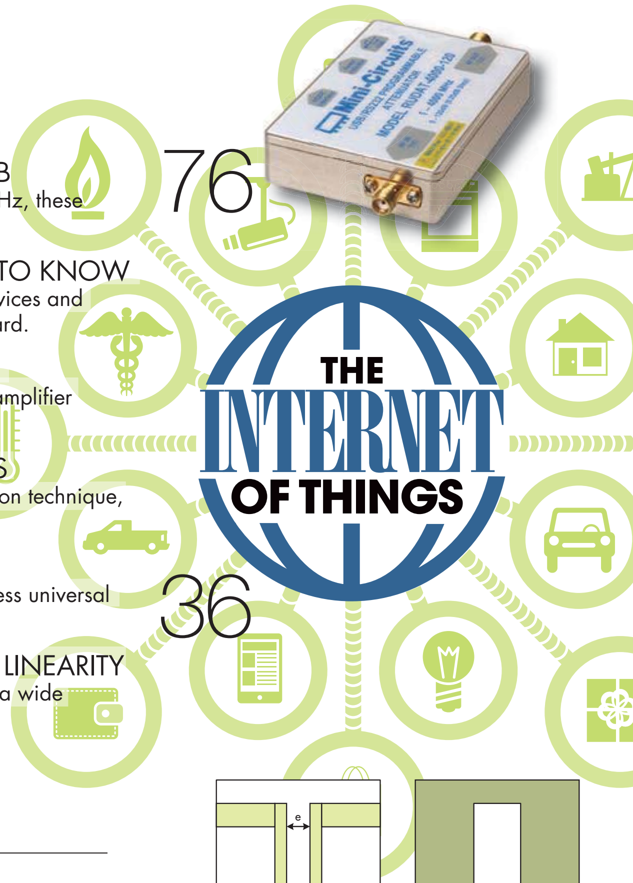

76

36

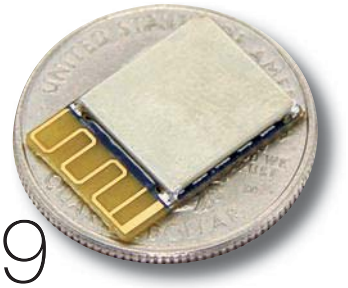

79

INDUSTRY TRENDS & ANALYSIS

PRODUCT TECHNOLOGY

NEWS & COLUMNS

JOIN US ONLINE

follow us @MicrowavesRF

become a fan at
facebook.com/microwavesRF

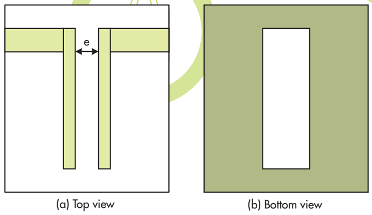

54

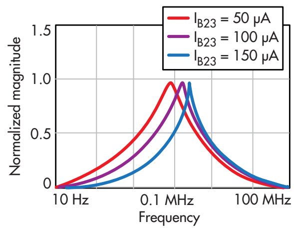

60

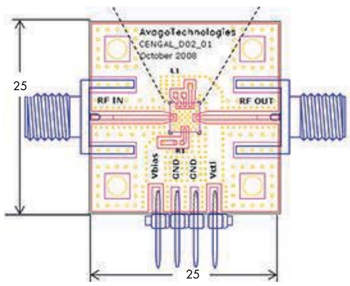

68

Keysight W1715EP SystemVue
MIMO channel builder

Keysight N9040B UXA signal analyzer
with 89600 VSA software

Keysight MIMO PXI test solution
with N7624/25B Signal Studio software for LTE-Advanced/LTE FDD/TDD and 89600 VSA software

Keysight E7515A UXM wireless test set
with E7530A/E7630A LTE-Advanced/LTE test/lab application software

Keysight Infiniium S-Series
high-definition oscilloscope
with N8807A MIPI DigRF v4 (M-PHY) protocol decode software

Keysight N5182B MXG X-Series
RF vector signal generator
with N7624/25B Signal Studio software for LTE-Advanced/LTE FDD/TDD

Keysight E6640B EXM wireless test set
with V9080/82B LTE FDD/TDD measurement applications and N7624/25B Signal Studio software for LTE-Advanced/LTE FDD/TDD

HARDWARE + SOFTWARE

The more complex your LTE-A design, the more you need help from test and measurement experts. Keysight is the only company that offers benchtop, modular and software solutions for every step of the LTE-A design process. From R&D to manufacturing, we can give you the expertise, instruments and applications you need to succeed.

- *Complete LTE-Advanced design and test lifecycle*
- *Identical software algorithms across platforms*
- *300+ software applications for the entire wireless lifecycle*

PEOPLE

We know what it takes for your designs to meet LTE-A standards. After all, Keysight engineers have played major roles in LTE-A and other wireless standards bodies, including 3GPP. Our engineers even co-authored the first book about LTE-A design and test. We also have hundreds of applications engineers. You'll find them all over the world, and their expertise is yours for the asking.

- *Representation on every key wireless standards organization globally*
- *Hundreds of applications engineers in 100 countries around the world*
- *Thousands of patents issued in Keysight's history*

KEYSIGHT
TECHNOLOGIES

Unlocking Measurement Insights

onmicrowaves&rf.com

MAN AND MACHINE: BONDED TOGETHER WITH RF GLUE

http://mwrf.com/test-measurement-generators/man-and-machine-bonded-together-rf-glue

This year will see the advancement of a revolution in connectivity between man and data. The depth and design of this connectivity will bring us closer to technology and our bodies while enhancing our ability to compete electronically on the battlefield. In short, RF technologies is making possible advancements that were once relegated to pure fantasy.

INTERVIEW:

AARON PARTRIDGE, SiTIME

http://mwrf.com/components/inside-track-aaron-partridge-sitime

The size, weight, and limited integration potential of traditional timing solutions have been a limiting factor in many low-cost and high-performing RF and electronic devices. Aaron Partridge, SiTime's chief scientist and founder, discusses how MEMS timing solutions are changing the game, opening the doors to low-cost RF and Internet of Things devices.

join us online

twitter.com/MicrowavesRF facebook.com/microwavesrf

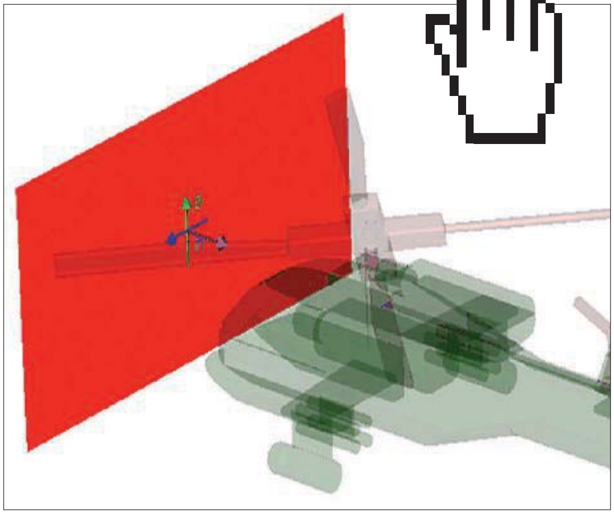

HOW TO EM SIMULATE LARGE AND COMPLEX OBJECTS

http://mwrf.com/software/how-em-simulate-large-and-complex-objects

To reduce costly trial-and-error troubleshooting and speed design cycles, EM simulators are using specialized methods, software, and hardware techniques. These features enable them to provide significant details into the EM behavior of massive objects and simulation environments.

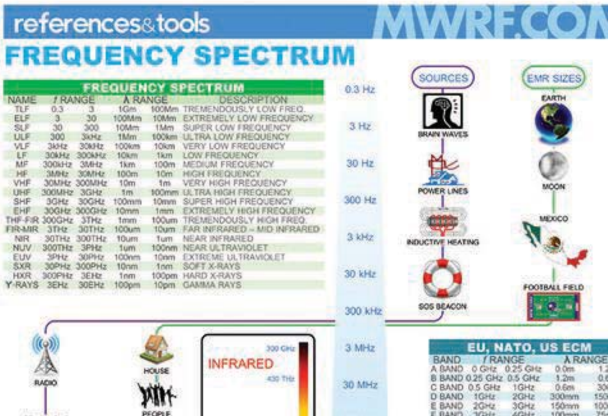

REFERENCES & TOOLS

http://mwrf.com/references-tools

Visit our online References & Tools section to quickly and easily download tables covering topics such as Connector Frequency, which include Coaxial and Waveguide; Frequency Nomenclature: Kilohertz to Terahertz; Frequency Spectrum & Allocations; and Wireless Coexistence: From 300 MHz to 6 GHz.

UP TO **100 Watt**

AMPLIFIERS

NOW! **100 kHz to 18 GHz**

from $995 ea. qty. (1-9)

High-powered performance across wide frequency ranges. These class A/AB linear amplifiers have set a standard throughout the RF & microwave industry. Rugged and reliable, they feature over-voltage and over-temperature protection, including the ability to withstand opens and shorts! And they're all in stock, whether with a heat sink/fan (for design labs and test benches), or without (for quick integration into customer assemblies). Go to minicircuits.com, where it's easy to select the models that meet your needs, including new features like TTL-controlled RF output. Place an order today, and you can have them in your hands as soon as tomorrow—or if you need a custom model, just give us a call for an engineer-to-engineer discussion of your requirements!

Model	Frequency (MHz)	Gain (dB)	Pout @ Comp. 1 dB (W)	Pout @ Comp. 3 dB (W)	$ Price (Qty. 1-9)
ZVE-3W-83+	2000-8000	35	2	3	1295
ZVE-3W-183+	5900-18000	35	2	3	1295
NEW ZHL-4W-422+	500-4200	25	3	4	1570
NEW ZHL-5W-422+	500-4200	25	3	5	1670
ZHL-5W-2G+	800-2000	45	5	6	995
ZHL-10W-2G	800-2000	43	10	13	1295
• ZHL-16W-43+	1800-4000	45	13	16	1595
• ZHL-20W-13+	20-1000	50	13	20	1395
• ZHL-20W-13SW+	20-1000	50	13	20	1445
LZY-22+	0.1-200	43	16	32	1495
ZHL-30W-262+	2300-2550	50	20	32	1995
ZHL-30W-252+	700-2500	50	25	40	2995
LZY-2+	500-1000	47	32	38	2195
LZY-1+	20-512	42	40	50	1995
• ZHL-50W-52+	50-500	50	40	63	1395
• ZHL-100W-52+	50-500	50	63	79	1995
• ZHL-100W-GAN+	20-500	42	79	100	2395
ZHL-100W-13+	800-1000	50	79	100	2195
ZHL-100W-352+	3000-3500	50	100	100	3595
ZHL-100W-43+	3500-4000	50	100	100	3595
LZY-5+	0.4-5	52.5	100	100	1995

Listed performance data typical, see minicircuits.com for more details.
• Protected under U.S. Patent 7,348,854

Mini-Circuits®

www.minicircuits.com P.O. Box 350166, Brooklyn, NY 11235-0003 (718) 934-4500 sales@minicircuits.com

Editorial

NANCY K. FRIEDRICH
Content Director
nancy.friedrich@penton.com

M&A Deals Jumpstart IoT

By now, I assume that everyone is familiar with the promise of the Internet of Things (IoT). With the IoT in place, devices will be so interconnected that they will open communications between ourselves and our homes, appliances, cars, and more. Billions of sensors will be in place to continuously monitor the various aspects of our lives. Between the required sensing technologies, data processing, communications support, and more, however, a lot has to be put into place to enable the IoT.

In "4 Major M2M and IoT Challenges You Need to Know" (page 36), for example, Technology Editor Jean-Jacques DeLisle provides an overview of some key concerns that need to be resolved and kept in mind: standards development and interoperability; trading off low power versus data rate; security; and interference and spectrum challenges. Due to all of the hype and interest around the IoT, many companies are looking to make big deals now in order to jumpstart their ability to overcome these challenges.

According to 451 Research (https://451research.com/), acquirers spent $14 billion to acquire more than 60 IoT-related companies in 2014. The firm notes that last year's number translates into a fortyfold increase in acquirer spending compared to 2013. They also involved a lot of major players, such as Google, Samsung, Cisco, Intel, and Qualcomm.

Drilling down, 451 Research revealed that last year's M&A activity was almost evenly split between IoT-enabling horizontal infrastructure and vertical applications. About 20 acquisitions targeted the infrastructure arena. The impetus behind those deals was the aspects needed to make the IoT work effectively: a wide range of sensors, semiconductors, software platforms, security infrastructure, and connectivity technologies.

In terms of vertical mergers and acquisitions, 451 Research cites the transport and logistics segment as the most active with 11 business transactions. Given all the attention paid to remote healthcare monitoring, wireless hospitals, and more, it is not surprising that fitness and healthcare ranked a close second among the verticals with 10 deals.

Clearly, major investments are being made in enabling the IoT, and those investments will continue to rise. They will inspire IoT-focused research and development across myriad of categories. For the microwave and RF industry, this should certainly translate into a major growth period while the IoT ramps up. mw

MCL B 744 ADP-2-10
MCL A 745 ADPQ-140-2
MCL B 744 ADP-2-10
MCL B 744 ADP-2-10
MCL QBA-12-2 071838
MCL SBA-2-20 071840
MCL BP2C
MCL BP4C

FEBRUARY | 2015 microwaves&rf

A Penton® Publication

EDITORIAL

CONTENT DIRECTOR: **NANCY K. FRIEDRICH** nancy.friedrich@penton.com
TECHNICAL CONTRIBUTOR: **JACK BROWNE** jack.browne@penton.com
TECHNICAL ENGINEERING EDITOR: **JEAN-JACQUES DELISLE** jean-jacques.delisle@penton.com
CONTENT PRODUCTION DIRECTOR: **MICHAEL BROWNE** michael.browne@penton.com
PRODUCTION EDITOR: **JEREMY COHEN** jeremy.cohen@penton.com
CONTENT PRODUCTION SPECIALIST: **ROGER ENGELKE** roger.engelke@penton.com
ASSOCIATE CONTENT PRODUCER: **ILIZA SOKOL** iliza.sokol@penton.com
ASSOCIATE CONTENT PRODUCER: **LEAH SCULLY** leah.scully@penton.com

ART DEPARTMENT

GROUP DESIGN DIRECTOR: **ANTHONY VITOLO** tony.vitolo@penton.com
SENIOR ARTIST: **JIM MILLER** jim.miller@penton.com
CONTRIBUTING ART DIRECTOR **RANDALL L. RUBENKING** randall.rubenking@penton.com

PRODUCTION

GROUP PRODUCTION MANAGER: **CAREY SWEETEN** carey.sweeten@penton.com
PRODUCTION MANAGER: **VICKI MCCARTY** vicki.mccarty@penton.com
CLASSIFIED PRODUCTION COORDINATOR: **LINDA SARGENT** linda.sargent@penton.com

AUDIENCE MARKETING

USER MARKETING DIRECTOR: **BRENDA ROODE** brenda.roode@penton.com
USER MARKETING MANAGER: **DEBBIE BRADY** debbie.brady@penton.com
FREE SUBSCRIPTION/STATUS OF SUBSCRIPTION/ADDRESS CHANGE/MISSING BACK ISSUES
T | 866.505.7173 microwaves&RF@halldata.com **F** | 847.763.9673

SALES & MARKETING

AL, AR, CT, DE, FL, GA, IA, IL, IN, KS, KY, LA,MA, MD, ME, MI, MN, MO, MS, NC, NE, NH, NJ, NY, OH, OK, RI, SC, TN, PA, VA, VT, WV, E/CANADA:
MANAGING DIRECTOR: **TRACY SMITH** **T** | 913.967.1324 **F** | 913.514.6881 tracy.smith@penton.com

REGIONAL SALES REPRESENTATIVES
AZ, NM, TX: **BILL YARBOROUGH** **T** | 713.636.3809 **F** | 913.514.7251 bill.yarborough@penton.com
AK, CA, CO, ID, MT, ND, NV, OR, SD, UT, WA, WI, WY, W/CANADA: **JAMIE ALLEN** **T** | 415.608.1959 **F** | 913.514.3667 jamie.allen@penton.com

PLEASE SEND INSERTION ORDERS TO: orders@penton.com
PENTON REPRINTS: **WRIGHT'S MEDIA** **T** | 877.652.5295 penton@wrightsmedia.com
CIRCULATION: **CUSTOMER SERVICE** **T** | 866.505.7173 **F** | 847.763.9673 microwaves&rf@halldata.com

INTERNATIONAL SALES
EUROPE: **TRACY SMITH** **T** | 913.967.1324 **F** | 913.514.6881 tracy.smith@penton.com
PAN-ASIA: **HELEN LAI** **T** | 886 2-2727 7799 helen@twoway-com.com
LIST RENTALS, CUSTOMER SERVICE--SUBSCRIPTIONS:
ONLINE MARKETING MANAGER: **SARAH NOWOWIEJSKI** **T** | (212) 204 4295 sarah.nowowiejski@penton.com

ONLINE

PRODUCT DEVELOPMENT DIRECTOR: **RYAN MALEC** ryan.malec@penton.com

DESIGN ENGINEERING & SOURCING GROUP

VICE PRESIDENT & MARKET LEADER: **BILL BAUMANN**
EXECUTIVE DIRECTOR OF CONTENT AND USER ENGAGEMENT: **NANCY K. FRIEDRICH**
GROUP DIRECTOR OF OPERATIONS: **CHRISTINA CAVANO**
GROUP DIRECTOR OF MARKETING: **JANE COOPER**

PENTON MEDIA INC.

CHIEF EXECUTIVE OFFICER: **DAVID KIESELSTEIN** david.kieselstein@penton.com
CHIEF FINANCIAL OFFICER: **NICOLA ALLAIS** nicola.allais@penton.com
SENIOR VP, DESIGN ENGINEERING GROUP: **BOB MACARTHUR** bob.macarthur@penton.com
1166 AVENUE OF THE AMERICAS, 10TH FLOOR NEW YORK, NY 10036 **T** | 212.204.4200

Penton

Electronic Design | Machine Design | Microwaves & RF | Medical Design | Source ESB | Hydraulics & Pneumatics | Global Purchasing | Distribution Resource | Power Electronics | Defense Electronics | Electronic Design Europe | Engineering TV

RF Amplifiers and Sub-Assemblies for Every Application

Delivery from Stock to 2 Weeks ARO from the catalog or built to your specifications!

- Competitive Pricing & Fast Delivery
- Military Reliability & Qualification
- Various Options: Temperature Compensation, Input Limiter Protection, Detectors/TTL & More
- Unconditionally Stable (100% tested)

ISO 9001:2000 and AS9100B CERTIFIED

OCTAVE BAND LOW NOISE AMPLIFIERS

Model No.	Freq (GHz)	Gain (dB) MIN	Noise Figure (dB)	Power-out @ P1-dB	3rd Order ICP	VSWR
CA01-2110	0.5-1.0	28	1.0 MAX, 0.7 TYP	+10 MIN	+20 dBm	2.0:1
CA12-2110	1.0-2.0	30	1.0 MAX, 0.7 TYP	+10 MIN	+20 dBm	2.0:1
CA24-2111	2.0-4.0	29	1.1 MAX, 0.95 TYP	+10 MIN	+20 dBm	2.0:1
CA48-2111	4.0-8.0	29	1.3 MAX, 1.0 TYP	+10 MIN	+20 dBm	2.0:1
CA812-3111	8.0-12.0	27	1.6 MAX, 1.4 TYP	+10 MIN	+20 dBm	2.0:1
CA1218-4111	12.0-18.0	25	1.9 MAX, 1.7 TYP	+10 MIN	+20 dBm	2.0:1
CA1826-2110	18.0-26.5	32	3.0 MAX, 2.5 TYP	+10 MIN	+20 dBm	2.0:1

NARROW BAND LOW NOISE AND MEDIUM POWER AMPLIFIERS

Model No.	Freq (GHz)	Gain (dB) MIN	Noise Figure (dB)	Power-out @ P1-dB	3rd Order ICP	VSWR
CA01-2111	0.4 - 0.5	28	0.6 MAX, 0.4 TYP	+10 MIN	+20 dBm	2.0:1
CA01-2113	0.8 - 1.0	28	0.6 MAX, 0.4 TYP	+10 MIN	+20 dBm	2.0:1
CA12-3117	1.2 - 1.6	25	0.6 MAX, 0.4 TYP	+10 MIN	+20 dBm	2.0:1
CA23-3111	2.2 - 2.4	30	0.6 MAX, 0.45 TYP	+10 MIN	+20 dBm	2.0:1
CA23-3116	2.7 - 2.9	29	0.7 MAX, 0.5 TYP	+10 MIN	+20 dBm	2.0:1
CA34-2110	3.7 - 4.2	28	1.0 MAX, 0.5 TYP	+10 MIN	+20 dBm	2.0:1
CA56-3110	5.4 - 5.9	40	1.0 MAX, 0.5 TYP	+10 MIN	+20 dBm	2.0:1
CA78-4110	7.25 - 7.75	32	1.2 MAX, 1.0 TYP	+10 MIN	+20 dBm	2.0:1
CA910-3110	9.0 - 10.6	25	1.4 MAX, 1.2 TYP	+10 MIN	+20 dBm	2.0:1
CA1315-3110	13.75 - 15.4	25	1.6 MAX, 1.4 TYP	+10 MIN	+20 dBm	2.0:1
CA12-3114	1.35 - 1.85	30	4.0 MAX, 3.0 TYP	+33 MIN	+41 dBm	2.0:1
CA34-6116	3.1 - 3.5	40	4.5 MAX, 3.5 TYP	+35 MIN	+43 dBm	2.0:1
CA56-5114	5.9 - 6.4	30	5.0 MAX, 4.0 TYP	+30 MIN	+40 dBm	2.0:1
CA812-6115	8.0 - 12.0	30	4.5 MAX, 3.5 TYP	+30 MIN	+40 dBm	2.0:1
CA812-6116	8.0 - 12.0	30	5.0 MAX, 4.0 TYP	+33 MIN	+41 dBm	2.0:1
CA1213-7110	12.2 - 13.25	28	6.0 MAX, 5.5 TYP	+33 MIN	+42 dBm	2.0:1
CA1415-7110	14.0 - 15.0	30	5.0 MAX, 4.0 TYP	+30 MIN	+40 dBm	2.0:1
CA1722-4110	17.0 - 22.0	25	3.5 MAX, 2.8 TYP	+21 MIN	+31 dBm	2.0:1

ULTRA-BROADBAND & MULTI-OCTAVE BAND AMPLIFIERS

Model No.	Freq (GHz)	Gain (dB) MIN	Noise Figure (dB)	Power-out @ P1-dB	3rd Order ICP	VSWR
CA0102-3111	0.1-2.0	28	1.6 Max, 1.2 TYP	+10 MIN	+20 dBm	2.0:1
CA0106-3111	0.1-6.0	28	1.9 Max, 1.5 TYP	+10 MIN	+20 dBm	2.0:1
CA0108-3110	0.1-8.0	26	2.2 Max, 1.8 TYP	+10 MIN	+20 dBm	2.0:1
CA0108-4112	0.1-8.0	32	3.0 MAX, 1.8 TYP	+22 MIN	+32 dBm	2.0:1
CA02-3112	0.5-2.0	36	4.5 MAX, 2.5 TYP	+30 MIN	+40 dBm	2.0:1
CA26-3110	2.0-6.0	26	2.0 MAX, 1.5 TYP	+10 MIN	+20 dBm	2.0:1
CA26-4114	2.0-6.0	22	5.0 MAX, 3.5 TYP	+30 MIN	+40 dBm	2.0:1
CA618-4112	6.0-18.0	25	5.0 MAX, 3.5 TYP	+23 MIN	+33 dBm	2.0:1
CA618-6114	6.0-18.0	35	5.0 MAX, 3.5 TYP	+30 MIN	+40 dBm	2.0:1
CA218-4116	2.0-18.0	30	3.5 MAX, 2.8 TYP	+10 MIN	+20 dBm	2.0:1
CA218-4110	2.0-18.0	30	5.0 MAX, 3.5 TYP	+20 MIN	+30 dBm	2.0:1
CA218-4112	2.0-18.0	29	5.0 MAX, 3.5 TYP	+24 MIN	+34 dBm	2.0:1

LIMITING AMPLIFIERS

Model No.	Freq (GHz)	Input Dynamic Range	Output Power Range Psat	Power Flatness dB	VSWR
CLA24-4001	2.0 - 4.0	-28 to +10 dBm	+7 to +11 dBm	+/- 1.5 MAX	2.0:1
CLA26-8001	2.0 - 6.0	-50 to +20 dBm	+14 to +18 dBm	+/- 1.5 MAX	2.0:1
CLA712-5001	7.0 - 12.4	-21 to +10 dBm	+14 to +19 dBm	+/- 1.5 MAX	2.0:1
CLA618-1201	6.0 - 18.0	-50 to +20 dBm	+14 to +19 dBm	+/- 1.5 MAX	2.0:1

AMPLIFIERS WITH INTEGRATED GAIN ATTENUATION

Model No.	Freq (GHz)	Gain (dB) MIN	Noise Figure (dB)	Power-out @ P1-dB	Gain Attenuation Range	VSWR
CA001-2511A	0.025-0.150	21	5.0 MAX, 3.5 TYP	+12 MIN	30 dB MIN	2.0:1
CA05-3110A	0.5-5.5	23	2.5 MAX, 1.5 TYP	+18 MIN	20 dB MIN	2.0:1
CA56-3110A	5.85-6.425	28	2.5 MAX, 1.5 TYP	+16 MIN	22 dB MIN	1.8:1
CA612-4110A	6.0-12.0	24	2.5 MAX, 1.5 TYP	+12 MIN	15 dB MIN	1.9:1
CA1315-4110A	13.75-15.4	25	2.2 MAX, 1.6 TYP	+16 MIN	20 dB MIN	1.8:1
CA1518-4110A	15.0-18.0	30	3.0 MAX, 2.0 TYP	+18 MIN	20 dB MIN	1.85:1

LOW FREQUENCY AMPLIFIERS

Model No.	Freq (GHz)	Gain (dB) MIN	Noise Figure dB	Power-out @ P1-dB	3rd Order ICP	VSWR
CA001-2110	0.01-0.10	18	4.0 MAX, 2.2 TYP	+10 MIN	+20 dBm	2.0:1
CA001-2211	0.04-0.15	24	3.5 MAX, 2.2 TYP	+13 MIN	+23 dBm	2.0:1
CA001-2215	0.04-0.15	23	4.0 MAX, 2.2 TYP	+23 MIN	+33 dBm	2.0:1
CA001-3113	0.01-1.0	28	4.0 MAX, 2.8 TYP	+17 MIN	+27 dBm	2.0:1
CA002-3114	0.01-2.0	27	4.0 MAX, 2.8 TYP	+20 MIN	+30 dBm	2.0:1
CA003-3116	0.01-3.0	18	4.0 MAX, 2.8 TYP	+25 MIN	+35 dBm	2.0:1
CA004-3112	0.01-4.0	32	4.0 MAX, 2.8 TYP	+15 MIN	+25 dBm	2.0:1

CIAO Wireless can easily modify any of its standard models to meet your "exact" requirements at the Catalog Pricing.

Visit our web site at **www.ciaowireless.com** for our complete product offering.

Ciao wireless

Ciao Wireless, Inc. 4000 Via Pescador, Camarillo, CA 93012

Tel (805) 389-3224 Fax (805) 389-3629 sales@ciaowireless.com

A MEASURE OF THE TIMES

Any present-day subway or bus trip will reveal more than one-half of the passengers with faces down in a smartphone or tablet. While it may be difficult to determine whether they're reading an associate's message, playing a game, or watching a television program without eavesdropping, it's clear how dominant of a role wireless technology is now playing in people's lives.

Of course, a growing number of wireless communications users translates into increasingly crowded bandwidths. In the evolution of wireless technologies, as cellular communications technologies developed from frequencies around 800 to 900 MHz to Personal Communications Services (PCS) frequencies around 1800 to 1900 MHz, higher-frequency communications products were developed with few cost penalties to users.

As different parts of the frequency spectrum have been gobbled up by different applications, microwave frequency bands have steadily become filled with different wireless applications and their products. This has left the higher-frequency portions of the spectrum, such as at millimeter-wave frequencies, as the place that might make the most sense for newer products.

But for millimeter-wave technologies to work economically for the masses, it must become possible to produce products based on those millimeter-wave technologies for relatively low costs. In particular, the capability to produce practically priced electronic communications products at millimeter-wave frequencies also calls for fast, accurate, reasonably priced test equipment.

The millimeter-wave frequency range has long been viewed as something of a technological mystery, typically the frequency range of astronomers and experimenters. It lacks the enticements of lower-frequency cellular-communications markets with their millions of users and needs for multiple millions of wireless electronic products.

Still, millimeter-wave devices and components will require aggressive product development and marketing of test equipment for those higher frequencies to enable millimeter-wave-frequency electronic products to become more commonplace among mass markets. The demand for wireless products and services is ever-growing. They can easily expand into the millimeter-wave frequency range if those products are priced right. Still, it will have to start with the test equipment.

Terrence Coleman

90mW I/Q Modulator

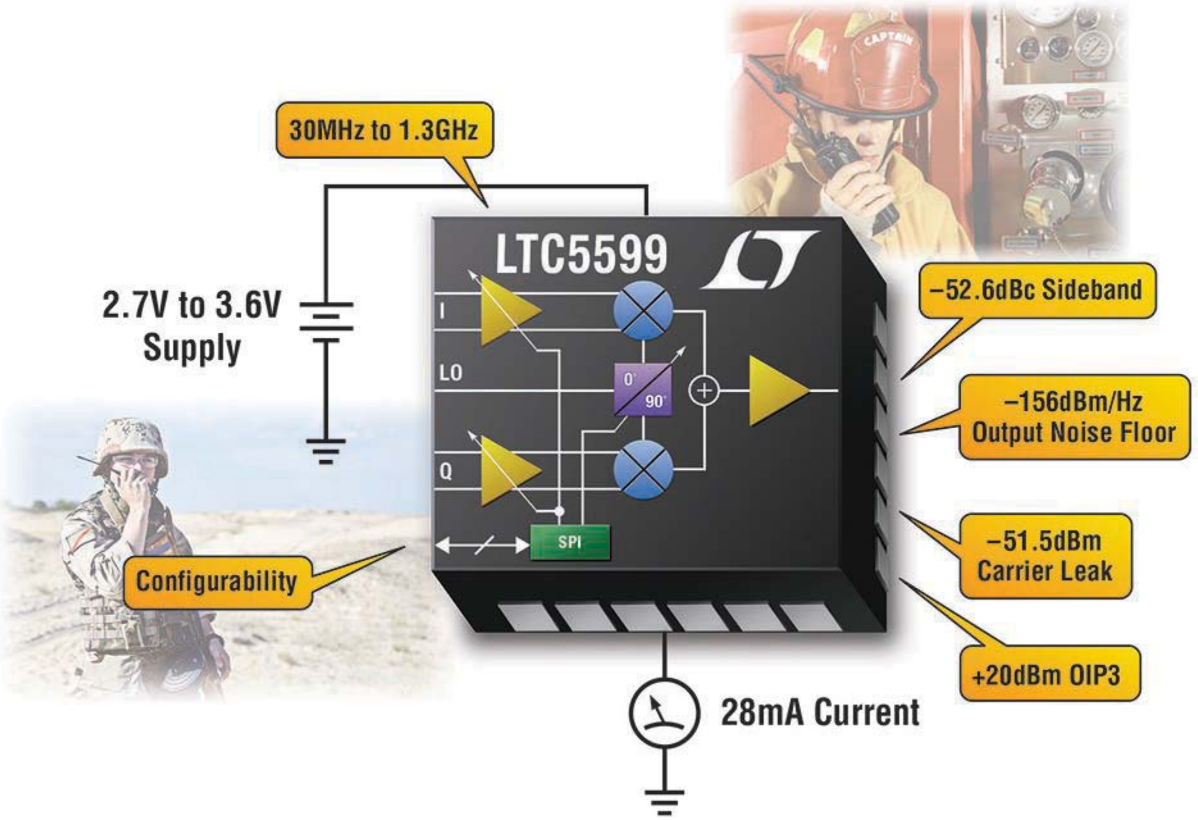

Powered from a single supply from 2.7V to 3.6V, the LTC®5599's 28mA supply current extends battery run time. The modulator offers superb –52.6dBc sideband and –51.5dBm carrier suppression—without the need of calibration. Its low noise floor of –156dBm/Hz and 20dBm OIP3 capability ensure outstanding transmitter performance. The LTC5599's built-in configurability allows users to optimize performance from 30MHz to 1.3GHz, minimizing external components and saving costs.

Features

Built-in Configurability Features:

- Gain Adjustable from 0dB to –19dB, with Supply Current Change from 35mA to 8mA
- Improves Sideband Suppression from –52.6dBc to –60dBc
- Reduces Carrier Leakage from –51.5dBm to –60dBm

Output Spectra (Optimized)

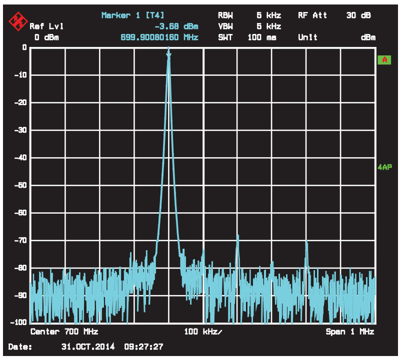

Info & Free Samples

www.linear.com/product/LTC5599

1-800-4-LINEAR

www.linear.com/solutions/5429

LINEAR TECHNOLOGY

News

DECOY JAMMER WITH RADIO DATA LINK Takes Flight

Raytheon, in collaboration with the U.S. Marine Corps and Air Force, successfully demonstrated the flight of a Miniature Air Launched Decoy Jammer (MALD-J) equipped with a radio data link. The data link helps expand the weapon's situational awareness and allows for in-flight targeting adjustments. The exercise, held at the U.S. Marine Corps Air Station in Yuma, Ariz., used the USMC's recently released Electronic Warfare Services Architecture protocol and a Tactical Targeting Network Technology radio.

MALD, a modular and programmable low-cost flight vehicle, weighs less than 300 pounds and has a range of approximately 500 nautical miles. MALD-J adds a radar-jamming capability to the basic platform. The ADM-160C MALD-J variant used in the demonstration is an autonomous stand-in-jammer that can also operate in decoy mode when selected by the warfighter. This serves to confuse enemy air defenses by duplicating friendly aircraft flight profiles and radar signatures.

As part of the demonstration, the MALD-J carried out its assigned radar-jamming mission on the range and then sent situation awareness data to the EW Battle Manager (EWBM). The EWBM used that information to adjust the MALD's mission while in flight. Various types of MALDs are currently in service, including the MALD-J, which was first delivered to the Air Force in 2012. ■

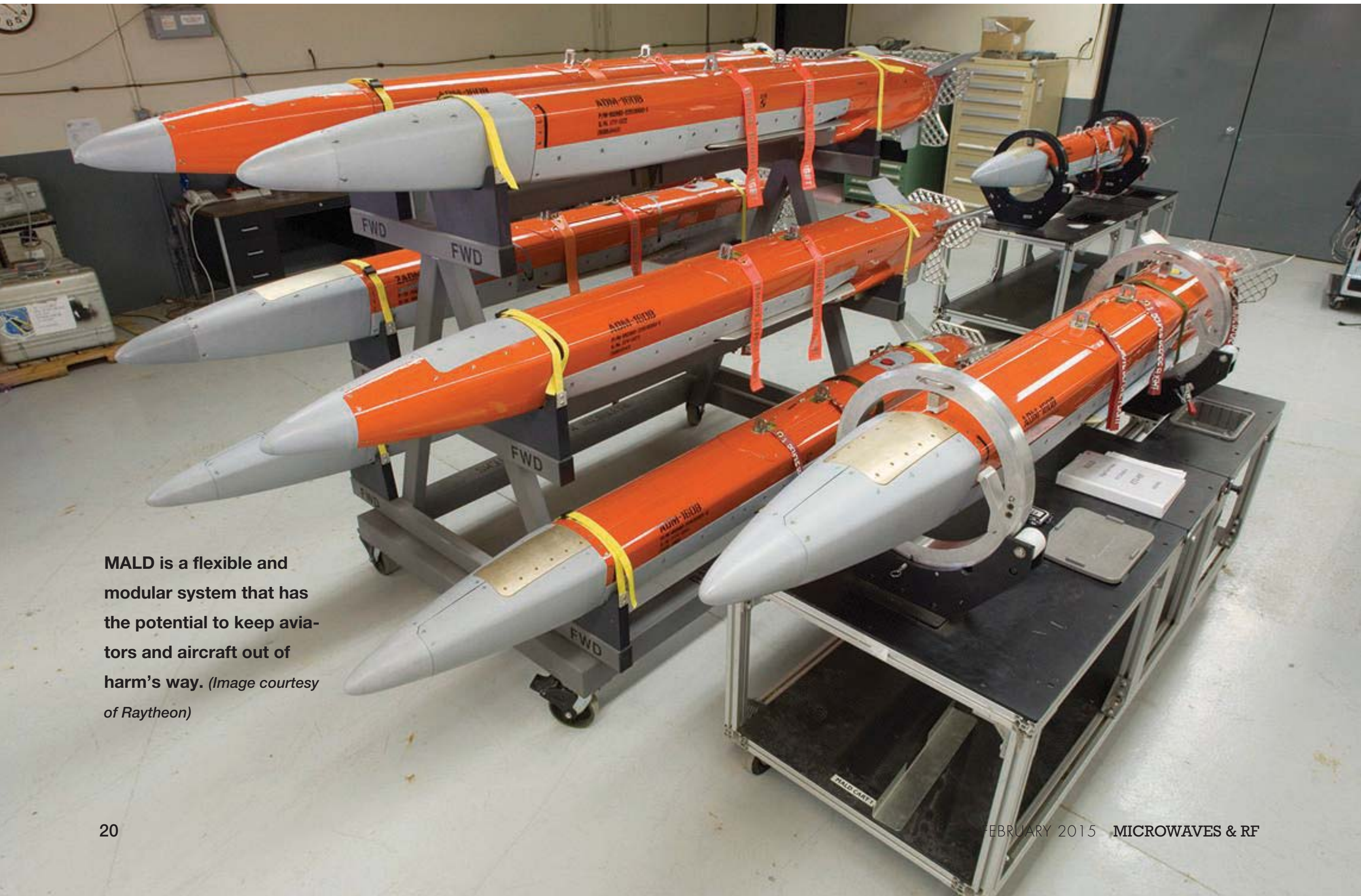

MALD is a flexible and modular system that has the potential to keep aviators and aircraft out of harm's way. *(Image courtesy of Raytheon)*

NYU WIRELESS TEAM Receives IEEE Award for 5G Research

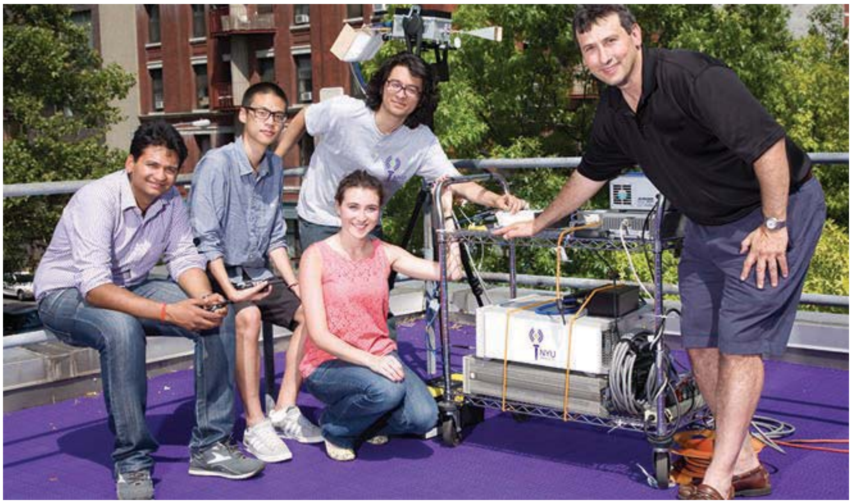

Theodore Rappaport (right) and members of NYU WIRELESS showcase some of their research. *(Image courtesy of NYU)*

IT'S ESTIMATED THAT bandwidth demand doubles annually, mirroring the surge in data-heavy devices. Efforts toward fulfilling that demand were recognized by the IEEE—it selected a research team led by Professor Theodore Rappaport, founder and director of the NYU WIRELESS research center, as the recipient of the 2015 IEEE Donald G. Fink Award for their work on new-generation wireless technology. The award is given to a single survey, review, or technical paper published in one of IEEE's 170 publications during the previous calendar year. Rappaport and WIRELESS's winning article was entitled "Millimeter Wave Mobile Communications for 5G Cellular: It Will Work."

The paper provided research results surveying the potential of a new segment of radio-wave spectrum that could increase mobile-network capacity 1000-fold or more. Among the top five downloaded papers by IEEE's 430,000 members, it explores the under-utilized millimeter-wave (mm-wave) frequency spectrum. Such portions of the spectrum could be used for future broadband cellular communication networks as a solution to the current global bandwidth shortage facing both wireless carriers and users.

Rappaport and his colleagues studied radio waves at 28, 38, 60, and 73 GHz—more than 10 times greater than the cellular frequency used today. Used in conjunction with new types of antennas, the signals can travel down city blocks by reflecting off buildings and even people. The FCC recently cited NYU WIRELESS research on its Notice of Inquiry to explore the feasibility and implementation of mobile technology in the mm-wave bands.

The paper's co-authors—Shu Sun, Rimma Mayzus, Hang Zhao, Yaniv Azar, Kevin Wang, George N. Wong, Jocelyn K. Schulz, Mathew Samimi, and Felix Gutierrez—include students from the NYU Polytechnic School of Engineering and Courant Institute of Mathematical Sciences. The award will be presented during the 2015 IEEE GLOBECOM held in San Diego, Calif. ■

BEYOND THE BULB: Lighting Gets Smarter

INNOVATIONS IN LIGHTING typically focus on building a better light bulb—from traditional bulbs, to compact fluorescents, to LEDs. To accelerate the development of the next step—connected lighting—Qualcomm Atheros and LIFX jointly developed a turnkey, Wi-Fi-based, smart-lighting platform. The hardware/open-source software combination suits lighting manufacturers of any size.

The platform consists of a lighting connectivity module (LCM) and a complete LED bulb design. Both feature

LIFX offers a variety of connected bulb options with a wealth of features. *(Image courtesy of LIFX)*

Qualcomm Atheros' QCA4002, a low-power Wi-Fi solution that connects directly to a home's Wi-Fi network without a hub or translator. The companies are also working with Arrow Electronics to globally distribute the solution, enabling more manufacturers to quickly develop smart-lighting products. The LCM is reportedly the first lighting product to receive "Designed for AllSeen" certification from the AllSeen Alliance, a cross-industry collaboration intent on advancing the Internet of Things (IoT) through open-source software. As a result, smart lights using the resolution can quickly get the same certification.

The platform is compatible with the AllSeen Alliance's open-source lighting service framework (LSF), which generally ensures interoperability with AllJoyn-enabled smart devices. By integrating the LCM, established lighting manufacturers can easily turn their products into smart lights with minimal communication issues.

The AllSeen Alliance's Connected Lighting Work Group aims to develop ways for IP-enabled, multicolor, and energy-efficient LED light bulbs to work in news ways with each other and the devices around them. ■

MICRO SATELLITE CONSTELLATION to Expand Worldwide Internet Access

ACCORDING TO THE International Telecommunications Union, more than half of the world's population still lacked Internet access as 2014 drew to a close. The OneWeb satellite system, formerly known as WorldVu, aims to bring high-speed Internet and telephony to that half via a fleet of 648 micro satellites. The telecommunications-class micro satellites will provide low-latency, high-speed Internet access directly to small user terminals deployed around the world.

The OneWeb terminals, which act as small cells, provide the given surrounding area with access to Wi-Fi, LTE, 3G, or 2G connections using an operator partner's licensed spectrum (or LTE/Wi-Fi on unlicensed spectrum). The satellites will operate in the Ku band, with approximately 20 satellites operating in each of the 20 different orbital planes for consistent coverage. Each satellite's phased-array antenna utilizing progressive pitch helps avoid interference with other Ku-band satellites.

Aside from typical phone, computer, and tablet connectivity, the low-earth-orbit constellation could also provide global emergency and first-responder access for various disaster situations.

Qualcomm and the Virgin Group have been announced as initial investors. Additional investors will be brought on to fund the construction, launch, and operation of the system. OneWeb also announced that Virgin Galactic's LauncherOne has been selected as the first satellite launch vehicle. Virgin Group founder Sir Richard Branson says by the time the second constellation is developed, more satellites will have been launched than what's currently orbiting the sky. ■

The OneWeb system of 648 telecom-class micro satellites will help provide high-speed Internet access via small user terminals. *(Image courtesy of OneWeb Ltd.)*

A4WP recently expanded the applicability of the Rezence technical specification to include the wireless charging of cell phones, smartphones, tablets, notebooks, laptops, and desktop PC peripherals. ***(Image courtesy of A4WP)***

MAJOR SHAKEUP IN Wireless-Charging Ecosystem

Two leaders in the wireless-charging arena—the Alliance for Wireless Power (A4WP) and the Power Matters Alliance (PMA)—are merging with an eye toward accelerating the global availability and deployment of wireless-charging technology. Expected to close by mid-2015, the merger is the bookend to a separate collaboration agreement announced in February 2014. Under the Letter of Intent, the joint effort will operate under a yet-to-be-announced name.

According to the two organizations, speeding the transition to volume economies of scale of wireless-power-transfer technology will not only benefit consumers, but mobile network operators,

consumer-facing brands, the consumer electronics industry, and the latter's semiconductor and manufacturing partners. It will ultimately broaden access to new battery-charging and power-management technologies across a wealth of devices, from Bluetooth headsets to wearables to tablets and laptops.

The A4WP also recently announced that its membership has doubled, and that it was able to expand the applicability of the Rezence technical specification to include the wireless charging of cell phones, smartphones, tablets, notebooks, laptops, and desktop PC peripherals. The Rezence specification, which was previously adopted by the PMA, is an industry-sponsored magnetic-resonance technical specification for transmitters and receivers in both single- and multi-mode configurations.

Rezence technology delivers wireless power solutions in the 1- to 50-W range and supports multi-device charging while preserving freedom of placement. Furthermore, it supports the charging of multiple devices with differing power requirements—all on the same charging surface. It's currently the only available industry-sponsored resonant wireless-charging standard.

The joint A4WP and PMA boards will include a roster of consumer brands and supply-chain and market leaders, including AT&T, Broadcom, Duracell, Flextronics, Gill Electronics, Integrated Device Technologies (IDT), Intel, Powermat, Qualcomm, Samsung Electronics, Samsung Electro-Mechanics, Starbucks, and WiTricity. ■

MARKET REPORT

PC SHIPMENTS TOTALED 79.4 million units in the third quarter of 2014, 0.5 percent down on the same quarter of 2013. Lenovo is still number one in global PC sales, with worldwide PC shipment market share of **19.8 percent.** HP is close behind with **17.9 percent** (and is number one in EMEA and the U.S.), Dell comes in at **12.8 percent,** Acer has **8.6 percent,** and Asus rounds it out with **7.3 percent.** All those firms saw healthy year-to-year growth (Asus more so than the rest, with a 16.9 percent boost), but shipments by vendors in the "others" category dropped 15.5 percent. *--Gartner*

KA-BAND SATELLITES FEATURE 90+ Beams for Broadband Access

CLAIMED TO DELIVER broadband speeds 100 times faster than the previous generation, Inmarsat's Global Xpress satellites should be able to provide connectivity just about anywhere—even the most inaccessible and remote regions of Earth. The fifth-generation satellites, built by Boeing, will mobilize the first globally available, high-speed mobile broadband service delivered through a single network operator. The new Gx network, which operates in the Ka-band, will complement Inmarsat's existing L-band fleet to deliver seamless broadband services at download speeds up to 50 Mb/s and uplink speeds up to 5 Mb/s.

The Gx fleet features a combination of 89 fixed narrow spot beams (generated by two transmit and two receive apertures) that provide high speed through compact terminals, as well as six steerable beams that can add capacity in real-time when needed. Each satellite has a mission lifespan of 15 years and uses five panels of ultra-triple junction gallium arsenide solar cells to generate 15 kW of power at the start of service (13.8 kW by the end of life). A xenon ion propulsion system (XIPS) handles all in-orbit maneuvering.

The first Gx satellite was launched in December 2013. The recently delivered second satellite launches this month, with the third scheduled for launch by the second half of the year. A fourth satellite is set to deliver in late 2016. ■

The fifth-generation Global Xpress satellites, pictured here in a Boeing facility, operate in the Ka-band to deliver high-throughput broadband access to remote areas. *(Image courtesy of Inmarsat)*

Company News

CONTRACTS

API Technologies Corp.—Received a $3 million order from a Fortune 50 company to produce secure communications products that will be used to support a U.S. C4ISR program. This first award is part of a multimillion-dollar program with additional awards expected in 2015.

Norsat International Inc.—Received an order for approximately $430,000 from a large international defense electronics company, to deliver its ATOM series Block Upconverter (BUC) products. This represents the second largest single order for the ATOM series, and builds on the momentum and success of the ATOM product line. Norsat has worked closely with this customer since the product was introduced in April 2014.

ATOM SERIES BUILDS MOMENTUM

SSL IN LATIN AMERICA DEAL

Northrop Grumman Corp.—Was selected by Lockheed Martin to provide its space inertial reference system for the U.S. Air Force Space-Based Infrared System's (SBIRS) fifth Geosynchronous Earth Orbit (GEO) satellite. Northrop Grumman will provide its Scalable Space Inertial Reference Unit (Scalable SIRU) for sensor pointing/stabilization and attitude control on the SBIRS GEO-5 mission. The company has also provided its Scalable SIRU for previous SBIRS GEO satellites.

Space Systems/Loral (SSL)—Was selected to provide a multimission communications satellite to Spanish satellite operator HISPASAT Group. The satellite, Amazonas 5, will be used for a broad range of services in Latin America.

FRESH STARTS

Aeris Communications—Has become the latest member of the International M2M Council (IMC) and will also be joining the IMC Board of Governors. The IMC mission is to increase M2M communications technology driving the growth of Internet of Things (IoT) deployments, particularly among enterprise organizations. Aeris joins 16 other companies on the IMC Board, including Deutsche Telekom, AT&T, and Verizon.

Analog Devices Inc.—Is celebrating its 50th anniversary by expanding support of FIRST (For Inspiration and Recognition of Science and Technology), a not-for-profit organization founded by inventor Dean Kamen to inspire young people's interest and participation in science and technology. ADI made donations of over $50,000 through a corporate sponsorship that will help fund FIRST events in New England and California, and as a diamond-level supplier to the FIRST Robotics Competition.

W. L. Gore & Associates—Has introduced the new online Microwave/RF Assembly Calculator to calculate insertion loss, VSWR, and other parameters of microwave/RF assemblies for different cable types. The calculator is particularly useful when the initial cable type is unknown and needs to be specified independent of the connector.

Astronics Corp.—Completed its acquisition of Armstrong Aerospace for approximately $52 million in cash on Jan. 14, 2015. Armstrong, located in Itasca, Ill., is a provider of engineering, design, and certification solutions for commercial aircraft, specializing in connectivity, in-flight entertainment, and electrical power systems. For 2014, Armstrong had sales of approximately $27 million.

CoorsTek—Has reached a definitive agreement with the Carlyle Group and Unison Capital Group to acquire Covalent Materials. The transaction closed on Dec. 26, 2014. With the addition of Covalent, CoorsTek will further its strength in engineered ceramics through a portfolio of over 300 materials.

Digi International—Announced an expanded global distribution agreement with Digi-Key, making Digi's complete product portfolio available through Digi-Key, including embedded system-on-modules; RF products, including XBee modules, gateways, modems, adapters, range extenders, and sensors; cellular gateways/routers; and Rabbit modules and single-board computers.

Isola Group Sar.l.—Launched a new Technical Education Series (TES) to address the increasingly important role of laminate materials in the overall process of system-level design. The TES was developed to update system-level designers on important aspects of laminate selection by means of an interactive viewing experience. Users can access the initial four videos within the TES by logging in at www.isola-group.com/TES.

Isola Asia Pacific (Taiwan) Inc.—Received ISO 50001:2011 certification by SGS, the global inspection, verification, testing and certification company. This certification recognizes that the company has integrated energy management into its overall efforts to improve quality and environmental management at its manufacturing facilities located in Yangmei and Taoyuan, Taiwan.

Lockheed Martin—Opened a new state-of-the-art collaboration center in Masdar City, Abu Dhabi, to explore innovation, advance security, and help to achieve the UAE's vision of building a strong, resilient economy. The Center for Innovation and Security Solutions (CISS) is the first of its kind outside the United States.

Murata Electronics North America Inc.—Has acquired all outstanding shares of Peregrine Semiconductor Corp., founder of RF silicon on insulator (SOI) and pioneer of advanced RF solutions. The cash transaction paid the holders of Peregrine common shares $12.50 per share.

San-tron Inc.—Appointed two new sales representatives: Sea-Port Technical Sales, which will handle the Pacific Northwest region, covering Idaho, Montana, Oregon, Washington, and British Columbia; and Coastal RF Systems, which will cover Southern California.

Inside TRACK with Lorne Graves,

Chief Technologist for Mercury Systems

Interview by JEAN-JACQUES DeLISLE

JJD: What is the goal of the OpenRFM architecture and potential standard?

LG: We are launching the OpenRFM initiative to streamline the integration of RF and digital subsystems in advanced sensor-processing applications. The goal is to create more affordable, flexible, and open solutions. Our desire is to see the formation of a complementary, industry-developed RF ecosystem that gives defense primes and the Department of Defense (DoD) maximum flexibility and adaptability for the rapid deployment of affordable EW and SIGINT systems. Such capability is critical to addressing evolving threats.

> **" 'RF middleware' is a term coined by myself and others that, simply put, is a software layer that provides a hardware abstraction**

JJD: What components comprise an open-architecture RF system?

LG: A common Open Systems Architecture (OSA) RF system would consist of an RF controller and one or more integrated microwave assemblies or multi-function RF circuits. They would be connected to a common control plane, such as Gigabit Ethernet, PCI-E, VME, or OpenVPX.

JJD: What interface technologies can communicate with an OpenRFM system?

LG: The OpenRFM architecture allows for a variety of interface connections. Along with those mentioned previously, you could have 10 Gigabit Ethernet, Serial Rapid I/O, and Serial Front Panel Data Port. These physical protocols could then use a transport layer, such as VITA-49 (also known as Vita Radio Transport), to send packetized data or receive commands. One of the compelling features of OpenRFM is that it is virtually "protocol-agnostic."

JJD: What is meant by the term "RF middleware"?

LG: "RF middleware" is a term coined by myself and others that work with the OpenRFM architecture. Simply put, it's a software layer that provides a hardware abstraction layer (HAL). That HAL is derived from the various protocols mentioned for control planes ranging to the low-level discrete control of RF control lines.

JJD: What time/cost savings are associated with a module-based design approach?

LG: The time and cost savings are tremendous. At Mercury, for example, we now have a single common test environment for all OpenRFM-based RF modules. Because the control software is universal, little effort is required to develop new test code for control. This aspect reduces the costs associated with integrating and testing the OpenRFM-compliant modules and infrastructures that are designed and implemented by customers. Another example is that standardized parts, such as common connectors and interface components, allow for greater interoperability and reuse across multiple applications and platforms. They deliver a better overall return on investment and a more affordable solution for the end users.

JJD: How is Mercury encouraging other organizations and companies to participate in the development and implementation of OpenRFM?

LG: We are trying to show tangible evidence that this architecture is well aligned with the DoD's directives to lower costs and increases the ability to rapidly and continuously upgrade critical defense electronics systems. We are developing interoperable RF, microwave, and digital modules and showing how we can reuse those modules. We can scale them to various platforms to reduce overall integration time and tighten schedules for RF subsystem development. Nothing breeds acceptance like success, and we are working to have real examples to show to a broad audience in the near future.

JJD: What types of configurability and upgradability are offered by an architecture such as OpenRFM?

LG: The possibilities are seemingly endless. For instance, if a system needed increased instantaneous bandwidth (IBW) or a particular filter changed on a signals-intelligence (SIGINT) subsystem, you could simply change that one module without having to change the system software. The configurability of newer systems provides many options. For example, you could use a receiver, synthesizer, and transmitter to build the RF section of an electronic warfare (EW) system. If a user wanted to build a multichannel SIGINT system, they could then use the same receiver and synthesizer modules as common building blocks to construct a new functional system.

"We expect to have at least three to four OpenRFM-based subsystems deployed with several customers by the end of this year."

JJD: How may the OpenRFM hardware and software impact the retrofitting, modernizing, and maintaining of aerospace EW systems?

LG: Retrofitting systems will allow for more competition in terms of the RF modules, reducing "vendor lock." At the same time, they will give systems integrators a quicker, easier, and more affordable path for future upgrades.

JJD: What external threats are encouraging the development of systems that can be rapidly upgraded and reconfigured?

LG: Many adversaries are already using readily available commercial technology for various EW, communications, and radar systems. This provides them with the ability to adapt quickly. To effectively counter these systems, we must be able to meet or exceed their rate of adaptability. Because it is based on an open-systems architecture approach, OpenRFM can help speed the rate of technology insertion in EW, SIGINT, and radar systems.

JJD: What systems could benefit from using OpenRFM?

LG: Consider, for example, an aging platform with custom hardware that is experiencing obsolescence issues. The system could be re-"architected" using the flexibility of OpenRFM to interface to the older control mechanisms at a line-replaceable-unit (LRU) level. The platform infrastructure (chassis, cooling, wiring, etc.) could then be preserved. In addition to saving millions of dollars, such an approach provides new capabilities to protect or defeat new threats.

JJD: Where is OpenRFM to date, and how do you see it developing in the next year?

LG: The first introductions of OpenRFM to the general industry began in October 2014. We have also discussed OpenRFM at the recent Embedded Technology Trends conference hosted by the VITA organization (www.embeddedtechtrends.com). The architecture is taking shape, as we have carriers in VME and VPX for OpenRFM modules. The first OpenRFM modules are being tested now. We expect to have at least three to four OpenRFM-based subsystems deployed with several customers by the end of this year. mw

SCIENTISTS COMPARE PHASE NOISE WITH VECTOR OFDM

ORTHOGONAL FREQUENCY DIVISION multiplexing (OFDM) is a specific subcase of vector OFDM (V-OFDM), which generally outperforms OFDM. To expand upon the study of V-OFDM techniques for single-transmit antenna systems, a phase-noise estimation and compensation method has been analyzed and developed by Ibo Ngebani, Yabo Li, Xiang-Gen Xia, Sami Ahmed Haider, Aiping Huang, and Minjian Zhao.

In an OFDM system, performance is degraded via intercarrier interference and common phase error, which result from the introduction of phase noise. In V-OFDM systems, however, phase noise results in inter-vector-block carrier interference and common-vector-block phase error (CVBPE). To successfully estimate phase noise, the researchers combined a linear minimum mean square error and maximum likelihood estimator. The phase-noise estimation technique for V-OFDM was found to be less complex than it is for OFDM systems. See "Analysis and Compensation of Phase Noise in Vector OFDM Systems," *IEEE Transactions on Signal Processing,* Dec. 2014, p. 6143-6157.

RESEARCHERS DEMONSTRATE SDR-BASED WIRELESS TOMOGRAPHY

AS THE INTERNET of Things (IoT) takes root, RF and wireless technologies are increasingly being used to enable sensing platforms. Taking this concept to the next step, RF sensing and tomography techniques were used to demonstrate an RF remote sensing concept by the research team of Jason Bonior, Zhen Hu, Terry N. Guo, Robert C. Qiu, James P. Browning, and Michael C. Wicks. With funding from the National Science Foundation, these researchers created images of single- and multi-target scenarios by employing automatic data-acquisition technology, an RF anechoic chamber, a software-defined radio (SDR), and phase reconstruction.

The experimental system implemented compared the results of a vector network analyzer (VNA) and universal serial radio peripheral (USRP)-based software-defined-radio (SDR) tomography device. Whereas the VNA is capable of measuring the actual scattering field, the SDR could only produce amplitude information without phase. The semidefinite relaxation method did provide a strong approximation of the amplitude and phase for these measurements. The measurements correlated strongly with the measured scattering field.

After confirming the viability of the phase-reconstructing methods, the researchers compared the VNA and SDR data with the magnitude take of the VNA data. Here, the amplitude-only information is fed into the processing methods.

With the phase-reconstructed data, it is possible to estimate both the dielectric constant of the target and its position. Unfortunately, the method used produced a consistent error in the target's position. Despite this issue, the experimental data succeeded in proving that RF tomography can be performed with an SDR along with phase-reconstruction techniques. It should be noted that this system used commercial-off-the-shelf (COTS) communications devices. See "Software-Defined-Radio-Based Wireless Tomography: Experimental Demonstration and Verification," *IEEE Geoscience and Remote Sensing Letters*, Jan. 2015, p. 175-179.

COMPARE HETNET COST AND CAPACITY FROM 0.7 TO 28 GHz

AS THE DEMAND for data grows, more companies are investing in a high-capacity office environment that offers continuous high-speed connectivity. Researchers Vladimir Nikolikj and Toni Janevski recently explored cost-analysis models for the following: 4G cellular bands, 5-GHz Wi-Fi, and a potential 5G system at 28 GHz. In this process, the duo considered a demand of 100 GB per user per month while factoring in the latest 3GPP Long Term Evolution (LTE) releases, upcoming radio-access technologies for millimeter-wave systems, and the propagation/path loss models to address millimeter-wave coverage concerns.

When considering range for the different technologies, the researchers used a dense urban environment. These factors limit the radio range at 900 MHz, 2.6 GHz, and 28 GHz, respectively, to 1.4, 0.57, and 0.1 km. At 5 GHz, for example, Wi-Fi is considered to have a 30-m range at a 1300-Mbps data rate. The bandwidth for the various technologies is considered as follows: 20 MHz for LTE-Advanced; 500 MHz for millimeter wave; and 80 for 5 GHz Wi-Fi. In megabits per second, the average site capacity for these radio-access-network (RAN) technologies are 228 (LTE-A), 2910 (millimeter wave), and 1300 (5-GHz Wi-Fi).

Once the models were developed for the RAN technologies, the researchers saw that costs scaled linearly for macrocell technologies like 4G and 5G. For moderate demands, the aggregated approach (using the 700-MHz and 2.6-GHz bands for 4G LTE-A) were the most cost-effective. Wi-Fi did prove cost-effective under extreme-demand levels for indoor scenarios. Considering long-term planning, however, the researchers recommend deploying pico-cell base stations for indoor and outdoor use with the 28-GHz millimeter-wave channel. See "A comparative cost-capacity modeling of wireless heterogeneous networks, implemented within the 0.7 GHz, 2.6 GHz, 5 GHz and 28 GHz bands," *2014 IEEE International Conference On Ultra-Wide-Band (ICUWB)*, Sept. 2014, p. 489-494.

JEAN-JACQUES DeLISLE | Technical Editor

THE INTERNET OF THINGS

4 Major M2M YOU NEED

With the explosion of machine-to-machine and Internet of Things devices and applications, more large technology companies are jumping on board with devices spanning from wearables to beacon modules.

There are so many considerations to take into account when implementing machine-to-machine (M2M) and industrial Internet of Things (IoT) technologies and every aspect must be carefully considered, ranging from cost and power to long-term product-life-cycle challenges and interference.

Even those companies armed with a solid standard—one that is efficient and sufficiently versatile for a variety of applications—may find that innate RF and infrastructure challenges continue to plague this emerging industry. Here are four critical areas to watch out for:

LOW POWER OR DATA RATE

The urge to acquire data, control, and intercommunicate throughout a connected-device environment can be quite costly in terms of power. Many wireless-device nodes only need to transmit data in a very limited and infrequent duty cycle. As a result, the power requirements for these types of devices is understandably low. The power requirement will be quite different for devices that are relaying large amounts of data or continuously gathering data from their surroundings.

The tradeoff between power efficiency and data rate extends from the base hardware and wireless protocol used to communicate to the sensors integrated into the platform and the RF environment in which the IoT device is communicating. Generally, a higher data rate and longer range correspond to a higher power requirement. If a device is more sophisticated, in terms of the data it can process and share, it will therefore be more limited in terms of range. It also will be more susceptible to the outside environment.

According to Greg Fyke, marketing director of IoT wireless products for Austin, Texas-based Silicon Labs, "Balancing data rate, range, and battery life are challenges for most low-power IoT platforms. An obvious way to increase the wireless transmitter's range is to boost the transmit output power to

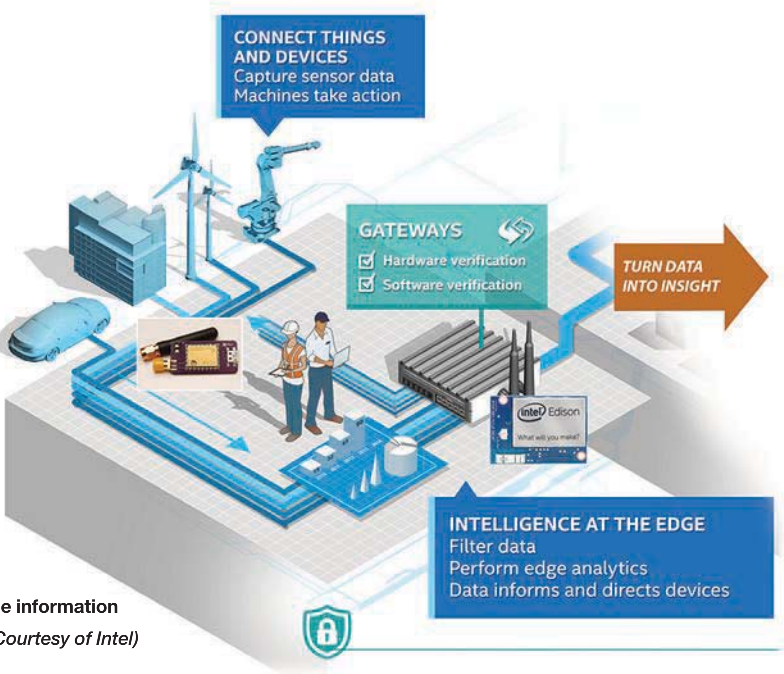

The expansive goal of many IoT platforms is to gather real-time sensor data in order to provide analysis-grade information for the optimization and study of intelligent systems. ***(Courtesy of Intel)***

and IoT Challenges TO KNOW

the maximum allowable level, but to realize low power in this scenario you have to architect your application to limit transmitter use and maximize the time spent in standby."

If the competing features of low power, range, and data rate are all critical, more investigation and development are needed for an appropriate wireless standard/protocol.

STANDARDS & INTEROPERABILITY

With an overwhelming number of proprietary and open M2M and IoT solutions available, there is a great deal of confusion over which to choose and under which circumstance it is best to deploy it. Many organizations are actively working to promote solutions that will unite M2M and IoT technologies—among them, m2mGlobal Alliance, Thread, Internet of Things Solution Alliance, AllSeen Alliance, and the Internet Protocol for Smart Objects Alliance. In addition, many competitors and various industrial partners are teaming to create solutions that can provide the necessary range of operation needed for IoT applications. These efforts involve merging a variety of disparate wireless technologies.

In these organizations, arguments are typically centered on the wireless hardware, software, and standards (*see Table at right*). A variety of standards, for example, are better suited to certain aspects of applications. Yet some standards are highly versatile. With many of these wireless standards, there are concerns about the cost of adoption and implementation, as well as the risk of obsolescence. As a result, many of the alliances are focusing on creating solutions that optimize the benefits of various existing wireless standards. In doing so, they hope to create standards and technologies that can coordinate devices operating on different standards.

"Recently, in M2M, we are seeing the development of platform applications that enable users to almost do a point-and-click app solution, such as Apple iOS, Thingworx, and our business," notes Alex Brisbourne, CEO of Kore, Alpharetta, Ga. "These companies are creating downstream libraries of pre-designed applications and solutions based on a variety of technologies. So if customers want a sensor application, they can choose from a variety of sensor providers and quite quickly build those solutions. These uniting platforms are still quite early in gestation. But this approach removes the mystery from having to deal with the numbers of proprietary devices and learning each individual one."

SECURITY & DEVICE SOPHISTICATION

When choosing or developing an M2M/IoT solution,

IOT WIRELESS TECHNOLOGIES

Technologies	Standards & Organizations	Network Type	Frequency (US)	Max Range	Max Data Rate	Max Power	Encryption
WiFi	IEEE 802.11 (a,b,g,n,ac,ad, and etc)	WLAN	2.4,3.6,5,60 GHz	100 m	"6-780 Mb/s 6.75 Gb/s @ 60 GHz"	1 W	WEP, WPA, WPA2
Z-Wave	Z-Wave	Mesh	908.42 MHz	30 m	100 kb/s	1 mW	Triple DES
Bluetooth	Bluetooth (formerly IEEE 802.15.1)	WPAN	2400-2483.5 MHz	100 m	1-3 Mb/s	1 W	56/128-bit
Bluetooth Smart (BLE)	IoT Interconnect	WPAN	2400-2483.5 MHz	35 m	1 Mb/s	10 mW	128-bit AES
Zigbee	IEEE 802.15.4	Mesh	2400-2483.5 MHz	160 m	250 kb/s	100 mW	128-bit AES
THREAD	IEEE 802.15.4 + 6LoWPAN	Mesh	2400-2483.5 MHz	160 m	250 kb/s	100 mW	128-bit AES
RFID	Many	P2P	13.56 MHz, etc.	1 m	423 kb/s	~1 mW	possible
NFC	ISO/IEC 13157 & etc	P2P	13.56 MHz	0.1 m	424 kb/s	1-2 mW	possible
GPRS (2G)	3GPP	GERAN	GSM 850/1900 MHz	25 km / 10 km	171 kb/s	2 W / 1 W	GEA2/GEA3/GEA4
EDGE (2G)	3GPP	GERAN	GSM 850/1900 MHz	26 km / 10 km	384 kb/s	3 W / 1 W	A5/4, A5/3
UMTS (3G) HSDPA/HSUPA	3GPP	UTRAN	850/1700/1900 MHz	27 km / 10 km	0.73-56 Mb/s	4 W / 1 W	USIM
LTE (4G)	3GPP	GERAN/UTRAN	700-2600 MHz	28 km / 10 km	0.1-1 Gb/s	5 W / 1 W	SNOW 3G Stream Cipher
ANT+	ANT+ Alliance	WSN	2.4 GHz	100 m	1 Mb/s	1 mW	AES-128
Cognitive Radio	IEEE 802.22 WG	WRAN	54-862 MHz	100 km	24 Mb/s	1 W	AES-GCM
Weightless-N/W	Weightless SIG	LPWAN	700/900 MHz	5 km	0.001-10 Mb/s	40 mW / 4 W	128-bit

another compromise arises in how secure the device or system needs to be. The level of security usually depends upon the application, which requires anything from maintaining consumer privacy to limiting cyber attacks against utilities. Unfortunately, as we rely more heavily on these systems, more opportunities arise for malicious conduct against them.

As noted by Daniel G. Steele, director of the OEM, Utility, and Energy Market for Freewave Technologies, "M2M, from a security perspective, has probably changed dramatically after 9/11. Some people are more aware from the cyber-attack side of the fence and informed about a lot of the attacks seen by SCADA networks. These issues are on everybody's mind now—especially with smart-grid applications and how they keep their networks secure."

From corporate espionage to denial-of-service (DOS) attacks, many connected systems face regular threats. As a result, Steele says, "Security needs to increase along with all the performance benefits we like to see. The focus shouldn't just be on what we expect with speed and connectivity but also, how secure is everything? We have to make sure no one is eavesdropping on our data packets or conversations."

The race for IoT system platforms focuses on a radio architecture with the smallest size, lowest power consumption, highest integration, and most versatility. *(Courtesy of Intel)*

Generally, adding security features to wireless systems requires more overhead in each packet sent. It also means adding components within the electronics. "There is a cost-analysis side of security features," says Kore's Brisbourne. "For example, if you are putting tens of thousands of devices in a network, how much processing can you have on that device for security? The security sophistication at the device level affects the relative balance of device cost, performance, and power. It is safe to say that there is a specific tension in a design engineer, urging him to look into this."

INTERFERENCE/FAILURES & SPECTRUM

To prevent interference and failure modes in M2M/IoT devices, reconfigurable networks must be created to ensure adequate operation. A variety of new networking standards and updates to old standards include techniques for networks to automatically decide workarounds. These adaptations are designed to work in scenarios ranging from fatal node failure to interference issues.

"Devices can fail so it is important for networks to have built-in resiliency," says Silicon Labs' Fyke. Mesh networks, such as ZigBee and Thread, are designed to self-heal and the network has the ability to intelligently redirect traffic if a device node is no longer available. In the event of a node failure, routes are dynamically updated to realize the most optimal path through the new network configuration. These fail-safe mechanisms in mesh networks ensure that messages can reliably reach their destination. The market won't tolerate an IoT platform where the lights turn on 'most' of the time. When you flip a light switch, the light must turn on every time."

As more wireless devices operate in a frequency swath within the RF environment, the greater the noise and interference will be in those frequencies. Many unintended and non-congestion-related aspects of interference, such as intermodulation and nonlinear effects, lead to other noise-causing issues. These performance-degrading issues exist, regardless if the frequency band is licensed or unlicensed.

Freewave's Steele says, "Another great challenge and the biggest complaint of the operators in the industry is why hasn't the FCC opened up more dedicated spectrum specifically for SCADA and M2M systems. The ISM band is great, along with the uniband and 5-GHz bands. But it is a double-edged sword if you don't have a radio product that can adapt and work around the noise potential."

He adds, "If you don't engineer the system well for noise, it can be your worst enemy. There are licensed systems around. With licensed systems, though, you generally have narrow bandwidths and can't operate at high capacity."

CONCLUSION: DO ENDLESS POSSIBILITIES EQUAL ENDLESS CONFUSION?

As mentioned, several organizations have been looking to create standards and technologies that will serve as the wireless "glue" that joins the various standards and wireless technologies. From a component level all the way to a protocol level, devices will then need to be optimized for flexible operation over common wireless standards. The resulting solutions could range from software-defined operation to highly capable, though specialized devices that are geared toward power optimization using a few critical wireless technologies.

"Traditionally, to enable multi-protocol support, one would need to use multiple radios, which can be expensive," says Fyke. "If you had a radio that was designed to support multiple protocols by time-slicing operation, you could enable multi-protocol support at a much lower cost point and still be able to address some really exciting use cases."

Although there are still many standards and challenges associated with implementing M2M/IoT networked systems, significant progress is being made in uniting current technologies. These approaches may take the form of new wireless standards or even devices that can operate using a variety of wireless standards and frequencies, which will, of course, be based on sophisticated protocols. Whatever solutions end up dominating, they will have to overcome the challenges of security, node failure, and ever-growing interference. mw

JEAN-JACQUES DELISLE | Technical Editor

What's the Difference Between Noise Terms and Noise Generators?

Because noise is a complex concept with many contributors and effects, confusion often arises about how noise is created and how it's described by engineers.

NOISE IS EVERYWHERE—YOU can't get rid of it, but rather can only hope to mitigate its effects in the signal chain. On top of that, noise isn't consistent. A good system design, therefore, includes additional overhead to account for noise generators.

Many different types of noise generators exist both inside and outside of components and systems. As a result, engineers use many terms to describe noise based on what, when, where, and how it's generated.

Noise is simply undesired energy outside of the signal that's manipulated by a system's design. Every component in a system generates noise. As such, there are terms to describe the noise contribution of a component and how it generates that noise.

Signal-to-noise ratio (SNR) compares the desired signal power to the noise power, or noise level, over a range of frequencies. SNR is typically given with respect to a frequency that relates to the operational frequency of a system. Usually, it's "average" SNR rather than "instantaneous."

While related to SNR, noise figure (NF) describes a component's or system's noise contribution to the signal chain. NF measures the input's SNR compared to the output's SNR. In other words, it tells how much the signal's SNR degrades as it passes through that component or system. The noise generators within a component or system tend to vary as a function of many different parameters. For this reason, NF is defined under certain conditions.

The noise floor, or noise power, will sometimes be confused with the noise figure. Within a signal chain, the noise floor represents the total measure of noise energy present within a signal created from noise generators and unwanted signal sources. To specify the targeted noise floor, it's categorized into the noise floor of both the test equipment (or instrumentation noise floor) and noise generators (or incidental noise). Incidental noise-floor conditions include temperature, atmospheric conditions, cosmic noise, and many other factors.

I CAN'T HEAR BECAUSE OF ALL THE NOISE!

Random thermal motion of charge carriers determines the thermal or Johnson-Nyquist noise generated within a conductor. Because thermal noise is basically white noise, it produces roughly equal power across the entire frequency spectrum. Unfortunately, every component within the signal chain will add to thermal noise within the signal. Therefore, it's essential to account for this noise. Components or systems that suffer most from thermal noise can be cooled to lessen its impact. But this method usually incurs costs, size, and complexity tradeoffs.

In terrestrial environments, electron charge action within the atmosphere and weather patterns will generate noise. Lightning discharges and thunderstorms are the primary contributors. As long-range noise contributors, several atmospheric incidences can induce this type of noise simultaneously. Understandably, this is the justification for some high-

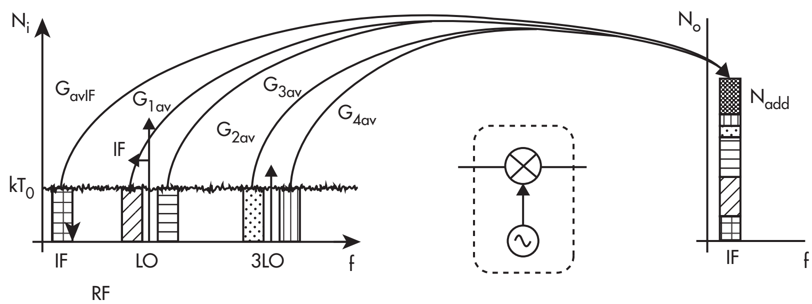

1. At the output of a mixer, the noise power at the intermediate frequency (IF) and the frequencies around the local oscillator (LO) and LO harmonics all contribute to the IF's noise.

priority satellite-communication systems that rely on multiple installations in geographically diverse locations.

Cosmic noise identifies closely to thermal noise in that many types of cosmic noise are ever-present. It includes cosmic microwave background radiation (CMBR), which may have been a product of the Big Bang and generally peaks in the microwave bands. Other examples of cosmic noise include solar activity and celestial objects inside and outside of our galaxy that emit electromagnetic (EM) radiation. Random celestial events can also induce unpredictable and often complex noise distribution, such as meteorites ionizing surrounding gases by entering our atmosphere, solar flares, and supernovae. Generally, shielding is the only way to mitigate comic-noise generators.

Another intrinsic noise generator to consider is flicker noise, 1/f noise, or pink noise. Flicker noise stems from direct current (dc) or resistive effects. One example is generation/recombination noise caused by the base current or inconsistencies in the conductive channel within a transistor or diode. Though predominantly a low-frequency phenomenon, flicker noise can occasionally be upconverted to frequencies within a significant range of the carrier frequency. For instance, this may occur during frequency generation or when mixer circuits are involved. Flicker noise can become significant in higher-current devices because its power tends to rise with increasing current.

Transit-time noise usually becomes an issue in frequencies above the very-high-frequency (VHF) band. This type of noise generates during amplification of a signal with a period that's in the same order of magnitude as the traveling time required for electronics to go from the emitter to collector in a bipolar junction transistor (BJT). This effect increases the transistor's noise input admittance of the transistor. It increases as a function of frequency.

In contrast, shot or Poisson noise is a function of the charges in a dc system arriving at inconsistent times. Typically, such noise isn't a concern for most electronics, which are generally more affected by flicker or thermal noise. These will swamp out the effects of shot noise.

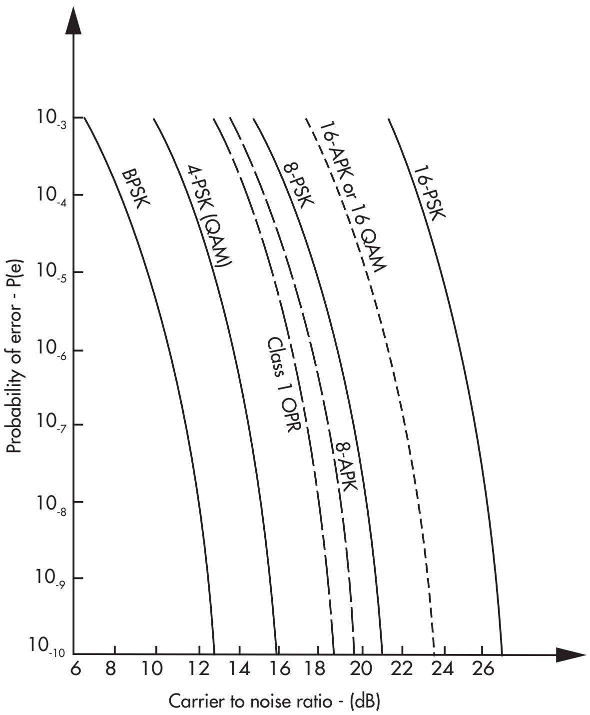

2. As the carrier-to-noise ratio decreases for digitally modulated data, it increases the probability of error. (Courtesy of Keysight)

An interesting characteristic of shot noise is that it's not influenced by temperature or frequency. Unlike flicker or thermal noise, it can significantly affect a circuit under low-temperature and high-frequency conditions. For highly sensitive receivers, such as the receivers used to measure CMBR, shot noise may limit the microwave imaging system's resolution.

These aspects and definitions are important to consider because of the effect noise has on modern digital communications systems. In highly sensitive digital receivers, noise directly impacts bit-error rate (BER) and the data rate of a channel (or channel capacity). By employing techniques like spread spectrum, a receiver system can demodulate signals below the noise floor. However, this method requires significantly more bandwidth to achieve the same data rate in a less noisy system.

Often, a set of components within a design will include a specification for the maximum allowable noise contribution. This specification ensures that the overall system operates within reliable and robust ranges that add margin for intermittent noise effects, such as incidental and man-made noise. mw

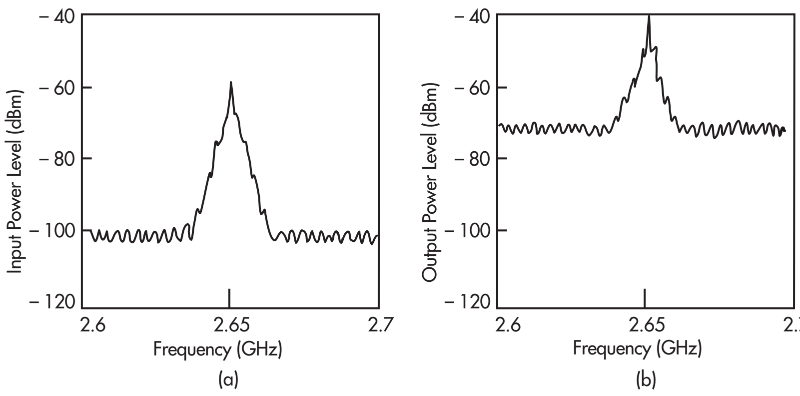

3. The additional noise figure of an amplifier compounds with the noise level of the input signal, amplifying the noise more than the desired signal. (Courtesy of Keysight)

JEAN-JACQUES DELISLE | Technical Editor

Software Reveals Cosite Challenges

As RF/microwave technology is increasingly incorporated into systems ranging from naval defense vessels to Internet of Things beacons, the number of antennas involved is creating a range of cosite complications.

UNLESS A RADIO installation is single-purpose and located far from any urban environment, it will undoubtedly have to overcome RF cosite issues. Cosite is a growing challenge for both RF system design engineers and radio technicians. As RF/microwave technologies become more accessible, so do the challenges of preventing these different RF systems from negatively impacting each other's performance. Mitigating the interference impact of other radio systems is critically important for high-sensitivity, high-throughput, and mission-critical systems. Examples of these systems range from an unmanned aerial vehicle (UAV) to a tactical communications system on a naval ship or a wireless sensor platform in a mesh network (*Fig. 1*).

For the vast majority of radio installations, troubleshooting cosite issues is a complex, time-consuming, and error-prone task. Compounding this scenario is the fact that it is difficult to predict cosite scenarios before they occur. As a result, it is challenging to determine the best-performing antenna configuration. The variables in the problem increase exponentially with the number of antennas involved.

Shawn Carpenter, vice president of marketing for Delcrosse Technologies, Champaign, Ill., provides an example. "Naval ships are floating antenna farms," he says, "and there is a great deal of interaction between RF systems that must be considered. A natural concern for antenna placement in naval environments is that of coupling to the host vessel and to other antennas." A specific challenge with naval vessels is that their radios range from redundant emergency radios in the megahertz range to millimeter-wave radar systems. This broad range of frequencies creates a nearly impossible troubleshooting scenario, as the equipment needed to measure all of these interactions would require tens of gigahertz of bandwidth.

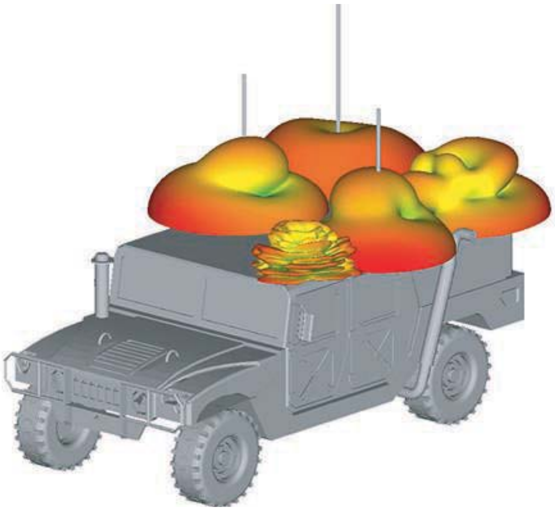

1. To ensure reliable operation, modern military vehicles usually carry a variety of different tactical and emergency radio equipment along with several redundant systems. *(Courtesy of Delcrosse)*

OPTIMIZING ANTENNA PLACEMENT

There is hope, though, as the latest EMI/cosite software has been developed using techniques that can optimize antenna placement. Such placement is based on profile models of commercial and military radios. Software suites, such as Ansys HFSS, FEKO, Delscrosse EMIT, Andro E3Expert, and others use specialized EM simulation techniques to efficiently gauge the performance of a variety of antennas and radio technology. To do this, they rely on antenna platforms imported from computer-aided design (CAD) models. Several of these software suites will even incorporate parameterized antenna models and simulate installed antenna performance and interactions from those models.

In a cosite prediction, the power received by the different antennas must typically be accounted for with each piece of radio hardware. Best practices—often developed by field experience in optimizing antenna placement—would be required to effectively use the information from the EM simulation (*Fig. 2*). However, it would be nearly impossible to account for

2. Business and commercial radio installations are often a conglomerate of different radio technologies and frequencies, making them an ideal breeding ground for cosite issues.

nonlinearities, intermodulation distortion, reflections, mixing action, and other potential causes of re-radiated or internal interference. Fortunately, the latest software designed for cosite analysis and interference mitigation offers the ability to include system-level models of amplifiers, filters, cables, and even complete radios.

"Using asymptotic EM simulation, we can study the installed performance of individual antennas and arrays," notes Carpenter. "EM simulation also enables us to perform antenna-to-antenna coupling in a fraction of the time and cost that would be required to install and measure these effects on an actual ship, for example." For many simulation scenarios, the antenna platform could be highly complex and require more advanced computational enhancement techniques. Carpenter says, "These simulations make it possible to study a multitude of antenna placements in terms of their installed far-field radiation patterns, local RF intensity levels, sidelobe levels, and coupling to other antennas in the scenario. Once the antenna coupling between RF systems is understood, it is possible to progress to RF cosite interference mitigation."

ANALYZING THE SIMULATION

Once the models of the antennas on the antenna platform are in place, the cosite simulation process incorporates those models into a cosite analysis mode or software package. Some of these software packages also include libraries of pre-built radio-configuration and component-level models, which allow a radio-hardware-inclusive cosite and interference simulation to be rapidly created. Including system- and component-level considerations enables transmit and receive paths to be considered separately. Self-interference effects can even be predicted.

To easily interpret the cosite and interference effects on the various transceivers, many of these software suites offer interference mapping. This aspect can be further investigated using one-on-one and multiple-on-one analysis. In addition to providing access to individual transceiver interactions, these tools can reveal the compound effects of either noise or direct interference on each individual receiver.

The quality and thoroughness of the EM simulation directly impacts the simulation's ability to identify interference scenarios. For EM simulations, a more detailed simulation also demands more computational resources. That computational requirement grows as a function of rising frequency and larger total simulation area.

For example, a car may require simulation volume of roughly 5 × 3 × 2 m. At 2.6 GHz (a necessary simulation range to capture all common radio frequencies deployed in car scenarios), the car is beyond 40 wavelengths of the maximum simulation frequency. It therefore requires over 100 million mesh cells. In comparing mesh size to total simulation volume, the computational time necessary could be days—even with a high-performing computing platform.

GPUs CHANGE THE GAME

To augment the computational power of a machine without demanding a significant investment, graphics processing units (GPUs) and software suites have recently been used. They are designed to profit from a GPU as a computing cluster.

Matthew Miller, president of Delcross Technologies, notes, "GPUs have been a game-changing technology for the SBR+ technique, providing anywhere from 20X to 200X acceleration factors with a single consumer-grade GPU card. For example, for a $300 to $400 investment in a GPU card, a simulation that used to take 24 hours to run now completes in under 15 minutes. We recently ran into a problem involving a 94-GHz antenna mounted to a Blackhawk helicopter. At 94 GHz, the Blackhawk is over 6000 wavelengths in dimension. Using a five-node cluster that we purchased for $20,000, we were able to compute the installed antenna performance in 143 seconds."

Clearly, EM cosite and interference software is being rapidly developed to reduce interference—from a radio-hardware design perspective all the way to antenna and device placement. As wireless capabilities continue to be incorporated into virtually everything, however, the environment is only becoming more highly congested and interference-prone. This issue applies whether the focal point is a connected home, automobile, or the body of the latest fighter jet.

Meanwhile, other issues are complicating these matters. Spectrum regulation, for example, was not designed to consider such a widespread demand for spectrum. Much like noise pollution in cities, the effects of ever-growing noise generators are creating a more complex and difficult environment for RF equipment, making it hard for that equipment to operate effectively. Thankfully, EM cosite and interference software is increasingly being used as an accepted best practice to meet the challenges of an ever-more-active wireless world. mw

CHUNHUA WANG | Professor
School of Computer and Communication, Hunan University, Changsha, People's Republic of China; e-mail: wch1227164@sina.com

WEN WANG | Postgraduate Student
College of Information Science and EngineeringHunan University, Changsha, People's Republic of China; e-mail: hellowordwen@gmail.com

Low-Power UWB CMOS LNA Gains 4 to 5 GHz

Running on very low power and voltage levels, this ultrawideband amplifier builds upon 0.18-μm silicon CMOS semiconductor technology to achieve low noise levels with generous gain.

Ultrawideband (UWB) communications offers a great deal of flexibility and versatility for modern users, but it requires advanced analog signal processing, including wideband amplifiers. To meet the growing needs for UWB applications, a low-noise amplifier (LNA) for low-voltage, low-power use was designed for fabrication using 0.18-μm silicon CMOS technology developed by Taiwan Semiconductor Manufacturing Corp. (TSMC; www.tsmc.com).

The LNA operates in the 4- to 5-GHz range and meets the Chinese specifications for UWB systems targeting broadband input matching. In addition, a transconductance (g_m) boosting technique helps improve the gain and noise-figure performance levels. Needing less than 0.9-mW total power consumption, the LNA features a low supply voltage of +0.6 V dc.

Since 2002, the Federal Communications Commission (FCC) has authorized UWB systems for use from 3.1 to 10.6 GHz in the United States. The technology offers high data rates at low power levels. In 2008, the Ministry of Industry and Information Technology (MITT) in China allocated the 4.2- to 4.8-GHz frequency band for UWB applications in that country.[1]

LNAs—crucial building blocks for wireless receiver front ends—must meet several requirements for practical use. As the first component following an antenna, an LNA must provide full bandwidth impedance matching with low noise figure, sufficient power gain. and acceptable gain flatness. In addition, many wireless UWB applications require low-voltage operation with low power consumption to extend operation under battery power.

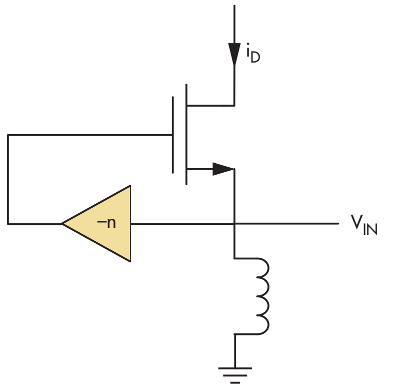

1. This simple schematic diagram shows a basic CG LNA using the g_m-boosting technique.

TYPES OF LNAS

A number of CMOS LNAs have been developed for UWB receiver systems.[2-9] A conventional distributed amplifier (DA),[10-12] for instance, absorbs the parasitic capacitance of the input transistor as part of the transmission line, and thus delivers good wide-frequency performance. However, these amplifiers are rather large in size with relatively high power consumption, making them of limited interest for low-power applications. There's also the resistive feedback topology,[13-15] which provides broadband matching with level gain over wide bandwidths. But it's still difficult to satisfy high-gain and low-noise-figure requirements simultaneously by taking this approach.

Amplifier designs have employed passive filtering for extended bandwidths.[16-19] By adding a passive inductive-capacitive (LC) network to a conventional cascode structure, a narrowband LNA can be extended to an UWB LNA with good performance in power gain, input matching, and noise figure. But stacking MOS transistors increases the voltage requirements, which more or less negates this approach. On top of that, additional inductors in the LC filter consume physical area and lead to higher costs.

Due to its simplicity, the common-gate (CG) amplifier has become a somewhat popular wideband-amplifier topology.[20,21] Proper transconductance of the input transistor achieves wideband matching and high gain. However, parasitic capacitance in this approach could significantly deteriorate noise figure and gain. A g_m-boosting technique[22,23] can overcome these limitations, although the additional g_m stage also leads to higher power dissipation.[24]

NEW UWB LNA APPROACH GETS A BOOST

The latest design concept used to conquer the limitations of these LNA design approaches for UWB leverages a novel current-reuse g_m-boosted structure. The CG amplifier design employs a common-source (CS) stage to achieve the g_m boost; this stage shares bias current with the LNA's CG stage. Incorporating a forward body bias technique effectively reduces the operating voltage of this LNA. As a result, the LNA design achieves excellent electrical performance at reduced supply voltage and power dissipation, suiting it for low-voltage Chinese UWB applications.

With the current-reuse CG configuration, this new LNA is able to meet impedance-matching requirements for UWB applications, whereas a CS LNA configuration needs additional techniques (and larger circuit size) to fulfill UWB matching requirements. The CG LNA features a simple, robust matching architecture, with good linearity and low power consumption. Because the voltage gain of a CG LNA approach is generally inferior to that of a CS LNA, it uses a g_m-boosting technique.

A CG amplifier's noise performance also comes up short versus that of a CS design. Once again, the g_m-boosting approach can be used, this time to help the noise figure. Neglecting induced gate noise, the noise factor of a basic CG LNA has a minimum NF[26] according to Eq. 1:

$$F = 1 + \gamma/\alpha \quad (1)$$

where α and γ are bias-dependent parameters.

It's usually difficult to achieve a noise figure of under 3 dB with a CG LNA approach, and the noise performance typically deteriorates at higher frequencies. A CG LNA also requires an input transconductance of 20 mS for input matching at 50 Ω, which translates into high power consumption. By boosting the transductance, the CG LNA design can be improved.

Figure 1 illustrates a g_m-boosting approach, where an inverting replica signal with an amplitude n is provided from the source to the gate terminal. Consequently, it boosts the effective transconductance by a factor of (1 + n):

$$g_{m,\,eff} = (1 + n)g_m \quad (2)$$

The noise factor (F) becomes:

$$F = 1 + (\gamma/\alpha)[1/(1 + n)]\big|_{(1+n)g_m R_s = 1} \quad (3)$$

A number of g_m-boosting methods are presented in the technical literature, either by using active circuitry or passive transformers. For example, a capacitive cross-coupling technique[28] can boost transconductance by a factor of 2. But the need for a differential architecture adds complexity and increases power consumption. A transformer-based approach[23,26] is easy to implement, but doesn't suit UWB applications due to process nonlinearities. Also, the inductors' parasitic resistance can degrade noise-figure performance.

A g_m-boosting CG UWB LNA approach was unveiled in refs. 22 and 27, with a CS stage to provide inverting g_m-boosting gain. This active amplifier approach[28] provides larger inverted amplitudes than other methods. But the CG stage and the g_m-boosting circuits are biased separately using different dc voltage paths, which increases total power dissipation compared to simpler biasing methods.

To minimize power dissipation in the proposed UWB LNA design, a current-reuse architecture is used with the CG stage and g_m-boosting circuit stacked together. Sharing current between the g_m-boosting stage and the CG stage

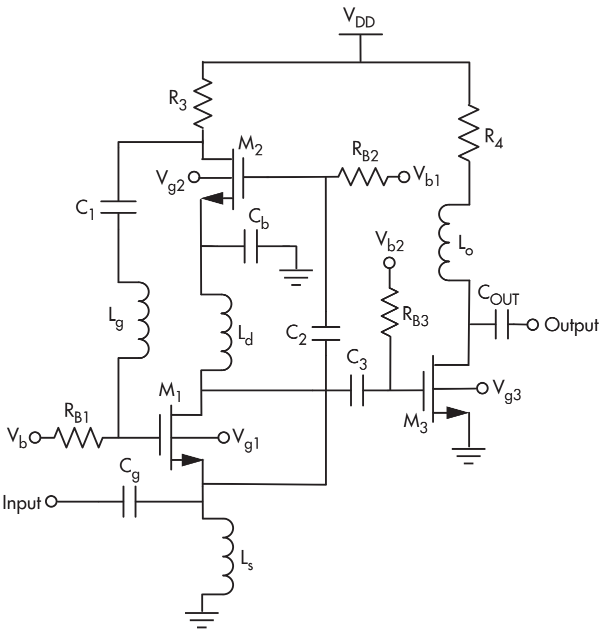

2. This schematic diagram shows the layout for the proposed UWB CG LNA.

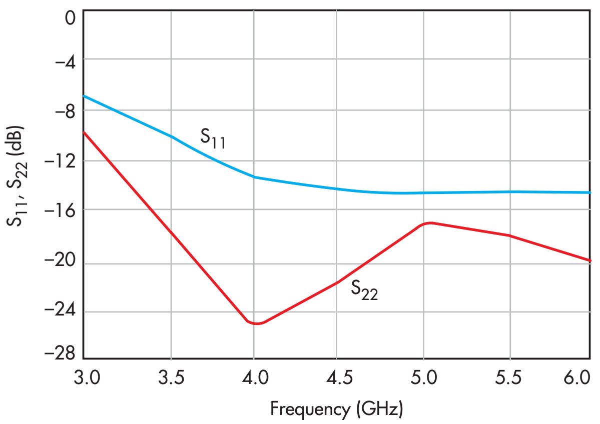

3. S_{11} and S_{22} behavior for the proposed LNA indicate good impedance matching.

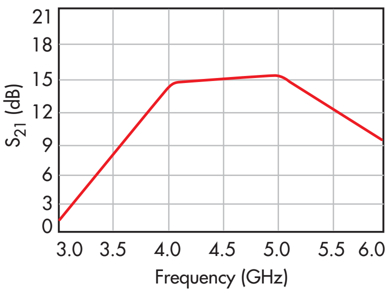

4. These plots show the simulated S_{21} results for the proposed LNA.

COMPARING UWB CMOS LNAs

Reference	This work	1	7	13	14	16
Technology (μm)	0.18	0.13	0.18	0.18	0.18	0.18
Bandwidth (GHz)	4-5	4.2-4.8	3-5	3.1-4.9	6-8.5	3.1-10.6
V_{dd} (V)	0.6	1.2	1.8	1.0	1.8	1.8
Noise figure (dB)	2.3-2.6	2.3-3.7	3.8-3.9	4.5-5.0	3.95-6.81	3.1-6
IIP3 (dBm)	−3	−2	−10	−5	—	−7
S_{11} (dB)	≤12	≤9	≤10	≤5.6	≤10	≤9
S_{21} (dB)	14.5-15.3	28#	11	10.3*	14.3*	13.5-16
S_{22} (dB)	≤16	≤10	≤15	≤8.6	≤14.9	—
Power (mW)	0.9	21.6	5.6	2.39	5.26	11.9

* maximum power gain # tunable maximum gain

minimized dc consumption. Also, a forward body bias technique[29] helps relieve the high-voltage supply caused by the stacked structure.

FORWARD BODY BIAS

Technologically, the most efficient way to reduce amplifier power consumption is through supply voltage scaling. However, a cascade arrangement's performance will degrade as the supply voltage decreases. For the proposed LNA design, which has two MOSFETs stacked in the first stage, a low supply voltage is impractical. At a supply voltage of +1 V dc, the NMOS transistors still operate in a weak inversion region.

To solve this problem, a forward body bias technique was applied to minimize the threshold voltage, V_{th}. In a standard silicon CMOS process, the dc bias at the body terminal can manipulate the threshold voltage, adding one more degree of freedom to a circuit design. Typically, the threshold voltage of an n-channel MOSFET is given by Eq. 4:

$$V_{th} = V_{th0} + \gamma[(\varphi_f - V_{bs})^{0.5}] - (2\varphi_f)^{0.5} \quad (4)$$

Thus, the source-to-body voltage V_{bs} can manipulate the threshold voltage (V_{th}). Voltage V_{th0} is the threshold voltage when $V_{bs} = 0$, γ = the bulk threshold parameter, and φ_f is a semiconductor parameter with a typical value in the range of 0.3 to 0.4 V.[29] With the forward body bias technique, the MOSFETs can operate acceptably at a reduced bias voltage.

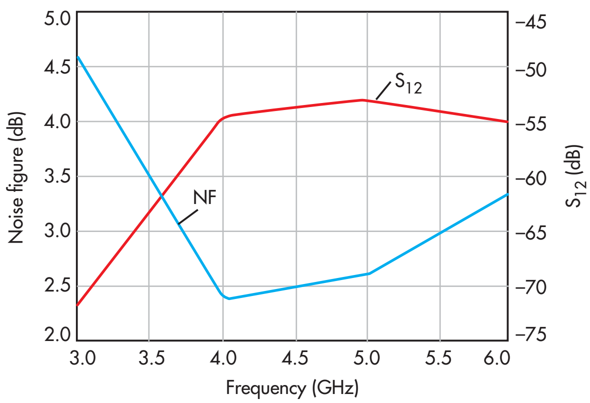

5. Simulation revealed good results in terms of noise figure and S_{12} behavior for the proposed UWB LNA.

TWO-STAGE ARCHITECTURE

The proposed low-power LNA adopted a two-stage architecture *(Fig. 2)*. The first stage is a CG stage with low input impedance and broadband characteristics, with noise figure almost independent of frequency of operation. The CG stage also eliminates the Miller effect and provides high isolation from output return signals. The g_m-boosting inverting stage, CS NMOS amplifier M_2, overcomes the inherent low transconductance of the CG LNA, thus improving gain and noise figure as in Eqs. 2 and 3.

To minimize current dissipation, the CG LNA and g_m-boosting stages are biased using the same dc path, which helps achieve good input matching and noise performance without increasing device size or power dissipation. To boost gain, the CS active device, M_3, is designed into the second stage.

At the input stage, gate capacitor C_g and source inductor L_s are part of the matching network to match the input port to 50 Ω. The series-resonant LC tank with gate inductor L_g and capacitor C_1 provide low-impedance ac coupling paths between the drain of M_2 and the gate of M_1. Capacitor C_b is a bypass capacitor that makes high-frequency ac current flow to ground, avoiding signal interference coupling back to M_1. Drain inductor L_d acts as an RF choke to isolate devices M_1 and M_2.

The input RF signal is simultaneously fed to the source of M_1 and the gate of M_2 for amplification; with one path through M_2, an inverting signal is applied back to the gate of M_1. This increases the equivalent transconductance ($g_{m,\,eff}$) of M_1, leading to a reduction in the CG LNA's noise figure.

To ensure sufficient gain across the full frequency range, the CS amplifier is used in the second stage. A shunt peaking inductor (L_0) and resistor R_4 are used to achieve an extension of LNA bandwidth.

SIMULATION RESULTS

The proposed UWB LNA design was simulated with com-

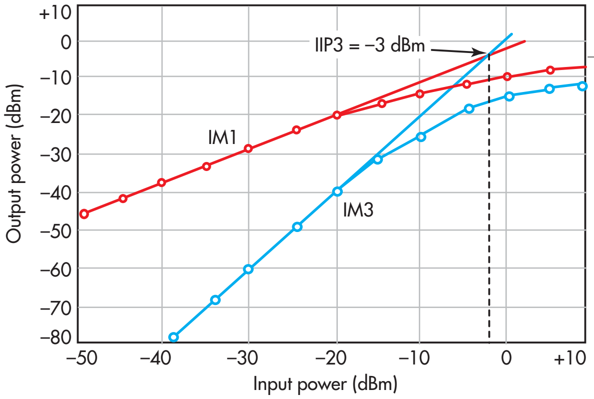

6. The LNA's linearity can be gauged by this plot of IIP3 performance at 4.5 GHz.

mercial computer-aided-engineering (CAE) software—the Advanced Design System (ADS) from Agilent Technologies (now Keysight Technologies). The simulation was based on TSMC's 0.18-µm CMOS technology.

Figure 3 shows the simulated input reflection coefficient S_{11} and output reflection coefficient S_{22}, which are below −12 and −16 dB, respectively, indicating good impedance matching. *Figure 4* shows the LNA's forward transmission, S_{21}, which ranges from 14.5 to 15.3 dB with gain variations as small as 0.8 dB.

The amplifier design achieves good reverse isolation, with S_{12} of better than −50 dB, and the simulated noise figure ranges from 2.3 to 2.6 across the frequency range *(Fig. 5)*. The linearity is also acceptable *(Fig. 6)*, with input third-order-intercept point (IIP3) of −3 dBm at 4.5 GHz. The total power dissipation for the LNA design is 0.9 mW from a +0.6-V dc supply.

The *table* summarizes the proposed UWB LNA's performance and compares it with previously reported CMOS UWB LNAs. Even while operating with low power and voltage levels, the new proposed LNA achieves quite respectable impedance matching, low noise figure, and high power gain. These simulation results suggest that the proposed UWB LNA design is well suited for broadband and UWB receiver applications that require minimized power consumption. mw

ACKNOWLEDGMENT

The authors would like to thank the Open Fund Project of Hunan University's Key Laboratory (Project No.12K012).

REFERENCES

1. Fei-hua Chen, Shui-yang Lin, Ling-yun Li, and Xiao-Wei Sun, "4.2-4.8 GHz CMOS Variable Gain LNA for Chinese UWB Application," International Conference on Microwave and Millimeter Wave Technology, 2010, pp.1922-1924.
2. Ro-Min Weng, Chun-Yu Liu, and Po-Cheng Lin, "A Low-Power Full-Band Low-Noise Amplifier for Ultra-Wideband Receivers," IEEE Transactions on Microwave Theory and Techniques, 2010, pp. 2077-2083.
3. Chen-Ming Li, Ming-Tsung Li, Kuang-Chi He, and Jenn-Hwan Tarng, "A Low-Power Self-Forward-Body-Bias CMOS LNA for 3–6.5-GHz UWB Receivers," IEEE Microwave and Wireless Components Letters, 2010, pp. 100-102.
4. Alireza Dehqan, Ehsan Kargaran, Khalil Mafinezhad, and Hooman Nabovati, "An Ultra Low Voltage Ultra Low Power CMOS UWB LNA Using Forward Body Biasing," IEEE International Midwest Symposium on Circuits and Systems, 2012, pp. 266-269.
5. Giuseppina Sapone and Giuseppe Palmisano, "A 3–10-GHz Low-Power CMOS Low-Noise Amplifier for Ultra-Wideband Communication," IEEE Transactions on Microwave Theory and Techniques, 2011, pp. 678-686.
6. Yanjie Wang and K. Iniewski, "A Low Power CMOS Low Noise Amplifier for 3-l0 GHz Ultra-wideband Wireless Receivers," IEEE International Midwest Symposium on Circuits and Systems, 2006, pp. 353-357.
7. Liu Jinhua, Chen Guican, and Zhang Hong, "A 3-5-GHz gm-Boosted Common-Gate CMOS UWB LNA with a Common-Source Auxiliary Circuit," International Conference on Microwave and Millimeter Wave Technology (ICMMT), 2008, pp. 1342-1345.
8. Bo-Yang Chang and C. F. Jou, "Design of a 3.1-10.6-GHz Low-Voltage, Low-Power CMOS Low-Noise Amplifier for Ultra-wideband Receivers," Asia-Microwave Conference Proceedings, 2005.
9. Zhe-Yang Huang, Che-Cheng Huang, Chun-Chieh Chen, and Chung-Chih Hung, "A 1-V, 2.39-mW Capacitor-coupling Resonated Low Noise Amplifier for 3-5-GHz Ultra-Wideband System," IEEE International SOC Conference, 2007, pp. 101-104.
10. Yueh-Hua Yu, Emery Chen, and Deukhyoun Heo, "A 0.6-V Low Power UWB CMOS LNA," IEEE Microwave and Wireless Components Letters, 2007, pp. 299-231.
11. Brian M. Ballweber, Ravi Gupta, and David J. Allstot, "A Fully Integrated 0.5–5.5-GHz CMOS Distributed Amplifier," IEEE Journal of Solid-State Circuits, 2000, pp. 231-239.
12. Yueh-Hua Yu, Yi-Jan Emery Chen, and Deukhyoun Heo, "An Ultra-low Voltage UWB CMOS Low Noise Amplifier," Asia-Pacific Microwave Conference, Yokohama, Japan, 2006, pp.313-316,2006.
13. Zhe-Yang Huang, Che-Cheng Huang, and Chun-Chieh Chen, "A CMOS Low-Noise Amplifier with Impedance Feedback for Ultra-Wideband Wireless Receiver System," IEEE International Symposium on VLSI Design, Automation, and Test, 2008, pp. 51-54.
14. A. Djugova, J. Radic, and M. Videnovic-Misic, "A 0.18-{LC MU}m CMOS Low Power LNA for 6–8.5 GHz UWB Receivers," International Semiconductor Conference, 2011, pp. 215-218.
15. Chang-Wan Kim, Min-Suk Kang, and Phan Tuan Anh, "An Ultra-Wideband CMOS Low Noise Amplifier for 3–5-GHz UWB System," IEEE Journal of Solid-State Circuits, 2005, pp. 544-547.
16. Yi-Jing Lin, S.S. H. Hsu, Jun-De Jin, and C.Y. Chan, "A 3.1–10.6 GHz Ultra-Wideband CMOS Low Noise Amplifier With Current-Reused Technique," IEEE Microwave and Wireless Components Letters, 2007, pp. 232-234.
17. Youngsung Lee, Nackgyun Seong, Y. Jang, and Jaehoon Choi, "Design of Folded-cascode UWB Low Noise Amplifier with Low Power Consumption," International Conference on Advanced Communication Technology, 2011, pp. 214-217.
18. Pang-Hsing Chen and Jeng-Rern Yang, "A 3-10 GHz Low Power Ultra-Wideband CMOS LNA," IEEE International RF and Microwave Conference, 2011, pp. 356-358.
19. H.L. Kao, Albert Chin, K.C. Chang, and S.P. McAlister, "A Low-Power Current-Reuse LNA for Ultra-Wideband Wireless Receivers from 3.1 to 10.6 GHz," Topical Meeting on Silicon Monolithic Integrated Circuits in RF Systems, 2007, pp. 257-260.
20. Zhang Heng, Fan Xiaohua, and E. S. Sinencio, "A Low-Power, Linearized, Ultra-Wideband LNA Design Technique," IEEE Journal of Solid-State Circuits, 2009, pp. 320-330.
21. J.-Y. Lee, H.-K. Park, H.-J. Chang, and T.-Y. Yun, "Low-power UWB LNA with common-gate and current-reuse techniques," IET Microwaves, Antennas & Propagation, 2011, pp. 793-799.
22. Yu Wu Chung, Yi-Kai Lo, and Min-Chiao Chen, "A 3–10 GHz CMOS UWB Low-Noise Amplifier With ESD Protection Circuits," IEEE Microwave and Wireless Components Letters, 2009, pp. 737-739.
23. Jeffrey S. Walling, Sudip Shekhar, and David J. Allstot, "A gm-Boosted Current-Reuse LNA in 0.18-µm CMOS," IEEE Radio Frequency Integrated Circuits (RFIC) Symposium, 2007, pp. 613-616.
24. H.-H. Hsieh, J.-H. Wang, and L.-H. Lu, "Gain-Enhancement Techniques for CMOS Folded Cascode LNAs at Low-Voltage Operations," IEEE Transactions on Microwave Theory and Techniques, 2008, pp.1807-1816.
25. W. Zhuo, X. Li, S. Shekhar, and S. H. K. Embabi, "A Capacitor Cross-Coupled Common-Gate Low-Noise Amplifier," IEEE Transactions on Circuits and Systems II: Express Briefs, 2005, pp. 875-879.
26. Li Xiaoyong, S. Shekhar, and D.J. Allstot, "Low-Power gm-boosted LNA and VCO Circuits in 0.18-µm CMOS," 2005 IEEE International Solid-State Circuits Conference (ISSCC) digest, 2005, pp. 534-615.
27. T.K.K. Tsang, Lin Kuan-Yu, and M. N. El-Gamal, "Design Techniques of CMOS Ultra-Wide-Band Amplifiers for Multistandard Communications," IEEE Transactions on Circuits and Systems II: Express Briefs, 2008, pp. 241-218.
28. Peng Wang; F. Jonsson, and Zheng Li-Rong, "A Novel Low-power Fully-differential Current-reuse Cascaded CG-CS-LNA for 6-9-GHz UWB Receivers," 17th IEEE International Conference on Electronics, Circuits, and Systems (ICECS 2010), December 12-15, 2010, Athens, Greece, pp.1188-1191.
29. Meng-Ting Hsu and Kun-Long Wu, "Design of UWB Low Power Low Noise Amplifier with Body Bias Technique," Proceedings of the 2011 Asia-Pacific Microwave Conference (APMC 2011), Melbourne, Australia, pp. 227-230.

WU GUO-AN | Professor ZHANG BI-XIA | Master's Degree Candidate XU QIN-FEN | Lecturer LI WEN-GUANG | Lecturer
Institute of Microwave Technology Application, Huazhong University of Science and Technology, Wuhan, 430074, People's Republic of China

Bandpass Filter Passes 2.4- and 5.2-GHz Bands

This bandpass filter design employs an aperture-backed compensation technique, along with numerous enhancements to screen the two key wireless bands at 2.4 and 5.2 GHz.

As communications systems have spread, dual-band filters become ever-more essential components in RF front-end modules for sorting and screening signals in different frequency bands. A great deal of research has been conducted on different methods for realizing such filters.[1-5] In one approach,[2] two homocentric microstrip perturbed ring resonators were fabricated on the same layer to obtain dual-mode dual-band filter responses. The resonators were fed by coplanar waveguide (CPW), resulting in a wide range of external quality factors (Qs).

In another approach,[3] two homocentric embedded defected-ground-waveguide (DGW) resonators were adopted for a dual-band filter design, each fed by a 50-Ω microstrip line. In another work,[4,5] a dual-band bandpass filter (BPF) with meander-loop resonator and complementary split-ring resonator defected ground structure (SRR DGS) was proposed. Finally, an aperture compensation technique was proposed for enhancing the coupling in the parallel-coupled microstrip lines employed in these filters,[6] although there's little research on combining dual-band filter designs with the aperture compensation technique.

For improved performance in dual-band communications applications, a dual-band BPF was developed. It features a dual-mode resonator and SRR DGS excited with common improved input/output (I/O) coupling structure using an aperture compensation technique. The improved I/O structure is designed to provide greater coupling than traditional coupling structures without adding size. The performance of the improved coupling structure was confirmed by means of two-port equivalent-circuit analysis. The coupling structure and filter achieves high selectivity through the use of several finite attenuation poles within the stopbands.

This new design approach also offers a great deal of flexibility in the manner of independently controllable center frequencies

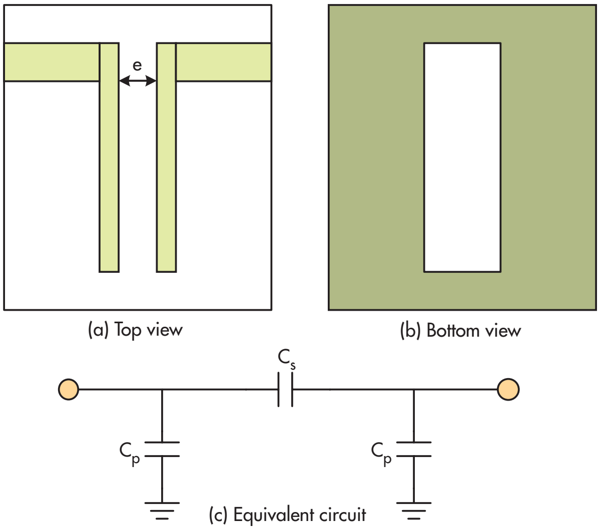

1. An improved input/output coupling structure was developed for the dual-band filter: (a) top view, (b) bottom view, and (c) equivalent circuit.

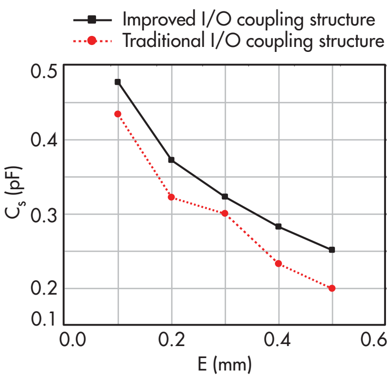

2. These simulations were performed for capacitance C_S in the coupling structure.

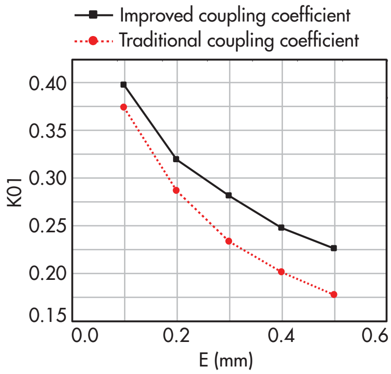

3. These simulations were performed for coupling coefficient K01 in the coupling structure.

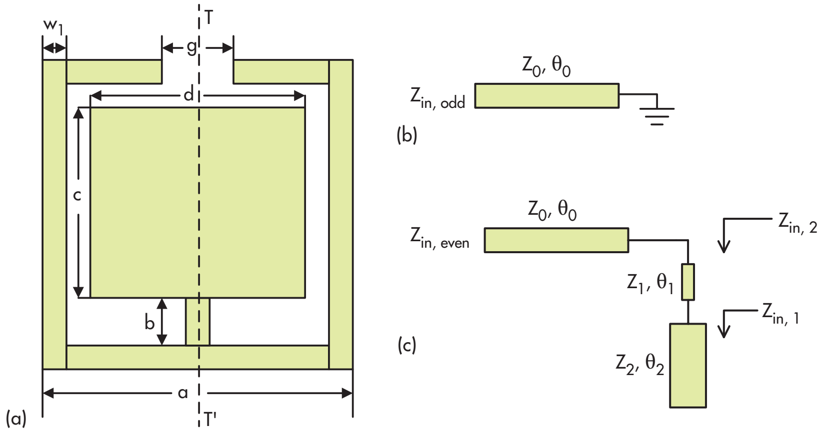

4. These diagrams show (a) the structure of the dual-mode resonator, along with (b) its odd-mode equivalent circuit and (c) its even-mode equivalent circuit.

within the passbands and bandwidths that can be tuned over a wide range. The filter structure is relatively simple and compact. The design approach was applied to the development of a dual-band filter for use at the wireless-local-area-network (WLAN) frequency bands of 2.4 and 5.2 GHz.

The new filter approach includes an improved I/O structure that employs an aperture compensation technique. *Figure 1(a)* shows a traditional I/O coupling structure with complete ground plane, while *Fig. 1(b)* offers the improved coupling structure with defected ground plane. Both can be equivalent to the structure shown in *Fig. 1(c)*. Equation 1 details the transfer function of the two-port network:

$$H(s) = (1/sC_{p2})/[1/sC_s + 1/ sC_{p1}] = C_s/(C_{p2} + C_s) \quad (1)$$

where it can be seen that the amplitude of H(s) is proportional to capacitance C_s. As the amplitude of H(s) is increased, the energy transferred between the two ports increases, which also means an increase in the coupling coefficient. The value of C_s changes according to the change of distance e *(Fig. 2)*. *Figure 2* indicates that an improved structure can provide greater coupling than conventional coupling structures. As evidence of this, *Fig. 3* shows simulated results of an improved input/output (I/O) coupling coefficient in comparison with a traditional I/O coupling coefficient. As seen in *Fig. 3*, it is possible to achieve stronger coupling with an improved structure in the same physical size as a conventional coupling structure.

The improved dual-mode resonator structure is shown in *Fig. 4(a)*. The dual-mode characteristics are realized by loading a stepped-impedance-line stub at the center of the open-loop resonator. Due to the fact that the resonator is symmetrical to the T-T′ plane, the odd- and even-mode method can be applied to analyze it. The equivalent circuit of *Fig. 4(b)* is able to be applied for analysis of the odd-mode excitation. Subsequently, the one-port input impedance of

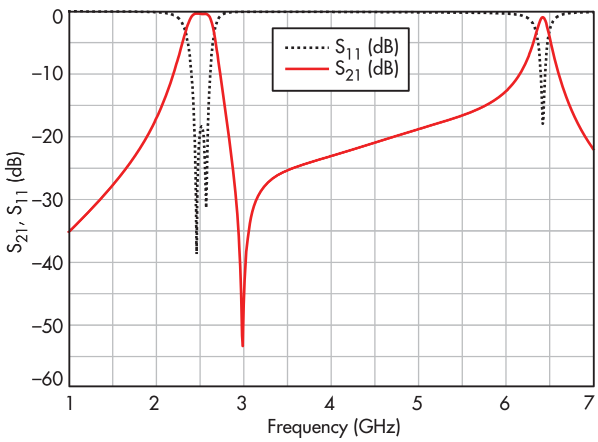

5. The plots show the responses of the filter with the dual-mode microstrip open-loop resonator.

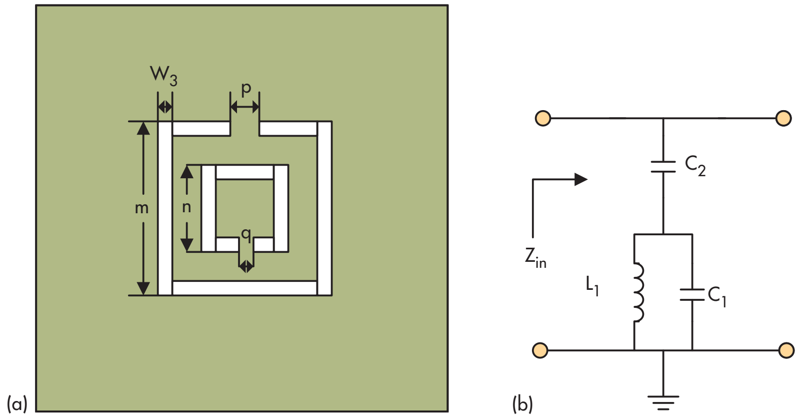

6. This is (a) the layout and (b) the equivalent circuit of the SRR DGS resonator used in the dual-band filter.

that equivalent circuit can be found with the help of Eq. 2:

$$Z_{in,odd} = jZ_0\tan\theta_0 \quad (2)$$

From the resonant condition that $Y_{in,odd} = 0$, the first odd-mode resonant frequency can be determined via Eq. 3:

$$f_{odd} = c/[4(2a - g/2)(\varepsilon_{eff})^{0.5})] \quad (3)$$

where:
c = the speed of light in free space, and
ε_{eff} = the effective dielectric constant of the substrate material.

For an even-mode excitation, the equivalent circuit of *Fig. 4(c)* should be applied. Its one-port input impedance can be found by means of Eqs. 4-6:

$$Z_{in1} = -j(1/ Z_2\tan\theta_2) \quad (4)$$

$$Z_{in2} = Z_1[(Z_{in1} + jZ_1\tan\theta_1)/(Z_1 + jZ_{in1}\tan\theta_1)] \quad (5)$$

$$Z_{in,\,even} = Z_0[(Z_{in2} + jZ_0\tan\theta_0)/(Z_0 + jZ_{in2}\tan\theta_0)] \quad (6)$$

From the resonance condition that $Z_{in,even} = 0$, it is possible to achieve the equality of Eq. 7:

$$R_1R_2\tan\theta_0\tan\theta_1\tan\theta\}_2 - R_1\tan\theta_0 - \tan\theta_1 - R_2\tan\theta_2 = 0 \quad (7)$$

where:
$R_1 = Z_1/Z_0$ and $R_2 = Z_1Z_2$.

Under the special condition that $Z_0 = Z_1 = Z_2$, the first resonant frequency can be found by applying Eq. 8:

$$f_{even} = c/[2(2a - g/2 + b + c)(\varepsilon_{eff})^{0.5}] \quad (8)$$

Equations 3 and 8 show that changing the values of b and c only affects the even-mode resonant frequency, leaving the odd-mode resonant frequency unchanged. By adjusting the values of b and c, the even-mode resonant frequency can be tuned while also adjusting the center frequencies and bandwidths.

Figure 5 shows the frequency response of a filter fabricated with a dual-mode microstrip open-loop resonator and the proposed improved I/O coupling structure. A transmission zero can be found in the stopband close to 3 GHz and the spurious passband at 6.4 GHz. Examination of the filter revealed that any shifting of the transmission zero and spurious passband can be linked to the stepped-impedance-line stub at the center of the open-loop resonator.

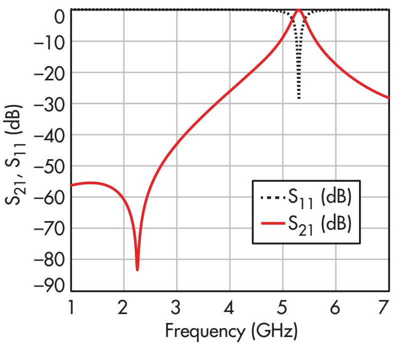

7. The plots show the forward and reverse return loss for the dual-band filter with SRR DGS resonator.

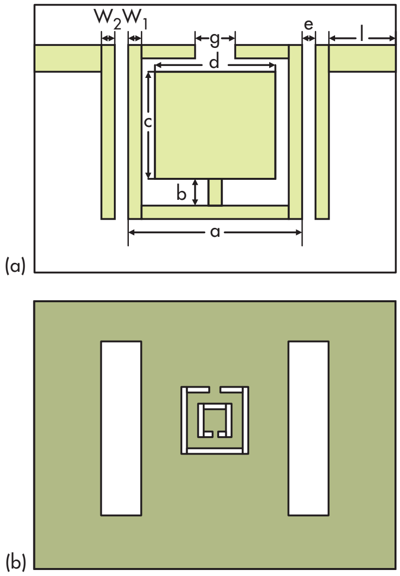

8. These layouts show the (a) top view and (b) bottom view of the dual-band filter.

Figure 6(a) shows the topology of the SRR DGS. From an equivalent circuit of the SRR DGS[7] shown in *Fig. 6(b)*, it is possible to find the location of the transmission zero for the SRR DGS cell according to the desired resonant frequency of the shunt circuit. This resonant frequency can be found using Eq. 9:

$$f_s = 1/2\pi[L_1(C_1 + C_2)]^{0.5}] \quad (9)$$

Figure 7 shows the S-parameter responses for the filter employing this SRR DGS resonator and its improved I/O coupling structure. By essentially combining two filters via a common, enhanced I/O coupling structure, the compact configuration of *Fig. 8* can be achieved. For the experimental dual-

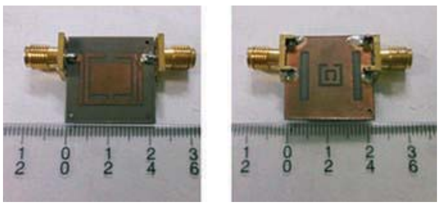

9. The photographs show the (a) top view and (b) bottom view of the fabricated filter.

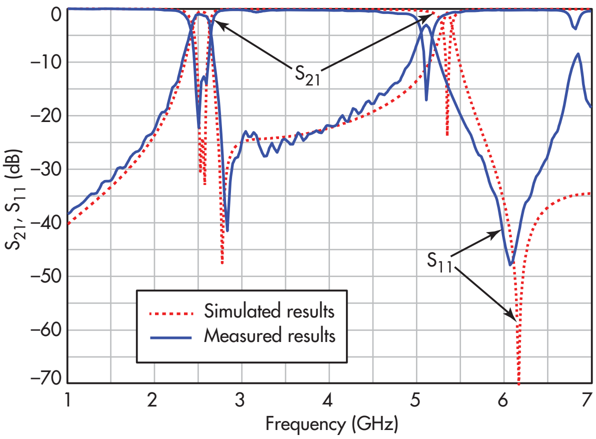

10. These plots compare the simulated and measured S-parameters for the proposed filter.

band BPF fabricated with this configuration, a circuit substrate with permittivity of 2.2 and thickness of 0.76 mm was used. Signals at different frequencies within a communications system may travel via different channels, but will pass through the common feed structure for the filter. The width of the filter's terminal microstrip line is 2.33 mm, so that it can be matched to 50-Ω systems. The filter measures around $0.22\lambda_g \times 0.22\lambda_g$, where λ_g is the guided wavelength at the center frequency of the lower passband.

Figure 9 is a photograph of the fabricated dual-band filter. Simulations and measurements were accomplished by means of the High Frequency Structure Simulation (HFSS 13.0) simulation software and model E5071C microwave vector network analyzer (VNA), respectively, both from Agilent Technologies (now Keysight Technologies).

Figure 10 presents simulated and measured results for the proposed filter. The two filter passbands are centered at 2.53 and 5.11 GHz, with minimum insertion losses of 1.1 and 3.0 dB, respectively, for the two passbands. The return losses within the two passbands were better than 14 dB. Two attenuation poles were realized for the dual-band BPF structure, at 2.83 and 6.08 GHz, which helped to greatly improve the selectivity of the proposed dual-band BPF. As can be seen from the plots, the measured results mainly agree with the simulated performance values. Discrepancies between the measured and simulated performance levels can be attributed to fabrication tolerances in realizing the dual-band filter on commercial microwave circuit substrate material. mw

REFERENCES

1. Jin Xu, Wen Wu, and Chen Miao, "Compact and Sharp Skirts Microstrip Dual-Mode Dual-Band Bandpass Filter Using a Single Quadruple-Mode Resonator (QMR)," IEEE Transactions on Microwave Theory & Techniques, Vol. 61, No. 3, March 2013, pp. 1104-1113.
2. Xiu Yin Zhang and Quan Xue, "Novel Dual-Mode Dual-Band Filters Using Coplanar-Waveguide-Fed Ring Resonators," IEEE Transactions on Microwave Theory & Techniques, Vol. 55, No. 10, October 2007, pp. 2183-2190.
3. H.W. Liu, L. Shen, Z.C. Zhang, J.S. Lim, and D. Ahn, "Dual-Mode Dual-Band Bandpass Filter Using Defected Ground Waveguide," Electronics Letters, Vol. 46, 2010, pp. 895-897.
4. G.-L. Wu, W. Mu, X.-W. Dai, and Y.-C. Jiao, "Design of Novel Dual-Band Bandpass Filter with Microstrip Meander-Loop Resonator and CSRR DGS," Progress in Electromagnetic Research, Vol. 78, 2008, pp. 17-24.
5. Jahyeon Lee and Yeongseog Lim, "A Dual-Band Bandpass Filter Using Capacitively I/O Coupling," Microwave & Optical Technology Letters, Vol. 55, 2013, pp.1823-1825.
6. Lei Zhu, Huizheng Bu, and Ke Wu, "Aperture Compensation Technique For Innovative Design Of Ultra-Broadband Microstrip Bandpass Filter," in IEEE MTT-S International Microwave Symposium Digest, 2000, pp.315-318.
7. B. Wu, B. Li, T. Su, and C.-H. Liang, Equivalent-Circuit Analysis and Lowpass Filter Design of Split-Ring Resonator DGS, Journal of Electromagnetic Waves and Applications, Vol. 20, 2006, pp. 1943-1953.

Amazingly Low Phase Noise

SAW VCO's

Features:

| Very Low Post Thermal Drift

| Small Size 0.5" x 0.5"

Note: * (0.75" x 0.75" models)

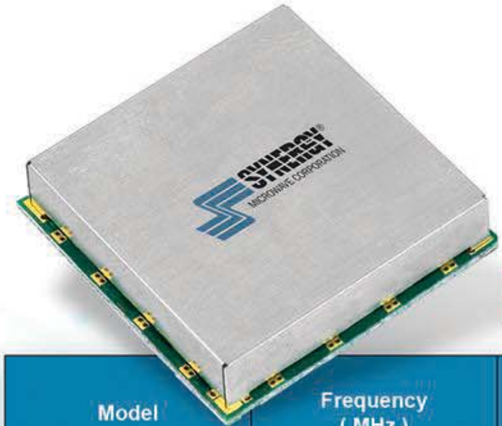

RoHS REL-PRO®
Patented Technology

Model	Frequency (MHz)	Tuning Voltage (VDC)	DC Bias VDC @ I [Max.]	Phase Noise @ 10 kHz (dBc/Hz) [Typ.]
HFSO800-5	800	1 - 12	+5 @ 20	-146
HFSO800-5H	800	1 - 12	+5 @ 20	-150
HFSO800-5L	800	1 - 12	+5 @ 20	-142
HFSO1000-5	1000	1 - 12	+5 @ 35	-141
HFSO1000-5L	1000	1 - 12	+5 @ 35	-137
HFSO1600-5	1600	1 - 12	+5 @ 100	-137
HFSO1600-5L	1600	1 - 12	+5 @ 100	-133
HFSO2000-5 *	2000	1 - 12	+5 @ 100	-137
HFSO2000-5L *	2000	1 - 12	+5 @ 100	-133

Talk To Us About Your Custom Requirements.

SYNERGY®
MICROWAVE CORPORATION

Phone: (973) 881-8800 | Fax: (973) 881-8361
E-mail: sales@synergymwave.com
Web: WWW.SYNERGYMWAVE.COM
Mail: 201 McLean Boulevard, Paterson, NJ 07504

SHAOJIANG LIN | Professor QINIAN SHI | Professor
School of Mechanical and Electrical Engineering, Hubei Polytechnic University, Huangshi 435003, People's Republic of China, e-mail: 1527762155@qq.com

CCCDTAs Form Flexible Biquad Filter

Through the use of current-controlled, current-differencing transconductance amplifiers (CCCDTAs) and a pair of capacitors, this resistorless universal biquad filter can achieve all basic filtering functions.

Filters have long been instrumental in cleaning and sorting signals. Likewise, the concept of a "universal" filter has long intrigued designers in search of flexible signal-processing solutions. In quest of that universal filter, which is a circuit that can realize all basic filtering functions, a transadmittance-mode (TA-M) universal biquad filter has been developed based on current-controlled, current-differencing transconductance amplifiers (CCCDTAs).

In a configuration with two CCCDTAs, two capacitors, and no resistors, this filter can realize all standard filtering functions. Among these are lowpass-filter (LPF), highpass-filter (HPF), bandpass-filter (BPF), bandstop-filter (BSF), and even all-pass filter (APF) responses using the same circuit structure. The design also offers great convenience, via electronic tuning of center frequency, quality factor (Q), and bandwidth. The TA gains of LPF, BPF, and HPF functions can be independently and electronically adjusted by means of bias currents to the CCDTAs. Since the CCCDTAs exhibit high input and output impedances, this flexible filter does not require impedance matching when cascaded with other circuits.

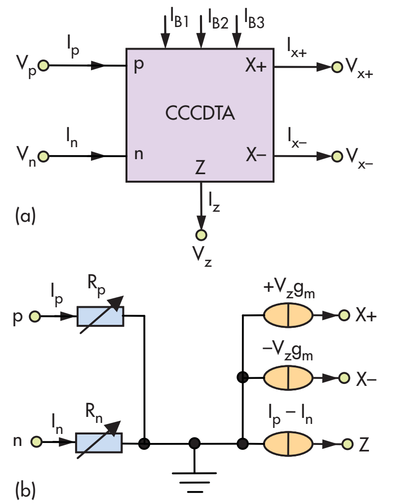

1. A current-controlled, current-differencing transconductance amplifier (CCCDTA) is represented by (a) this symbol and (b) this equivalent circuit.

Analog filters have long been essential building blocks for electronic design.[1,2] In recent years, a variety of current-mode (CM) and voltage-mode (VM) filter circuits have been developed with active devices, such as operational transconductance amplifiers (OTAs), current conveyors (CCs), and current differencing transconductance amplifiers (CDTAs). In many electronic systems, the use of voltage-to-current interface circuits is essential, since CM and VM circuits in these systems must be connected. In the process of making these voltage-to-current interfaces, it is also possible to realize signal processing, such as filtering, and the TA-M filter is a tremendous boost for these situations.[3]

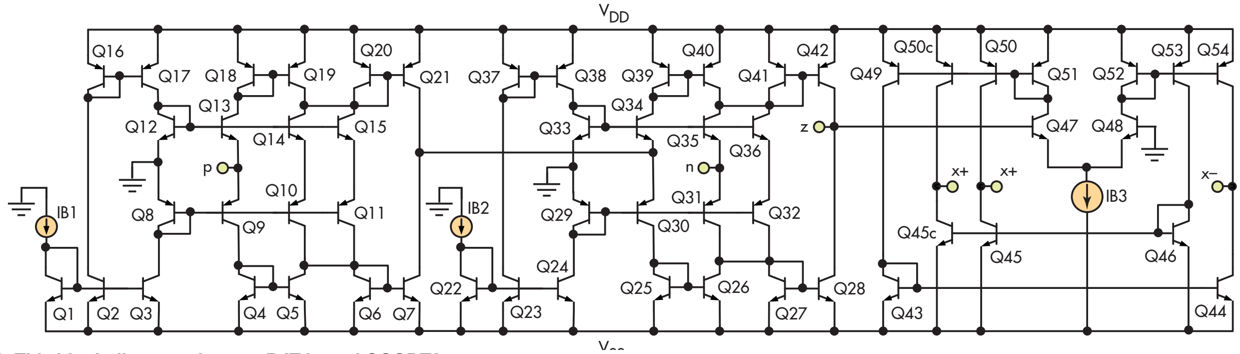

2. This block diagram shows a BJT-based CCCDTA.

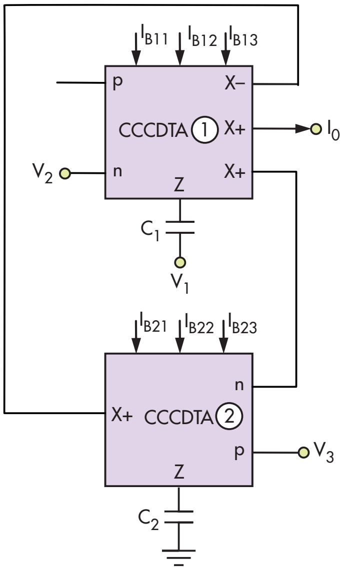

3. This block diagram shows a CCCDTA-based TA-M universal filter.

A number of TA-M filter studies have been published.[3-14] Unfortunately, all of these design efforts suffer from various shortcomings. Since a novel active-element design was first reported as a CCCDTA,[15] a wide range of CCCDTA-based applications have been realized.[15-24] The present design offers simplicity, electronic tenability, and high output impedance for versatility. Its parasitic resistance at two current input ports can be controlled by input bias current. As a result, in some circuit designs, there is no need for additional resistors to create an integrator circuit.

By exploring the capabilities of these CCCDTA designs, it was possible to create a novel TA-M universal biquad filter using CCCDTAs. The proposed circuit employs two CCCDTAs and two capacitors, one of which is permanently grounded. The circuit topology is suitable for integrated-circuit (IC) fabrication. With its three voltage input terminals and single current output terminal, the circuit can realize all standard filtering functions. Key parameters can be controlled by adjusting different bias currents for the CCCDTA.

The new CCCDTA design has been simulated with commercial software, and the simulations agree closely with theoretical analysis of the design. The *table* presents a comparison of the new design with previously published TA-M filters. This new design approach reduces the number of active and passive circuit elements required and overcomes some of the limitations of the earlier designs.

In general, a CCDTA can be represented by the diagram of *Fig. 1(a)* and the equivalent circuit of *Fig. 1(b)*. The matrix of Eq. 1 portrays the CCCDTA's terminal relationships:

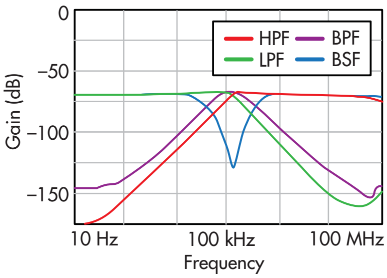

4. These gain-frequency curves represent TA-M LPF, BPF, and BSF responses.

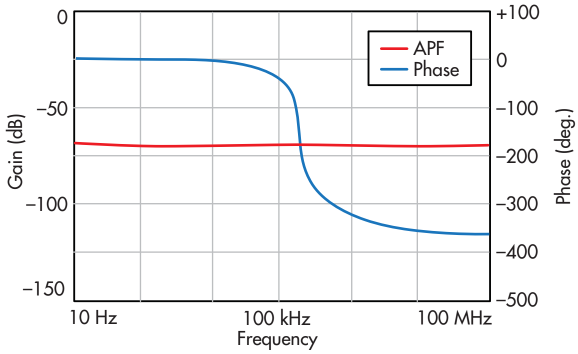

5. This plot shows the gain-phase simulation for a TA-M APF response.

THE COMPARISON RESULTS OF VARIOUS TA-M FILTERS

Topology	Number of active elements	Number of resistors	b	c	d	e	f
[3](CCII)	3	3	Yes	Yes	Yes	Yes	No
[5](CCIII)	3	0	No	Yes	Yes	Yes	No
[6](CCCII)	3	0	No	Yes	Yes	No	No
[7](PFTFN)	3	3	Yes	Yes	Yes	No	Yes
[8](CDTA)	2	2	No	No	Yes	Yes	No
[10](OTA)	4	0	Yes	No	Yes	No	No
[11](OTA)	7	0	No	No	Yes	No	No
[13](DVCC)	5	1	Yes	Yes	Yes	Yes	Yes
[14](VDTA)	2	0	No	No	Yes	Yes	No
Proposed (CCCDTA)	2	0	No	No	No	No	No

$$\begin{bmatrix} V_p \\ V_n \\ I_z \\ I_{x\pm} \end{bmatrix} = \begin{bmatrix} R_p & 0 & 0 & 0 \\ 0 & R_n & 0 & 0 \\ 1 & -1 & 0 & 0 \\ 0 & 0 & 0 & \pm g_m \end{bmatrix} \begin{bmatrix} I_p \\ I_n \\ V_x \\ V_z \end{bmatrix} \quad (1)$$

where:

p and n = positive and negative current input terminals with finite resistances R_p and R_n, respectively, at those terminals;

z and x = current output terminals, which have high output impedance;

g_m = the transconductance gain, which can be tuned by using the external bias current of the CCCDTA;

V_Z = the voltage drop at terminal Z, which is turned into a current output by means of a transconductance stage.

Figure 2 presents a realization of a proposed CCCDTA universal filter.[24] The circuit is comprised of a current-controlled current differencer and a multiple-output operational transconductance amplifier (MO-OTA). The current-controlled current differencer consists of bipolar transistors Q_1 through Q_{42}. Bipolar transistors Q_{43} through Q_{54} form an MO-OTA, which

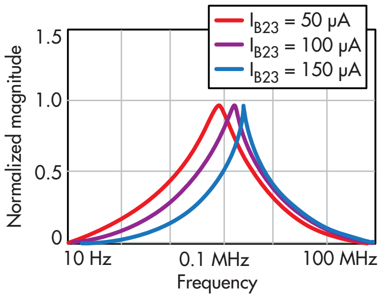

6. These plots show TA-M BPF responses for different values of I_{B23}.

is composed of transconductance circuits and multiple-output current mirror circuits. The transconductance gain and input resistance at two current input terminals (the p and n ports) can be directly controlled by the diverse bias currents of the CCCDTA, allowing for flexibility and versatility in many different applications.

In this CCCDTA design, resistances R_p and R_n and transconductance g_m can be expressed by means of Eqs. 2-4:

$$R_P = \frac{V_T}{2I_{B1}} \tag{2}$$

$$R_n = \frac{V_T}{2I_{B2}} \tag{3}$$

$$g_m = \frac{I_{B3}}{2V_T} \tag{4}$$

where:
V_T = the thermal voltage, and
I_{B1}, I_{B2}, and I_{B3} = the bias currents of the CCCDTA.

Figure 3 shows a circuit diagram of the designed transadmittance filter. From the diagram, it can be seen that a TA-M universal filter is relatively easy to realize by adopting minimum active and passive elements for the design. With its resistorless configuration, the filter design is also quite suitable for monolithic integration. Using Eqs. 1-4, the characteristic equations of *Fig. 3* are:

$$I_{out} = g_{m1}\frac{s^2V_1 - sV_2/C_1R_{1n} + V_3g_{m2}/C_1C_2R_{2p}}{\Delta(s)} \tag{5}$$

$$\Delta(s) = s^2 + sg_{m1}/C_1 + g_{m1}g_{m2}/C_1C_2 \tag{6}$$

where:
R_{in} = the finite negative input resistance of the CCCDTA, and
R_{ip} = the finite positive input resistance of the CCCDTA.

Through analysis of *Fig. 3* and Eqs. 5 and 6, the five current-transfer functions for the LPF, BPF, HPF, BSF, and APF responses can be obtained in the following ways. The LPF response can be achieved by means of Eq. 7 when $V_3 = V_{in}$ and $V_1 = V_2 = 0$:

$$T_{LP}(s) = \frac{I_o(s)}{V_{in}(s)} = \frac{g_{m1}g_{m2}/C_1C_2R_{2p}}{\Delta(s)} \tag{7}$$

The BPF response can be achieved by means of Eq. 8 when $V_2 = V_{in}$ and $V_1 = V_3 = 0$:

$$T_{BP}(s) = \frac{I_o(s)}{V_{in}(s)} = -\frac{sg_{m1}/C_1R_{1n}}{\Delta(s)} \tag{8}$$

The HPF function can be achieved with the aid of Eq. 9, when $V_1 = V_{in}$ and $V_2 = V_3 = 0$:

$$T_{HP}(s) = \frac{I_o(s)}{V_{in}(s)} = \frac{s^2g_{m1}}{\Delta(s)} \tag{9}$$

The BSF response can be gained with the help of Eq. 10 and when $I_{B12} = I_{B13}$ and $V_1 = V_3 = V_{in}$:

$$T_{BS}(s) = \frac{I_o(s)}{V_{in}(s)} = \frac{g_{m1}\left(s^2 + g_{m2}/C_1C_2R_{2p}\right)}{\Delta(s)} \tag{10}$$

The APF response can be achieved with the help of Eq. 11 and when $I_{B12} = I_{B13} = I_{B21}$ and $V_1 = V_2 = V_3 = V_{in}$:

$$T_{AS}(s) = \frac{I_o(s)}{V_{in}(s)} = \frac{g_{m1}\left(s^2 - 1/C_1R_{1n} + g_{m2}/C_1C_2R_{2p}\right)}{\Delta(s)} \tag{11}$$

From Eqs. 7-11, it is evident that Fig. 3 provides second-order LPF, BPF, HPF, BSF, and APF responses from the same circuit design through the selection of different input signals. It is also

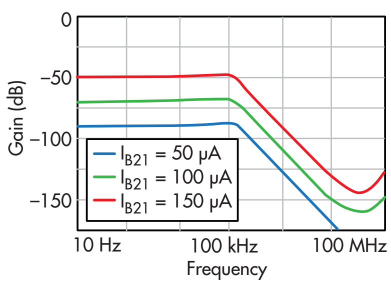

7. These plots show TA-M LPF responses for different values of I_{B21}.

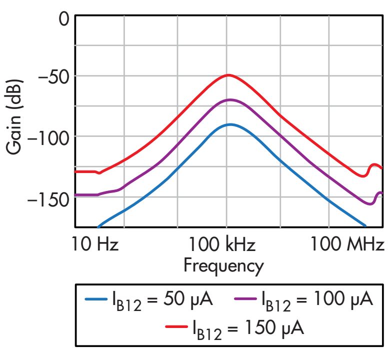

8. These plots show TA-M BPF responses for different values of I_{B12}.

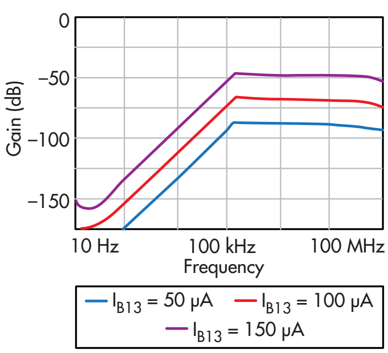

9. These plots show TA-M HPF responses for different values of I_{B13}.

Turn Smart Power Sensors into Low-Cost RF Power Meters!

USB & Ethernet POWER SENSORS from $695 ea. qty. (1-4)

Mini-Circuits' RF power sensors turn almost any Windows® or Linux® based computer into a low-cost testing platform for all kinds of RF components and applications. To give you even more options, our new PWR-8GHS-RC model allows easy remote signal monitoring and data acquisition with USB and Ethernet control.

With 7 different models in stock offering measurement speeds as fast as 10 ms*, dynamic range as wide as -35 to +20 dBm†, and measurement capability for continuous wave and modulated signals, chances are, we have a power sensor to meet your needs and fit your budget!

Our user-friendly GUI provides a full range of measurement tools including measurement averaging, time-scheduled measurements, multi-sensor support, and measurement applications supporting RF testing of couplers, filters, amplifiers and more! View data and graphs on-screen or export to Excel® for reporting and data analysis.

All Mini-Circuits power sensors fit in your pocket and come supplied with all the accessories you need for immediate use right out of the box. Visit minicircuits.com and place your order today for delivery as soon as tomorrow!

RoHS compliant

Model	Power Measurement	Frequency MHz	Control Interface	Price $ ea. (Qty 1-4)
PWR-2.5GHS-75 (75Ω)	Peak	0.1 to 2500	USB	795.00
PWR-4GHS	Peak	0.009 to 4000	USB	795.00
PWR-6GHS	Peak	1 to 6000	USB	695.00
PWR-8GHS	Peak	1 to 8000	USB	869.00
NEW! PWR-8GHS-RC	Peak	1 to 8000	USB & Ethernet	969.00
PWR-8FS	Peak	1 to 8000	USB	969.00
PWR-4RMS	Average	50 to 4000	USB	1169.00

**Measurement speed as fast as 10 ms for model PWR-8-FS. All other models as fast as 30 ms.*

†Dynamic range as wide as -35 to +20 dBm for model PWR-4RMS. All other models as wide as -30 to +20 dBm.

Excel is a registered trademark of Microsoft Corporation in the US and other countries.

Neither Mini-Circuits nor Mini-Circuits Power Sensors are affiliated with or endorsed by the owners of the above-referenced trademarks.

Mini-Circuits®

www.minicircuits.com P.O. Box 350166, Brooklyn, NY 11235-0003 (718) 934-4500 sales@minicircuits.com

532 rev A

apparent that there is no need for an external inverter and a matching element to realize BS and AP filters. The parameters of ω_0, Q, and ω_0/Q (bandwidth) for the proposed filter can be found from Eqs. 12-14:

$$\omega_o = \sqrt{\frac{g_{m1}g_{m2}}{C_1C_2}} = \frac{1}{2V_T}\sqrt{\frac{I_{B13}I_{B23}}{C_1C_2}} \quad (12)$$

$$Q = \sqrt{\frac{g_{m2}C_1}{g_{m1}C_2}} = \sqrt{\frac{I_{B23}C_1}{I_{B13}C_2}} \quad (13)$$

$$BW = \frac{\omega_o}{Q} = \frac{g_{m1}}{C_1} = \frac{I_{B13}}{2C_1V_T} \quad (14)$$

It is clear that all of the characteristic parameters of this filter can be electronically tuned by CCCDTA bias currents. Also, ω_0 and Q can be adjusted electronically and independently by means of I_{B23} without obstructing the value of ω_0/Q.

By using Eqs. 7-9, the transadmittance gain of the LPF, BPF, and HPF responses can be calculated by means of Eqs. 15, 16, and 17, respectively:

$$G_{LP} = \frac{1}{R_{2p}} = \frac{2I_{B21}}{V_T} \quad (15)$$

$$G_{BP} = \frac{1}{R_{1n}} = \frac{2I_{B12}}{V_T} \quad (16)$$

$$G_{HP} = g_{m1} = \frac{I_{B13}}{2V_T} \quad (17)$$

From these three expressions, it is easy to see that the transadmittance gains of the LP, BP, and HP filter functions can be independently and electronically modified by adjusting the different bias currents: I_{B21}, I_{B12}, and I_{B13}. The lowpass and bandpass gains—G_{LP} and G_{BP}, respectively—can be independently transformed by means of bias currents I_{B21} and I_{B12}, respectively, without the poly-frequency and bandwidth of the particular filter response.

Considering the CCCDTA's nonideal characteristics, its port relationship in *Fig. 3* can be rewritten as Eq. 18:

$$i_z = \alpha_p i_p - \alpha_n i_n, i_{x\pm} = \pm\beta g_m v_z \quad (18)$$

where:

α_{pi} ($\alpha_{pi} = 1 - \varepsilon_{pi}$, $|\varepsilon_{pi}| << 1$) and α_{ni}($\alpha_{ni} = 1 - \varepsilon_{ni}$, $|\varepsilon_{ni}| << 1$)

are parasitic current gains between p → z and n → z terminals of the ith CCCDTA, respectively, and

β_i ($\beta_i = 1 - \varepsilon_i$, $|\varepsilon_i| << 1$)

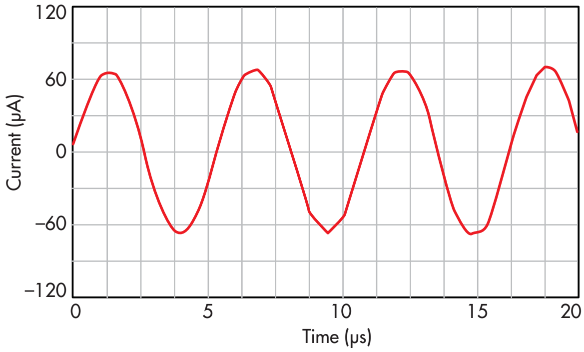

10. This is the TA-M APF response for a sinewave input signal.

is the parasitic transconductance tracking error from the z to the x terminals.

The circuit in *Fig. 3* was reanalyzed by using Eq. 18. The modified current transfer characteristic is approximated by Eq. 19:

$$\Delta(s) = s^2 + s\beta_1\alpha_{p1}g_{m1}/C_1 + \alpha_{p1}\alpha_{n2}\beta_1\beta_2 g_{m1}g_{m2}/C_1C_2 \quad (19)$$

From Eq. 19, the nonideal values of ω_0 and Q for the universal filter can be expressed by means of Eqs. 20 and 21, respectively:

$$\omega_o = \sqrt{\frac{\alpha_{p1}\alpha_{n2}\beta_1\beta_2 g_{m1}g_{m2}}{C_1C_2}} \quad (20)$$

$$Q = \sqrt{\frac{\alpha_{n1}g_{m2}C_1}{\alpha_{p1}\beta_1 g_{m1}C_2}} \quad (21)$$

The sensitivities of the active and passive components to ω_0 can be found by means of Eqs. 22 and 23:

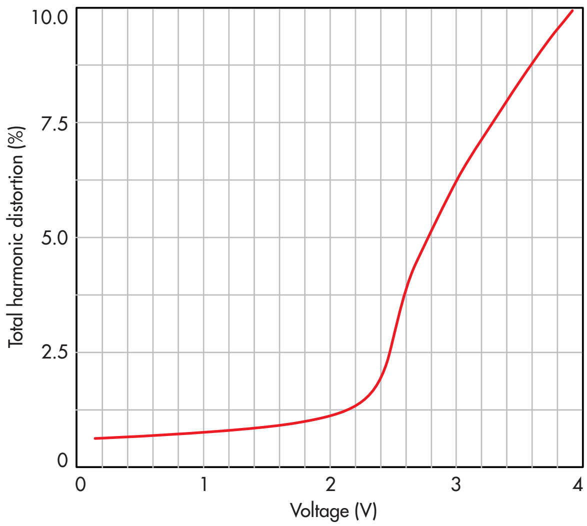

11. The linearity of the TA-M filter can be gauged by its low THD.

$$S^{\omega_o}_{\alpha_{p1},\alpha_{n2},\beta_1,\beta_2,g_{m1},g_{m2}} = 0.5,\quad S^{\omega_o}_{C_1,C_2} = -0.5 \qquad (22)$$

$$S^{Q}_{\alpha_{n1},g_{m2},C_1} = 0.5,\quad S^{Q}_{\alpha_{p1},\beta_1,g_{m1},C_2} = -0.5 \qquad (23)$$

It can be noted from Eqs. 22 and 23 that all sensitivities of the passive and active elements of the proposed TA-M filter do not exceed 50% in magnitude.

It was possible to simulate a TA-M filter as portrayed in *Fig. 3* by using the CCCDTA in *Fig. 2* simulated with the parameters of the PR200N and NR200N bipolar transistors of the ALA400 transistor array from AT&T in a PSPICE simulator.[25] The power supplies were set as $V_{DD} = -V_{SS} = 1.5$ V.

The universal filter was designed using passive component values of $C_1 = C_2 = 1$ nF. Bias currents for the CCCDTAs were chosen as $I_{B11} = I_{B22} = 500$ µA (for $R_{1p} = R_{2n} = 20\ \Omega$); $I_{B12} = I_{B21} = 100$ µA; and $I_{B13} = I_{B23} = 100$ µA (for $g_m = 1.2$ mS). Using Eq. 12, a polyfrequency of 190 kHz was achieved through these values. By selecting different input signals, it was possible to achieve simulated responses for LPF, BPF, HPF, and BSF functions *(Fig. 4)*. *Figure 5* offers simulated responses for the gain and phase of the APF function.

From *Figs. 4 and 5*, it is apparent that the proposed TA-M filter circuit can realize LP, HP, BP, BS, and AP functions depending upon input signal selection, without modifying the basic circuit framework. By setting different I_{B23} values, the different BPF magnitude responses of *Fig. 6* can be achieved. It is clear that the polyfrequency and Q of the filter can be adjusted electronically. The electronic tuning of gain for LPF, BPF, and HPF responses are achieved by changing bias currents from 50 to 150 µA while maintaining $C_1 = C_2 = 1$ nF, as shown in *Figs. 7 through 9*.

To test the large-signal behavior of the TA-M filter, a sinusoidal input at 190 kHz and 0.5 V was applied to the APF function with the circuit elements as established previously. *Figure 10* shows the results of the output transient response, while the total harmonic distortion (THD) is presented in *Fig. 11*.

In short, this is a single circuit that can be electronically tuned for different filter responses, and it can realize all standard filtering functions. Being completely without resistors, it is well suited for IC fabrication. MW

Note: For references, see the online version of this article at www.mwrf.com.

ACKNOWLEDGMENTS

The authors would like to thank the reviewers for their valuable comments and helpful suggestions. This work is supported by the foundation of outstanding youth science and technology innovation team of the Hubei Polytechnic University (No. 13xtx02) and the project planning of young teachers in enterprises of the Hubei Province (No. XD2014681), both of the People's Republic of China (PRC).

CHIN LEONG LIM | Engineer
Avago Technologies, Penang, Malaysia; www.avagotech.com

This compact voltage variable PIN-diode-based attenuator provides a wide attenuation range with outstanding linearity, suiting it for wireless communications systems at 3.5 GHz.

VARIABLE Blends Dynamic

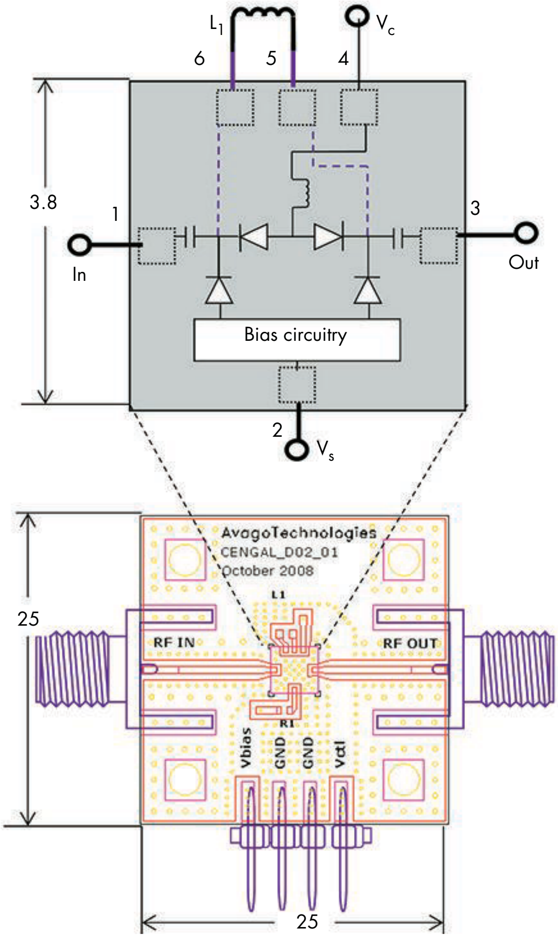

1. A 3.5-GHz attenuator capable of wide attenuation range and high linearity can be formed from one compact module and one external inductor.

Amplitude control is a critical function in many high-frequency communications and other systems, and often is handled by a voltage-variable attenuator (VVA). In wireless receivers and transmitters, for example, VVAs can provide automatic gain control. They also can help minimize amplifier gain variations with temperature and semiconductor process variations.[1] The π and bridge-T topologies are the most compact of the constant-impedance VVA configurations, since they are realized solely with lumped-element circuit components.[2,3]

The variable resistances of a VVA design can be approximated with either field-effect transistors (FETs) or positive-intrinsic-negative (PIN) diodes, although the latter will result in an attenuator with higher linearity.[4] While the basic π topology requires only three resistive elements, implementing this VVA with three diodes, as it was initially done, results in an asymmetrical circuit that is complicated to bias.[5,6] Consequently, a revision of the π VVA using four diodes has gained popularity because of its simpler biasing than the three-diode configuration.[7,8]

A π VVA has a limited frequency range that, according to some reports, reaches a maximum upper frequency limit of 1 GHz.[9] Its frequency response is bounded by the maximum attenuation degrading at 6 dB/octave due to signal leakage through the series diodes' parasitic elements. One way to circumvent this frequency ceiling is to apply parasitic cancellation on the affected diodes. Applying this technique to a π VVA fabricated with discrete compo-

ATTENUATOR

Range, Linearity

nents, it was possible to achieve about a 25-dB attenuation range at 3.8 GHz.[10]

However, the discrete implementation requires many components, and this consumes considerable space. To reduce the component count and size of the VVA from previous designs, the current work extends this technique to a standalone, highly integrated PIN-diode π VVA module. This report describes the design and characterization of a compact, high-performance 3.5-GHz VVA.

The heart of this attenuator design is a PIN diode VVA circuit in a multichip-on-board (MCOB) module.[11,12] Measuring $3.8 \times 3.8 \times 1\ mm^3$, the VVA is contained within a lead-less plastic package that integrates 13 passive devices and four diodes *(Fig. 1)*. Two voltage supplies are required to operate the VVA: a control-voltage (V_c at pin 4) variable over a range of 0 to +5 V dc and a +2.7-V dc reference voltage (V_s at pin 2). The control voltage is used to adjust the attenuation. The reference voltage, V_s, is used to control the current relationship between the series and the shunt arms. In this way, V_s is used to optimize the VVA's impedance matching over the attenuation range.

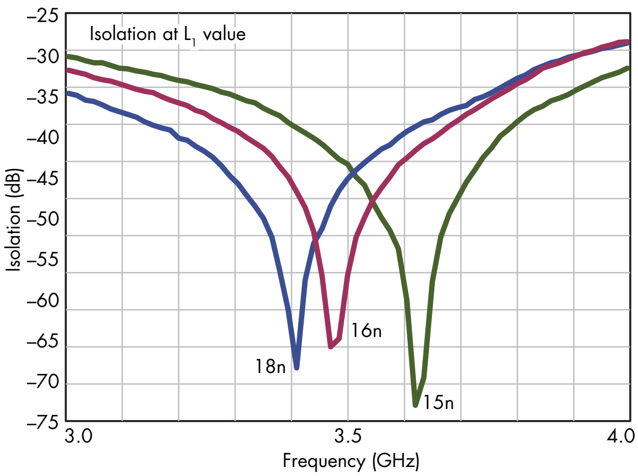

2. Of the three evaluated inductance values (15, 16, and 18 nH) from the Coilcraft 0603HP series, the 16-nH inductor positions the notch closest to the 3.5-GHz design target.

Without parasitic cancellation, the module's maximum attenuation is a modest 27 dB at 3.5 GHz. The module permits access to the series diodes through pins 5 and 6. Via these pins, an external inductor, L_1, can be connected in parallel with the series diodes. At resonance, its inductance and the diodes' capacitances will cancel, leaving the diodes' junction resistances in series with the signal path. Therefore, the problem of signal leakage through the parasitic capacitances is eliminated. However, the improvement is narrowband. Although the parasitic cancellation technique is demonstrated on this standalone VVA module, it should be applicable to any π VVA—whether it is a discrete or integrated-circuit (IC) design—as long as the series arm is accessible.

Excluding the connectors, the bill of materials (BOM) for this VVA solely consists of two components. Both are mounted on one side of a 10-mil-thick RO4350 printed-circuit board (PCB) from Rogers Corp. (www.rogerscorp.com). The component-less side of the PCB is glued to an FR-4 circuit-board layer for rigidity, as well as to increase the stack height to 1.6 mm, so as to suit the edge-mounted SMA receptacles. All measurements are referenced to these connectors; therefore, they include connector and PCB losses.

Computer circuit simulations can predict the correct L_1 inductance value if accurate circuit models of the inductor, module, and PCB are available. Due to the lack of resources to develop these models, it was decided to determine the L_1 value using the "cut-and-try" approach. After deciding on a 0603-size wirewound inductor series,[13] different L_1 values were substituted into the prototype circuit design to gauge the effects. Although the target resonant frequency was 3.5 GHz, the inductance granularity prevents this from happening.

Finally, an inductance value of 16 nH was chosen because the resulting notch it produced was closest to 3.5 GHz *(Fig. 2)*. The spacing between the notches is not consistent with

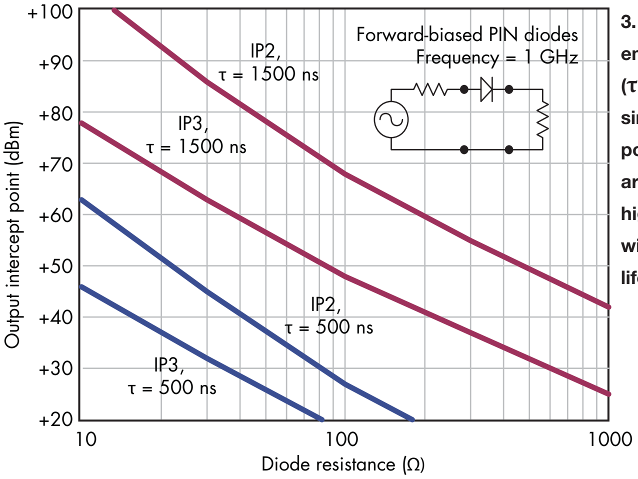

3. The VVA module employs long-lifetime (τ = 1500 ns) diodes since their intercept points (IP2 and IP3) are at least 30-dB higher than diodes with moderate lifetimes (τ = 500 ns).

the stated inductance values—this probably points to tolerance in either the inductance or the parasitic capacitance. Ideally, an inductor with tight tolerance should be specified for L_1 to minimize variation in the notch frequency. Although a multilayer inductor can be used to save cost, it is not recommended because of its higher parasitic capacitance and lower quality (Q) factor compared to a wirewound inductor.

For a VVA that is meant to pass complex, multitone waveforms, linearity can be a bottleneck and a problem when lacking. To understand the linearity performance of a VVA based on diodes requires some background knowledge of the diodes' distortion-generating mechanism. The subject VVA module's four diodes are forward-biased over most of the attenuation range, except at low control voltages (i.e., less than +1 V dc). In the forward-biased condition, distortion is created by RF currents modulating the charge density of the diode's intrinsic (I) layer.

The VVA module employs two techniques to minimize distortion. First, the two series diodes are oriented in the opposite direction to produce out-of-phase distortion so that their even-order distortion will be partially cancelled.[14,15] Secondly, the diodes are chosen for a large ratio of carrier lifetime π to on-state resistance.[16] These long-lifetime diodes (π = 1500 ns) can improve the VVA's third-order intercept by

SURVEYING VOLTAGE-VARIABLE-ATTENUATOR PERFORMANCES AT 3.5 GHZ

Reference	Topology	Semiconductor	Attenuation range* (dB)	IIP3** (dBm)
17	Hybrid coupled	GaAs pHEMT	19	+20
18	Hybrid coupled	PIN diode	23	+43
19	Hybrid coupled	PIN diode	24	+45
20	Digital step	GaAs MMIC	16	+53
21	Digital step	GaAs pHEMT	32	+58
22	Bridged-T	GaAs PIN diode	25	+9
23, 24	π	Si CMOS	33	+55
This work	π	Si PIN diode	45	+61

*One stage
**At minimum attenuation

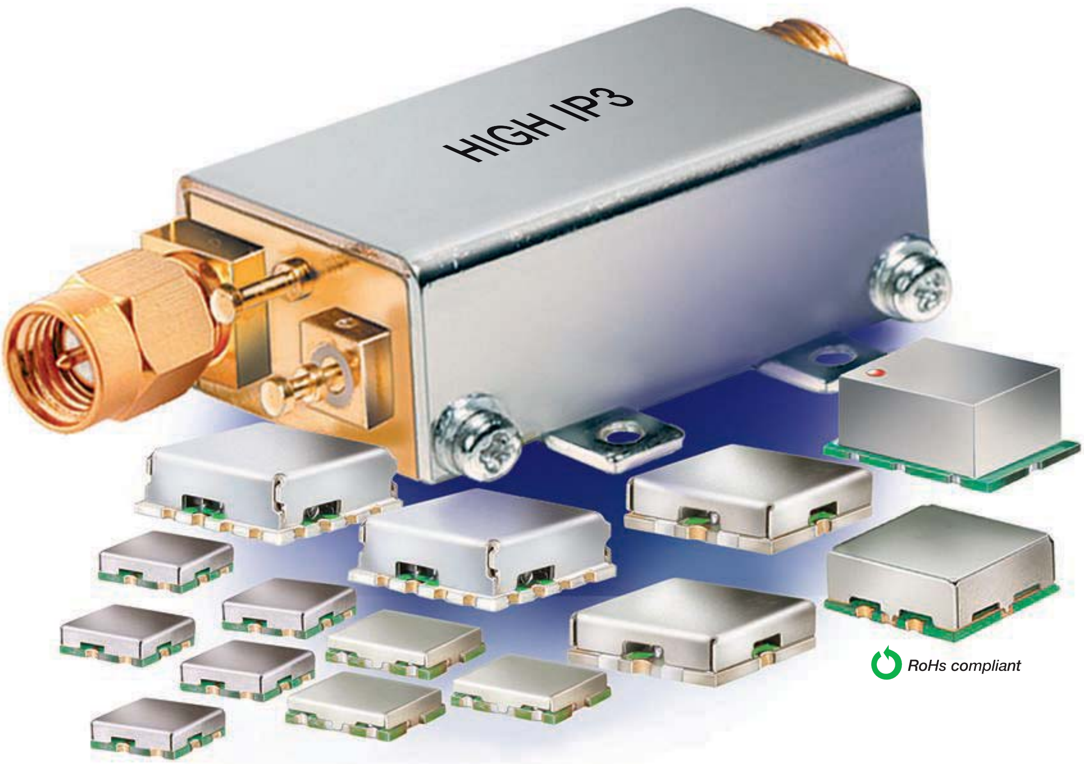
HIGH IP3
RoHs compliant

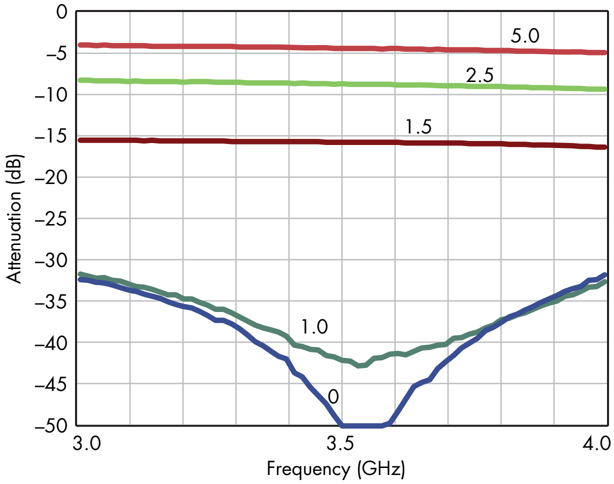

4. The 45-dB attenuation range of the VVA module is the highest ever reported for a single attenuator stage. Sweeping the control voltage from +5 to 0 V dc changes the attenuation from 4 to 50 dB at 3.5 GHz.

more than 30 dB compared to shorter-lifetime (500 ns) diodes *(Fig. 3)*. The long-lifetime diodes require approximately 10 times higher operating currents. However, this tradeoff is tolerable because intended applications are typically powered by mains supplies.

The VVA's attenuation is adjustable over a 45-dB range at 3.5 GHz. This represents the highest amount of attenuation yet reported in a single VVA stage *(see the table)*.[17-24] At the maximum control voltage (V_c = +5 V dc), the experimental minimum attenuation is about 4.4 dB *(Fig. 4)*, of which 0.3 dB is contributed by the PCB and connectors. At zero control voltage, a maximum attenuation of about 50 dB is achieved. The attenuation at 3.5 GHz is slightly less than the maximum possible because the notch is offset to 3.52 GHz. Compared to the original circuit, parasitic cancellation improves the maximum attenuation by about 22 dB.

The VVA input and output impedances remain stable over the attenuation range. The return loss measures better than 10 dB over 45 dB of change in attenuation *(Fig. 5)*. The impedance match is best at the attenuation midrange, but degrades toward either end of the attenuation range.

The experimental linearity performance of the VVA surpasses previous figures *(see the table)*. At minimum attenuation, the third-order input intercept point (IIP3) exceeds +61 dBm *(Fig. 6)*. This IIP3 is at its highest level because the control voltage

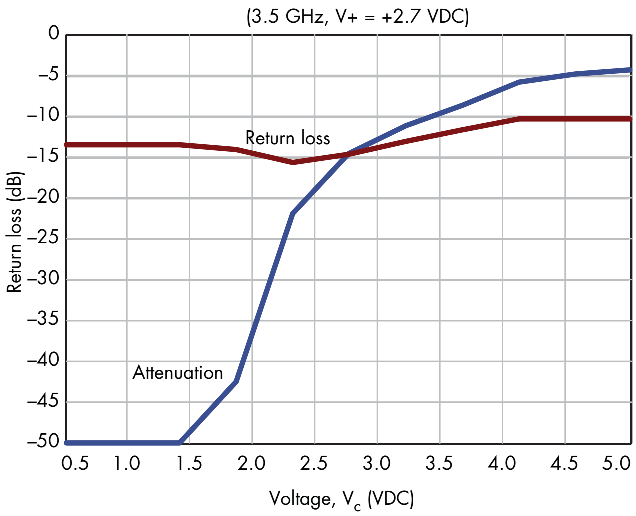

5. The 45-dB attenuation range is complemented by a better than 10-dB return loss.

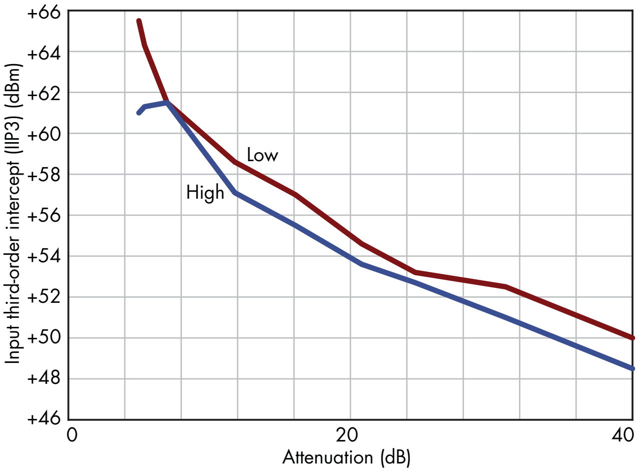

6. The compact VVA module achieves +61-dBm input third-order intercept point (IIP3) at minimum attenuation.

(V_c is at a maximum, hence heavily biasing the VVA's series diodes. The IIP3 gradually decreases with higher attenuation levels, but does not descend below +48 dBm over a 40-dB attenuation range.

Competing designs employ a varied range of topologies and semiconductors because there is no dominant configuration or all-around winner in this design comparison *(see the table)*. For example, the digital step topology can achieve a high IIP3 because its resistances are passive (non-semiconductor based), but its attenuation is not continuously adjustable. Compared to the rest of these design approaches, the current approach achieves the best attenuation range and linearity. Additionally, it is continuously adjustable, compact, simple, and low in cost.

In short, when using this design approach, the PIN diode π attenuator's operating frequency can be extended to the microwave range through the use of this parasitic cancelling technique. As this highly integrated VVA module has shown, this compact design is able to operate at 3.5 GHz using one external component. The design approach is compact and simple and relatively low in cost, but achieves a wide attenuation range with superior linearity. mw

ACKNOWLEDGMENT

The author thanks Y.M. Fong for designing the VVA module.

REFERENCES

1. C.L. Lim, "Wideband voltage variable attenuator with few components," Microwave Journal, December 2011, www.mwjournal.com.
2. K.C. Gupta, "Microwave Control Circuits," in Microwave Solid State Design, 2nd ed., I. Bahl and P. Bhartia, Eds., Wiley, New York, 2003, pp. 683-685.
3. Avago Technologies, application note 922, "Applications of PIN diodes," 1991, www.avagotech.com.
4. E. Higham, "Distortion in voltage-variable attenuators," Microwave Journal, December 1999, pp. 86-95.
5. R. Sydow, "PIN Diodes," in Capacitance Diodes, Tuner Diodes, Diode Switches, PIN Diodes Basics and Applications, ITT, 1976, pp. 55-58.
6. Ulrich L. Rohde and D.P. Newkirk, "PIN Diodes" in RF/Microwave Circuit Design for Wireless Applications," Wiley, New York, 2000, Section 2-1-3, p. 152.
7. Ray W. Waugh, "A Low Cost Surface Mount PIN Diode Pi Attenuator," Microwave Journal, Vol 35, No. 5, May, 1992, pp. 280-284.
8. S. Huettner, "Waugh Attenuator," in Microwaves 101, July 2011, www.microwaves101.com/encyclopedia/attenuator_waugh.cfm.
9. A. Grebennikov, "Attenuators," in RF and Microwave Transmitter Design, Wiley, New York, 2011, Section 13.4.
10. Avago Technologies, application note 5383, "Improving the maximum attenuation of the HSMP-3816 PI attenuator at 3.8 GHz," April 2008, www.avagotech.com.
11. Avago Technologies, datasheet, "ALM-38140," www.avagotech.com.
12. C.L. Lim, "VVA extends BW and dynamic range," Microwaves & RF, October 2011, pp. 54-62.
13. Coilcraft Industries, document 537-1, "Chip inductors – 0603HP series," May 2009, www.coilcraft.com.
14. R.W. Waugh, "A low distortion PIN diode switch using surface mount devices," Proceedings of the RF Expo West, February 1991, pp. 455-461.
15. Avago Technologies, application note 1049, "A low distortion PIN diode switch using surface mount devices," www.avagotech.com.
16. R.H. Caverly, "Distortion in RF and microwave control devices," Microwave Journal, December 1997.
17. Skyworks Solutions, product specification, "SKY12146-321LF: 3.0 – 3.8 GHz, 20 dB variable voltage attenuator," April 2011, www.skyworksinc.com.
18. Skyworks Solutions, product specification, "SKY12236-11: High IIP3, 2.6 to 5.0 GHz voltage-controlled variable attenuator," March 2014, www.skyworksinc.com.
19. Valpey Fisher product specification, "VFVA505-200," 2011, valpeyfisher.com.
20. Hittite Microwave, product specification, "HMC603QS16," www.hittite.com.
21. E.E. Austin, H. Cebi and J. Yang, "Tackling multi-bit attenuator designs," Microwaves & RF, March 2012, pp. 91-118.
22. K.W. Kobayashi, A.K. Oki, D.K. Umemoto, S. Claxton, and D.C. Streit, "GaAs HBT PIN diode attenuators and switches," IEEE Microwave Symposium Digest, 1993.
23. M. Granger-Jones, B. Nelson, and E. Franzwa, "A broadband high dynamic range voltage controlled attenuator MMIC with IIP3> +47dBm over entire 30-dB analog control range," IEEE Microwave Symposium Digest, 2011.
24. D. Walraven amd E. Franzwa, "RFSA2013 and RFSA2023 broadband high performance voltage-controlled attenuators, Microwave Product Digest, June 2011.

PINPOINT THE HIGH-FREQUENCY RESISTANCE OF TOROIDAL WINDINGS

IN HIGH-FREQUENCY DESIGNS, overcoming the challenge of calculating the resistance of single- and double-layer toroidal inductors can provide design benefits over the commonly used guess-and-check method.

Relatively accurate formulas exist for calculating the high-frequency (HF) resistance of a solenoidal inductor (accurate to between 5% and 10%). Historically, however, the approximations for toroidal inductors have been unmanageably inaccurate when the wiring diameter is greater than or equal to the skin depth.

To help conquer this problem, Micrometals produced an application note that discusses the simulation and modeling of toroidal windings at high frequencies. The note, "Calculating The High Frequency Resistance of Single and Double Layer Toroidal Windings," details the development of formulas and graphs for accurately calculating the resistive losses of single-layer toroidal windings.

Micrometals Inc., 5615 E. LA Palma Ave., Anaheim, CA 92807-2109, (714) 970-9400, www.micrometals.com

The multidimensional complexity of a toroidal winding system goes beyond the scope of an analytical technique. With the use of electromagnetic (EM) finite-element-analysis technology, though, many experiments can be run on various toroidal-winding configurations. In addition, it's possible to model and describe the parameter interactions using an adapted formula. The note describes the necessary assumptions for this process, such as the consideration of precision manufacture. After all, non-uniformities would unreasonably increase complexity.

The formulas for the single-layer windings also assume a generously sized wire diameter. It must be sufficiently large to keep the separation distance between the windings and the magnetic core's surface to less than 4%. Many of the parameters that define the effects of core proximity and eddy current are complex derivatives of other parameters. As a result, two correction factors from the simulation study are used instead of derived formulas.

When comparing the two-layer toroidal winding versus the singular, the former results in a significantly higher resistance at high frequencies. Such increased resistance is a product of the high-frequency current riding along the wire surface, which creates eddy-current losses in the secondary layer. These losses offset the lower-conduction losses that stem from having greater conductive surface area.

In conclusion, the note shows that the single-layer toroidal winding suffers the least loss with solid conductors. Spacing the round wires does not reduce the eddy-current losses enough to counteract the total loss per winding width.

THESE 11 SPECIFICATIONS DEFINE PIN-DIODE SWITCHES

SYSTEM DESIGNERS MUST understand the realistic and essential parameters of PIN-diode switches in order to specify them within designs.

American Microwave Corp., 7309-A Grove Rd., Frederick, MD 21704, (301) 662-4700, www.americanmic.com

PIN-diode switches come in many shapes, sizes, and operation ranges. When planning a project, system-level designers need to account for several to thousands of these switches. Thus, a detailed knowledge of the parameters of a PIN-diode switch becomes paramount, since they form part of the device's signal chain. To illuminate the most essential parameters, American Microwave offers an application note titled "How To Specify Pin Diode Switches." The document expounds upon the six key, and five secondary, PIN-diode parameters that are required to specify PIN diodes within a system.

Of the hundreds of device parameters, the six key PIN-diode switch specs include type, operating frequency band, insertion loss, isolation, switching speed, and power handling. Switch type can range from single to multiple poles and from single-throw to 32 throws. The more complex a switch, the less common it will be in the marketplace. According to the note, this factor also applies to the frequency range of operation. While lower-frequency video and high-frequency switches are frequently found, extreme-microwave and millimeter-wave PIN diode switches tend to be less available.

Insertion loss and isolation are the electrical properties associated with quality of design and manufacture. Insertion loss depends on two factors: the conductor/transmission-line interconnect within the switch, and how well the signal paths are matched. In contrast, isolation depends on the series or shunt connection of the switch. A variety of techniques exist specifically for maximizing isolation at broadband or narrowband frequencies.

Two parameters at odds with each other are switching speed and power handling. Handling greater power requires a larger device. Increased size, in turn, multiplies the parasitics that lower switching speed.

The note breaks down the key specifications further by detailing five secondary parameters: logic-compatible driver type/speed, phase tracking, off-arm terminations, intercept point, and video transients. These parameters require a grasp of the switch's application, the specific requirements of its higher-level assembly, and compliance requirements. Many of these parameters demand tradeoff considerations. As a result, the note recommends a study of those tradeoffs in accordance with the value of the specification within the application.

JACK BROWNE | Technical Contributor

Attenuators Program 0.25-dB Steps to 120 dB

Covering frequency ranges from 1 to 4000 MHz and 1 to 6000 MHz, these programmable step attenuators are fast, accurate, and command as much as 120-dB attenuation.

Attenuation is an important electrical characteristic for a wide range of applications, from communications networks to measurement systems. Attenuators come in many shapes and sizes, ranging from tiny fixed components to large instruments. As a practical compromise in size—but not in performance—a pair of new programmable attenuators from Mini-Circuits operate over broad bandwidths as wide as 1 to 6000 MHz, with 110-dB or more precisely controlled attenuation that is adjustable in fine 0.25-dB steps.

These programmable attenuators are noteworthy for maintaining consistent attenuation with high accuracy across their 4- and 6-GHz frequency ranges and wide temperature ranges. They are well suited for controlling signal levels where needed, such as for testing or for protecting other components [e.g., low-noise amplifiers (LNAs) in receivers] from overload damage.

Model RCDAT-4000-120 *(Fig. 1)* features programmable 0-to-120-dB attenuation in 0.25-dB steps across a frequency range of 1 to 4000 MHz. In contrast, model RUDAT-6000-110 *(Fig. 2)* boasts programmable 0-to-110-dB attenuation in 0.25-dB steps across a frequency range of 1 to 6000 MHz. The attenuators differ somewhat with their control interfaces: The RCDAT-4000-120 provides Universal Serial Bus (USB) and RJ45 Ethernet ports, while the RUDAT-6000-110 includes USB and RS-232C ports.

Both attenuators are well-equipped for taming the attenuation levels in communications and automatic-test-equipment (ATE) systems—and even in manual test setups, where the flexibility in amplitude control and speed protects the measurements and test gear.

1. Model RCDAT-4000-120 is a programmable attenuator with 0-to-120-dB attenuation in 0.25-dB steps from 1 to 4000 MHz.

2. Model RUDAT-6000-110 is a programmable step attenuator with 0-to-110-dB attenuation in 0.25-dB steps from 1 to 6000 MHz.

The model RCDAT-4000-120 includes a dedicated microcontroller, broadband monolithic digital step attenuator (DSA), control ports, and input and output connectors, all packed into a compact housing measuring just 2.5 × 3.0 × 0.85 in. The DSA supports bidirectional operation with its SMA female signal connectors, which allows either connector to serve as an input or output port.

This attenuator commands a range of attenuation from 0 to 120 dB in 0.25-dB steps from 1 to 4 GHz, but also offers the fast switching speed essential for production-line testing and the high levels of accuracy needed for trusted testing. Model RCDAT-4000-120 can change attenuation states with high-speed switching speed of typically 650 ns, while also settling to new attenuation settings with remarkable stability and accuracy.

The attenuation accuracy for this DSA is typically ±0.5 dB or better across the full attenuation range, even at the highest attenuation settings and frequencies. The attenuation accuracy is consistent across the full attenuation range *(Table 1)* and with frequency.

Attenuation accuracy is quite impressive across all attenuation settings and frequencies. For example, from 1 to 4000 MHz and for attenuation settings from 0.25 to 10.00 dB, the attenuation accuracy is typically ±0.15 dB. The attenuation accuracy is a worst case of ±0.70 dB for attenuation settings from 90.25 to 120.00 from 1 to 2000 MHz; this level of accuracy improves to typically ±0.35 dB for this same range of attenuation settings for frequencies from 2000 to 4000 MHz.

The typical attenuation accuracy is ±0.55 dB for attenuation settings from 10.25 to 40.00 dB from 1 to 2000 MHz, and ±0.50

Ultra Small 2x2mm

2W ATTENUATORS DC-20GHz from $1.99 ea. (qty. 1000)

Save PC board space with our new tiny 2W fixed value absorptive attenuators, available in molded plastic or high-rel hermetic nitrogen-filled ceramic packages. They are perfect building blocks, reducing effects of mismatches, harmonics, and intermodulation, improving isolation, and meeting other circuit level requirements. These units will deliver the precise attenuation you need, and are stocked in 1-dB steps from 0 to 10 dB, and 12, 15, 20 and 30 dB.

The ceramic hermetic ***RCAT*** family is built to deliver reliable, repeatable performance from DC-20GHz under the harshest conditions. With prices starting at only $4.95 ea. (qty. 20), these units are qualified to meet MIL requirements including vibration, PIND, thermal shock, gross and fine leak and more, at up to 125°C!

The molded plastic ***YAT*** family uses an industry proven, high thermal conductivity case and has excellent electrical performance over the frequency range of DC to 18 GHz, for prices starting at $2.99 ea. (qty. 20).

For more details, just go to minicircuits.com – place your order today, and you can have these products in your hands as soon as tomorrow!

RoHS compliant

FREE Simulation Models! Modelithics®

http://www.modelithics.com/mvp/Mini-Circuits/

Mini-Circuits®

www.minicircuits.com P.O. Box 350166, Brooklyn, NY 11235-0003 (718) 934-4500 sales@minicircuits.com

515 rev E

TABLE 1: THE MODEL RCDAT-4000-120 ATTENUATION ACCURACY AT A GLANCE		
Frequency range (MHz)	Attenuation setting (dB)	Attenuation accuracy (dB)
1 to 2000	0.25 to 10.00	±0.15
1 to 2000	10.25 to 40.00	±0.55
1 to 2000	40.25 to 90.00	±0.50
1 to 2000	90.25 to 120.00	±0.35
2000 to 4000	0.25 to 10.00	±0.15
2000 to 4000	10.25 to 40.00	±0.50
2000 to 4000	40.25 to 90.00	±0.25
2000 to 4000	90.25 to 120.00	±0.35

dB for attenuation settings of 40.25 to 90.00 dB from 1 to 2000 MHz. Across the upper half of the frequency range, attenuation accuracy is typically ±0.50 dB for attenuation settings of 10.25 to 40.00 dB from 2000 to 4000 MHz, ±0.25 dB for attenuation settings of 40.25 to 90.00 dB from 2000 to 4000 MHz, and ±0.35 dB for settings of 90.25 to 120.00 dB from 2000 to 4000 MHz.

Of course, the RCDAT-4000-120 suffers some insertion loss of its own, as measured at its 0-dB attenuation setting as a function of frequency. The insertion loss is typically 6.5 dB from 1 to 2000 MHz and 9.0 dB from 2000 to 4000. The isolation between input and output ports with power on is typically 134 dB from 1 to 4000 MHz. Across that same frequency range, the programmable attenuator offers excellent linearity, as measured by its high input third-order intercept point (IIP3) of typically +53 dBm at a 0-dB attenuation setting.

The attenuator is closely matched to 50 Ω, with low VSWR of typically 1.30:1 for attenuation settings of 0 to 40 dB from 1 to 500 MHz and VSWR of typically 1.05:1 for attenuation settings of 40.25 to 120.00 dB from 1 to 500 MHz. For higher frequencies, the VSWR is typically 1.10:1 for attenuation settings from 0 to 20 dB for frequencies from 500 to 4000 MHz and typically 1.05:1 for attenuation settings from 20.25 to 120.00 dB from 500 to 4000 MHz.

Controlling the model RCDAT-4000-120 programmable step attenuator is a simple matter, since each attenuator is supplied with easy-to-install, user-friendly graphical-user-interface (GUI) software for a PC or laptop computer. The GUI software is written with API objects for Microsoft Windows operating environments, and complete programming instructions for 32- and 64-b Windows and Linux operating systems. The software provides clear, straightforward user screens whether under USB or Ethernet control, allowing users to set attenuation, sweep speeds and modes, and even hop modes.

For those in need of higher-frequency operation with slightly less attenuation, the model RUDAT-6000-110 programs 0.25-dB steps across an attenuation range of 0 to 110 dB and a frequency range of 1 to 6000 MHz. It measures a compact 2.0 × 3.0 × 0.6 in. with female SMA input and output connectors.

TABLE 2: THE MODEL RUDAT-6000-110 ATTENUATION ACCURACY AT A GLANCE		
Frequency range (MHz)	Attenuation setting (dB)	Attenuation accuracy (dB)
1 to 2000	0.25 to 10.00	±0.15
1 to 2000	10.25 to 40.00	±0.55
1 to 2000	40.25 to 90.00	±0.50
1 to 2000	90.25 to 110.00	±0.70
2000 to 4000	0.25 to 10.00	±0.15
2000 to 4000	10.25 to 40.00	±0.50
2000 to 4000	40.25 to 90.00	±0.25
2000 to 4000	90.25 to 110.00	±0.35
4000 to 6000	0.25 to 10.00	±0.10
4000 to 6000	10.25 to 40.00	±0.40
4000 to 6000	40.25 to 90.00	±0.60
4000 to 6000	90.25 to 110.00	±0.80

Like its lower-frequency counterpart, this programmable attenuator provides very good attenuation accuracy of typically ±0.45 dB across its wide frequency and attenuation ranges *(Table 2)*. Moreover, it features high-speed switching of attenuation settings, allowing for efficient and effective production testing.

Also like the lower-frequency attenuator, model RUDAT-6000-110 exhibits low VSWR across its wide frequency range. From 1 to 500 MHz, the VSWR is typically 1.30:1 for attenuation settings from 0 to 20 dB and 1.05:1 for attenuation settings from 20.25 to 110.0 dB. From 500 to 4000 MHz, the VSWR is typically 1.10:1 for attenuation settings from 0 to 20 dB and 1.05:1 for attenuation settings from 20.25 to 110.0 dB. From 4000 to 6000 MHz, the VSWR is typically 1.30:1 for attenuation settings from 0 to 20 dB and 1.15:1 for attenuation settings from 20.25 to 110.00 dB.

Model RUDAT-6000-110 is a true Plug & Play device, with no drivers required, and is supplied with operating software on a CD. It has some insertion loss, measured as the loss at a 0-dB attenuation setting, at typically 6.5 dB from 1 to 2000 MHz, 9.0 dB from 2000 to 4000 MHz, and 9.5 dB from 4000 to 6000 MHz. It exhibits typical input-output isolation of 124 dB from 1 to 6000 MHz, and achieves excellent linearity, with input IIP3 of typically +53 dBm from 1 to 3000 MHz and +51 dBm from 3000 to 6000 MHz, as measured with a 0-dB attenuation setting and +10-dBm test-signal input power.

These compact programmable attenuators are useful for a wide range of purposes, from communications systems to manual measurements and ATE applications. Both attenuators feature good electrostatic-discharge (ESD) tolerance for use in a wide range of systems and environments. mw

MINI-CIRCUITS, P.O. Box 350166, Brooklyn, NY 11235-0003; (718) 934-4500, FAX: (718) 332-4661, *www.minicircuits.com*

JEAN-JACQUES DELISLE | Technology Editor

5 Antenna Typologies Squeeze into IoT Modules

As Internet of Things modules continue to shrink and incorporate more wireless technologies, making space for antennas is becoming an increasingly significant challenge.

MODULES FOR INTERNET of Things (IoT) applications are swarming the consumer and industrial markets with the aim of sensing, computing, and connecting all things within reach. A wealth of clever strategies is needed to shrink the size of these devices while maintaining highly reliable remote performance under low-power conditions. As a result, IoT-module antenna designers face the restrictions of maintaining reasonable performance in ever-shrinking footprints and under extreme interference/cosite conditions.

Weighing cost, size, design effort, and manufacturing complexity, IoT modules make an engineer's design decisions much more challenging. Common IoT antenna typologies range from printed circuit board (PCB) designs to prefabricated chip antennas. The following antenna typologies each have their benefits and drawbacks, which we've listed to aid IoT module designers in making the right antenna decision for their applications (*see Table at right*).

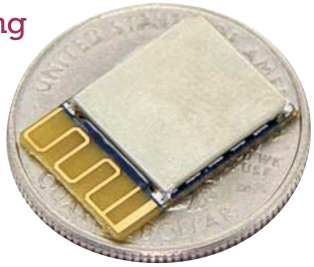

1. Antenna folding techniques can be used to minimize antenna dimensions, further decreasing the size and cost of IoT modules. ***(Courtesy of Seeed)***

PROS AND CONS OF ANTENNA STYLES

Antenna Style	Benefits	Drawbacks
Chip	Very small size even at low frequencies Extremely reproduceable Short design & test cycle Easy troubleshoot & retrofit	Midrange performance Midrange cost No flexibility of design Requires outside parts
Proprietary	Support from outside resource Quality custom design Limited design liability Generally short design & test cycle	Midrange cost Variable performance usually applications-specific No control of design Requires outside resource
Wired	Very low cost Low PCB footprint Highly accessible & flexible design Easy to EM simulate Wide frequency capability Can be designed for specific package Through-hole possible	Custom design & manufacturing required Reproduceability challenges Requires EM simulation for optimization Size increases as frequency decreases
Whip	High performance options Short design & test cycle Coaxial cable routing for flexible device design Can reduce cosite issues with multiple antenna using spatial diversity Easy to troubleshoot & retrofit	Coaxial connection requires connector More expensive than PCB & wire antenna Conducted emission tests required
PCB	Low cost Small size at high frequencies Free reference designs widely available Easy to EM simulate Highly reproduceable Performs well above 800 MHz Access to SMT matching components	Performance challenges below 500 MHz Size increases as frequency decreases Dedicated space on PCB required for all layers Multiple antennas increase PCB size Potential cosite issues with multiple antennas Antenna redesign requires board redesign

CHIP ANTENNAS

For the smallest form factors—even at low frequencies—chip antennas may be the best option for an ultra-crammed design. In addition to reducing the design effort required to implement an IoT solution, chip antennas could aid in maintaining low reproducibility issues when large manufacturing runs are required. However, chip antennas do add cost and design considerations. They have lower efficiency and lower bandwidths than other antenna typologies at comparable frequencies. And even if they have internal matching, external matching circuitry is most likely required to achieve datasheet performance. Chip antennas also can be sensitive to groundplane geometries.

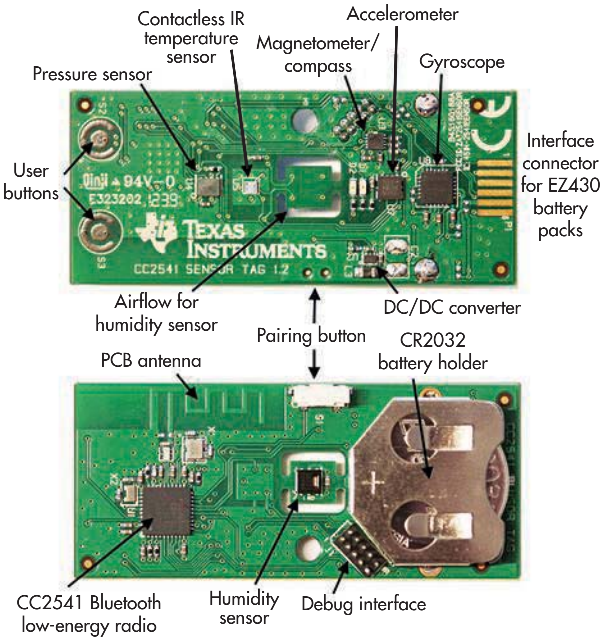

2. In complex IoT modules with many sensors, the PCB antenna can still dominate a significant portion of the PCB board. *(Courtesy of Texas Instruments)*

Given these points, it is crucial to adhere to the documented design guidelines for the chip antenna.

PROPRIETARY ANTENNAS

Proprietary antenna designs are owned by a designer or design company. Occasionally, these antennas also can be commissioned or custom-designed for specific applications. The cost for these antennas begins with the purchasing of the intellectual property (IP), although this option usually comes with support from the antenna design company. For companies that do not have antenna design expertise in-house, this design-sourcing option offers a chance to leverage the expertise of highly specialized designers skilled in this area. When considering proprietary antennas, it's critical to know the exact use case for the antenna. It is then possible to describe and design for the complete performance dynamics.

WIRED ANTENNAS

As one of the lowest-cost and highest-flexibility options, wired antennas can be applied to the majority of thrifty designs. Yet they do require additional design effort. These antennas generally demand electromagnetic (EM) simulation for optimal designs. They may even require custom designs based on the module's housing. Wired antennas also increase in size as frequency decreases, which may add to the manufacturing challenges associated with design reproducibility and reliability.

WHIP ANTENNAS

Whip antennas are one of the highest-cost antenna options. Yet they also are the highest-performing and may be the best fit if the module faces cosite issues with multiple transceivers. In addition to the up-front antenna cost, a connector will be needed on board. The design also will have to account for coaxial cable routing from the launching connector to the antenna module. For many whip antennas, emissions testing also will need to be performed.

PCB ANTENNAS

If a module demands low cost and reasonable design flexibility in a highly integrated printed circuit board, a PCB antenna may be the optimal choice. For large-scale manufacturing, PCB antennas tend to be the most cost-effective with the least reproducibility issues. In addition, there are many free reference designs for PCB antennas ranging from large and low-frequency to highly compact and high-frequency single-ended and differential antennas. Many low-cost or free EM-simulation software packages also aid in designing these antennas. They could even accelerate the matching circuitry design. mw

TO BALUN OR NOT TO BALUN?

FOR IoT APPLICATIONS, the limited space and exact positioning of the microcontroller unit (MCU) and sensors tend to limit the antenna's geometric flexibility. Although they're highly efficient and wideband, differential antennas typically require more space and precise design geometries—features that aren't available on most crammed IoT PCBs. Many IoT antennas are therefore single-ended, which allows them to take advantage of the isolated ends and crammed footprints of IoT-module PCBs.

Most IoT RF integrated circuits (RFICs) have differential transceiver (TRX) ports to the antenna. Using a single-ended antenna architecture therefore requires a balun. A balun also is needed when unbalanced transmission lines, such as coaxial cables, are used to feed the antenna. However, baluns add cost and require valuable PCB real estate near the MCU. Single-ended antenna options also tend to perform less efficiently than differential ones. Given the compressed antenna-typology geometry options, though, the IoT module designer may not have much choice.

3. Some highly complex IoT modules require multiple wireless technology transceivers. *(Courtesy of Link-One)*

JACK BROWNE | Technical Contributor

Switch Controls DC To 8 GHz

Based on UltraCMOS semiconductor technology, this 8-GHz switch is truly dc coupled in a miniature surface-mount package, with low harmonic distortion, for a variety of applications.

RF/MICROWAVE COMPONENTS ARE often touted as "dc-coupled" products that are capable of transferring signals at 0 Hz. This is important for maintaining the integrity of certain digital and analog signals, especially in mixed-signal applications where a variety of different signal types might be in evidence. Unfortunately, a number of components are dc coupled in name only and fail the test when processing signals at 0 Hz.

One exception is the model PE42020 single-pole, double-throw (SPDT) surface-mount switch from Peregrine Semiconductor. With a frequency range of 0 Hz to 8 GHz, this rugged little switch is truly dc coupled and capable of handling a good amount of RF/microwave power for its size. It is well suited for applications in communications and test that combine dc, RF/microwave, analog, and digital signals.

Model PE42020 is a wideband SPDT switch that is truly capable of channeling signals at 0 Hz and with an upper-frequency range of 8 GHz.

The PE42020 SPDT switch *(see photo)* is fabricated with UltraCMOS, Peregrine's patented silicon-on-insulator (SOI) technology on a sapphire substrate. Peregrine's HaRP technology, which essentially provides the performance of GaAs with the economy of silicon CMOS, supports high linearity with low harmonic distortion to help maintain signal integrity across wide frequency bandwidths.

The PE42020 switch, which is supplied in a 20-lead 4 × 4 × 0.85 mm QFN package, can be configured as an absorptive or open-reflective switch via single-pin control. It's able to handle maximum ac or dc voltage of ±10 V on its RF ports, and is rated for maximum RF power of +30 dBm at dc and +38 dBm at 8 GHz.

This broadband switch features a notable total-harmonic-distortion (THD) specification of –84 dBc, measured at 1 kHz into a 300-Ω load. It exhibits low insertion loss between switched ports, at no more than 0.7 dB and typically 0.6 dB at 0 Hz; no more than 1.00 dB and typically 0.85 dB from dc to 3 GHz; no more than 1.30 dB and typically 1.00 dB from 3 to 6 GHz; and no more than 1.35 dB and typically 1.10 dB from 6 to 8 GHz. The isolation between ports varies with frequency, but is at least 46 dB and typically 48 dB from 0 Hz to 3 GHz; at least 35 dB and typically 37 dB from 3 to 6 GHz; and at least 30 dB and typically 34 dB from 6 to 8 GHz.

The switch can handle hot switching, when RF power is applied to the switch during the switching process, at input levels to +27 dBm when operating at positive and negative supply voltages of +15 V and –15 V (it is rated for slightly less hot-switching power at lower supply voltages).

The switching speed, from 50% of a control signal to 10% or 90% of the RF signal, is 14 μs or less and typically 10 μs. The settling time, from 50% of the control signal to 0.05 dB of the final switched value, is 45 μs or less and typically only 35 μs.

The switch, which is designed for operating temperatures from –40 to +85°C, offers an input 1-dB compression point of typically +38 dBm from 40 MHz to 8 GHz. The input third-order intercept point (IIP3) is typically +62 dBm at 836 and 1900 MHz, +61 dBm at 2.7 GHz, and +55 dBm at 4.8 GHz.

To assist adopters of the switch, Peregrine Semiconductor offers a switch evaluation board for the PE42020, complete with connections to 50-Ω transmission lines via SMA connectors. The evaluation board is constructed with four metal layers on low-loss printed-circuit-board (PCB) material, including 4350B circuit material from Rogers Corp. (www.rogerscorp.com).

In addition to the RF connector, a 50-Ω through transmission line is available via SMA connectors for the purpose of de-embedding the losses of the PCB when evaluating the performance of the switch. mw

PEREGRINE SEMICONDUCTOR CORP., 9380 Carroll Park Dr., San Diego, CA 92121; (858) 731-9400, FAX: (858) 731-9499, *www.psemi.com*

This index is provided as an additional service by the publisher, who assumes no responsibility for errors or omissions.

Subscription Assistance and Information:
(ISSN 0745-2993)
Microwaves & RF is published monthly. Microwaves & RF is sent free to individuals actively engaged in high-frequency electronics engineering. In addition, paid subscriptions are available. Subscription rates for U.S. are $95 for 1 year ($120 in Canada, $150 for International). Published by Penton Media, Inc., 9800 Metcalfe Ave., Overland Park, KS 66212-2216. Periodicals Postage Paid at Kansas City and additional mailing offices. POSTMASTER: Send change of address to Microwaves & RF, Penton Media Inc., P.O. Box 2095, Skokie, IL 60076-7995. For paid subscription requests, please contact: Penton Media Inc., P.O. Box 2100, Skokie, IL 60076-7800. Canadian Post Publications Mail agreement No. 40612608. Canadian GST# R126431964. Canada return address: IMEX Global Solutions, P.O Box 25542,London, ON N6C6B2.

Back issues of MicroWaves and Microwaves & RF are available on microfilm and can be purchased from National Archive Publishing Company (NAPC). For more information, call NAPC at 734-302-6500 or 800-420-NAPC (6272) x 6578.

Penton Revised Privacy Policy

At Penton, we constantly strive to improve our products, including by changing our use of the information we collect from you. We now share information with other subscribers to our services and/or third party vendors who are our partners so that they can provide you additional opportunities and benefits. Some partners may analyze our sites to identify future improvements or to offer additional products you may want.

Visit **http://www.penton.com/privacy-policy/** to read our updated Privacy Policy.

EMI Tester Scans 20 Hz to 3.6 GHz

KEYSIGHT'S N9038A MXE electromagnetic-interference (EMI) receiver comes with a frequency range of 20 Hz to 3.6 GHz (and a price tag that's been downsized accordingly) for applications not requiring EMI compliance testing at higher frequencies. The receiver suits electromagnetic-compatibility (EMC) testing for a wide array of electronic products, across fields that include automotive, industrial, scientific, medical, consumer, and military markets. The receiver complies with CISPR 16-1-1 standards for commercial products and the MIL-STD-461 standard for military testing. With options, the MXE receiver can be equipped with frequency ranges of 20 Hz to 3.6, 8.4, 26.5, or 44 GHz. It costs $61,000 and up; availability is from stock.

KEYSIGHT TECHNOLOGIES INC., 1400 Fountaingrove Pkwy., Santa Rosa, CA 95403; (707) 577-2663, *www.keysight.com*

High-Power Amps Boost 87.5- to 230-MHz Apps

THE ACS series of high-power amplifiers will take on applications such as electromagnetic-interference (EMI) testing and FM broadcasting that range from 87.5 to 230.0 MHz. For example, the AFM-1500 high-power amplifier will target FM broadcast applications. Based on silicon MOSFET device technology, the amplifier provides 1500 W output power from 87.5 to 108.0 MHz. It accepts input signals to 2.5 W to achieve the maximum rated output power. Supplied in a 19-in. rack-mount enclosure, the amplifier operates on 100 A at +27 V dc with BNC connectors and forced-air cooling using external fans. Outputs from two amplifiers can be combined for 3 kW, and four amplifiers can be combined for 5-kW transmit power.

COM-POWER CORP., 114 Olinda Dr., Brea, CA 92823; (714) 528-8800, FAX: (714) 528-1992, *www.com-power.com*

Tuning-Control Switches Aid Antenna Adjustments

A pair of high-performance tuning-control switches, developed by Peregrine Semiconductor and available via Richardson RFPD, target antenna adjustments from 100 to 3000 MHz. Models PE613010 and PE613050 are based on Peregrine's UltraCMOS device technology, a patented variation of silicon-on-insulator (SOI) technology. Model PE613010 features low on-resistance of 1.2 Ω with insertion loss of 0.2 dB at 900 MHz and 0.4 dB at 1900 MHz. It can handle power levels

to +38 dBm with an electrostatic-discharge (ESD) tolerance of 2 kV, based on the human body model (HBM). Model PE613050 also exhibits low on-resistance of 1.6 Ω with insertion loss of 0.25 dB at 900 MHz and 0.40 dB at 1900 MHz. It handles power levels to +38.6 dBm at 900 MHz and +37.6 dBm at 2200 MHz. ESD tolerance is 2 kV per the HBM. The switches offer power-supply ranges of +2.3 to +4.8 V dc and +2.3 to +5.5 V dc, respectively.

RICHARDSON RFPD, 1950 South Batavia Ave., Ste. 100, Geneva, IL 60134; (630) 262-6837; *www.richardsonrfpd.com*

OCXOs Can Take the Heat

Vectron's OX-206 line of oven-controlled crystal oscillators (OCXOs) is intended for applications requiring extended-temperature operation. According to the company, the OCXOs will provide reliable operation at temperatures to +95°C. Available in standard clock frequencies from 10 to 20 MHz, the devices achieve stabilities of better than ±10 ppb across operating temperatures from –40 to +95°C, with phase noise as low as –150 dBc/Hz offset far from the carrier. They measure 25.0 × 25.0 × 13.2 mm.

VECTRON INTERNATIONAL, 267 Lowell Rd., Ste. 102, Hudson, NH 03051; (603) 598-0070, FAX: (603) 598-0075, *www.vectron.com*

Get a piece of the ARRA pie...

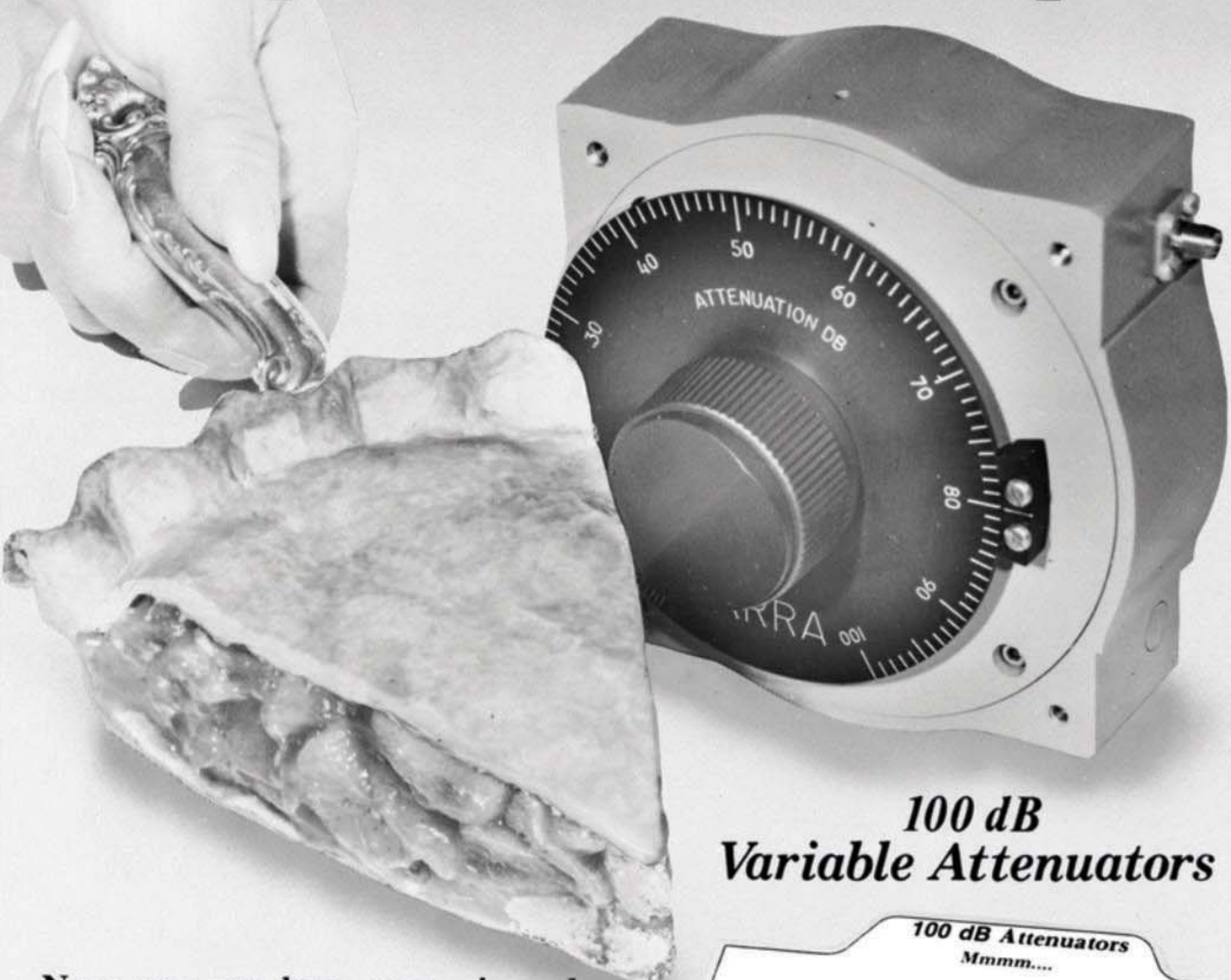

100 dB Variable Attenuators

100 dB Attenuators
Mmmm....

Freq Range	Atten vs Freq dB	Model #
500 - 1000 MHz	1.5	2952 - 100
900 - 1300 MHz	0.75	2-3952 - 100
1000 - 2000 MHz	1.5	3952 - 100X
2000 - 4000 MHz	1.5	4952 - 100 X
4000 - 8000 MHz	1.5	5952 - 100X

Insertion loss - 6 dB
VSWR - 1.5
Power - 15 cw
Temperature -30 to +120 C

Now, you can have your pie and eat it too! Only from ARRA! Four models that cover the 500 to 8000 MHz frequency range! Available in lower attenuation ranges. *Customerized to your requirements with little or no additonal charge.* Top performance. Super dial accuracy.

- Direct reading dial
- Extremely high reliability
- Non-contacting movable parts (our special recipe)
- High power version available (up to 200 W)
- Usage will not change calibration
- Attenuation will not vary with temperature
- Excellent phase characteristics
- Type N standard SMA connectors available

Applications include:
•TACAN •DME/IFF •Lab standards •Altimeter
Or any other requirements needing high attenuation and accurate dial reading.

Visit our website at www.arra.com
E-Mail: sales@arra.com

Some of the best attenuator recipes you can find are cooking at ARRA right now! Send for your copy today and get a piece of the ARRA pie.

...the last word in variable attenuators

ARRA INC.

15 Harold Court • Bay Shore NY 11706-2296

Tel 631-231-8400 Fax 631-434-1116

defenseelectronicsmag.com

defense electronics

A Special Section to PENTON'S DESIGN ENGINEERING & SOURCING GROUP 02/03 2015

The M8195A arbitrary waveform generator packs as many as four differential channels with 65 GSamples/s sampling rate and 20-GHz bandwidth into a single AXIe module.

Sources Generate WIDE RANGE OF SIGNALS

JACK BROWNE | Technical Contributor

SIGNAL GENERATORS have long been wideband in nature, as have sources of signals for testing and operating both military and aerospace systems. Nowadays, they are increasing in their modulation capabilities as those systems to be tested gain in complexity. At one time, military signal sources were generally associated with pulsed signals, for radar system testing. But many applications now require continuous-wave (CW) signals, often with some form of elaborate digital modulation format.

Military and aerospace signal sources are still largely wideband sources, such as the 2-to-18-GHz signal sources popularized for electronic-warfare (EW) testing, and an increasing number of signal sources are being offered for frequencies through 40 GHz and even to 70 GHz. Another trend in RF/microwave signal sources is the growing number of test signal sources in modular formats, like VXI modules. The use of modules allows rapid interchanging of instrument functions within one rack, along with the capability of fitting more functionality within smaller spaces (to learn more about modular test solutions, including analyzers, see the special report beginning on p. S14).

As an example, the M8195A arbitrary waveform generator (AWG) from Keysight Technologies (www.keysight.com) leverages several innovative technologies to provide current state-of-the-art capabilities in signal generation. For one thing, it is a physical departure from the traditional 19-in. instrument rack-mount form factor, with all necessary components and circuits fitting within a single AXIe module *(see photo)*. That single one-slot AXIe module contains four digital-to-analog converters (DACs) capable of generating four differential output signals. This generates the complex signals required by military users by

(continued on p. S28)

CURTISS-WRIGHT ADVANCES RUGGED COTS Enclosure

THE DEFENSE Solutions division of Curtiss-Wright Corp. (www.curtisswright.com) has introduced the industry's first rugged air-cooled three-unit (3U) nine-slot D2D chassis in a three-quarter air-transport-rack (3/4-ATR) enclosure. The firm's new Hybricon D2D-34TLA enclosure allows a system integrator to use the same commercial-off-the-shelf (COTS) enclosure throughout a system's lifetime, from development phases through deployment.

The nine-slot Open-VPX 34TLA enclosure is well suited for aerospace and defense applications. Using the enclosure eliminates the need to design a custom backplane for system since the D2D-34TLA chassis employs a standard COTS backplane and input/output (I/O) cables, using standard +28-VDC power supplies and industrial-grade fans for

(continued on p. S8)

defense electronics

In This Issue

C1

S14

S18

S24

FEATURES

NEWS SHORTS

CONTRACTS

Penton
inform engage advance

Making the Move to Modular Test

MODULAR MEASUREMENT technologies have made great strides over the last several decades. Commercial, industrial, and military users of test equipment now enjoy an unprecedented selection of test instruments in modular form (see. p. S24), from audio through microwave frequencies. The excellent track record of the VXI modular format, with its 25-year history, has shown that it is reliable even across the environmental extremes faced by many military users.

In addition, the performance levels achieved in some recent products introduced in the AXIe and PXIe modular instrument formats show that these mechanical structures and electronic bus configurations sacrifice nothing in terms of performance compared to older test instrument setups. Still, adoption of test equipment that slides into a standardized module-holding chassis can be as much of a philosophical as a technological decision.

"Old-guard" engineers might remember when the VXI modular format was first introduced … and the skepticism throughout the high-frequency industry that such "toy-like" products could ever perform at the level of those trusted rack-mount instruments. To this day, many engineers still feel that way. While they might eye the specifications for the latest analyzer or arbitrary waveform generator (AWG) introduced in one of the modular instrument formats, the equipment that they depend upon is all contained within 19-in. enclosures.

Adoption of critical test functions in modular form requires a willingness to abandon a long-trusted approach and to start with a new outlook on how measurements can be performed. A modular format offers many benefits, with the small size and conservation of power compared to full-sized instruments quite appealing to any electronic-facility manager.

To the working engineer, the flexibility to add or subtract test functions, such as a signal source or a digitizer, as needed represents a huge extension of engineering capabilities for any project. The fact that the functionality of a modular test system can be easily modified within one or two modular instrument chassis that can be moved around an engineering facility, and quickly reprogrammed by means of a commercial measurement software, makes modular measurement solutions quite attractive to many users.

For the most part, these modular test-equipment users are part of the next generation of engineers: younger users willing to try a new format because they did not grow up with the rack-and-stack instruments of their predecessors. de

JACK BROWNE, *Technical Contributor*

FEBRUARY/MARCH | 2015

defense electronics

A Penton® Publication

EDITORIAL

CONTENT DIRECTOR: **NANCY K. FRIEDRICH** nancy.friedrich@penton.com
TECHNICAL CONTRIBUTOR: **JACK BROWNE** jack.browne@penton.com
TECHNICAL ENGINEERING EDITOR: **JEAN-JACQUES DELISLE** jean-jacques.delisle@penton.com
CONTENT PRODUCTION DIRECTOR: **MICHAEL BROWNE** michael.browne@penton.com
PRODUCTION EDITOR: **JEREMY COHEN** jeremy.cohen@penton.com
CONTENT PRODUCTION SPECIALIST: **ROGER ENGELKE** roger.engelke@penton.com
ASSOCIATE CONTENT PRODUCER: **ILIZA SOKOL** iliza.sokol@penton.com
ASSOCIATE CONTENT PRODUCER: **LEAH SCULLY** leah.scully@penton.com

ART DEPARTMENT

GROUP DESIGN DIRECTOR: **ANTHONY VITOLO** tony.vitolo@penton.com
SENIOR ARTIST: **JIM MILLER** jim.miller@penton.com
CONTRIBUTING ART DIRECTOR **RANDALL L. RUBENKING** randall.rubenking@penton.com

PRODUCTION

GROUP PRODUCTION MANAGER: **CAREY SWEETEN** carey.sweeten@penton.com
PRODUCTION MANAGER: **VICKI MCCARTY** vicki.mccarty@penton.com
CLASSIFIED PRODUCTION COORDINATOR: **LINDA SARGENT** linda.sargent@penton.com

AUDIENCE MARKETING

USER MARKETING DIRECTOR: **BRENDA ROODE** brenda.roode@penton.com
USER MARKETING MANAGER: **DEBBIE BRADY** debbie.brady@penton.com
FREE SUBSCRIPTION/STATUS OF SUBSCRIPTION/ADDRESS CHANGE/MISSING BACK ISSUES
T | 866.505.7173 microwaves&RF@halldata.com **F** | 847.763.9673

SALES & MARKETING

AL, AR, CT, DE, FL, GA, IA, IL, IN, KS, KY, LA,MA, MD, ME, MI, MN, MO, MS, NC, NE, NH, NJ, NY, OH, OK, RI, SC, TN, PA, VA, VT, WV, E/CANADA:
MANAGING DIRECTOR: **TRACY SMITH** **T** | 913.967.1324 **F** | 913.514.6881 tracy.smith@penton.com

REGIONAL SALES REPRESENTATIVES
AZ, NM, TX: **BILL YARBOROUGH** **T** | 713.636.3809 **F** | 913.514.7251 bill.yarborough@penton.com
AK, CA, CO, ID, MT, ND, NV, OR, SD, UT, WA, WI, WY, W/CANADA: **JAMIE ALLEN** **T** | 415.608.1959 **F** | 913.514.3667 jamie.allen@penton.com

PLEASE SEND INSERTION ORDERS TO: orders@penton.com
PENTON REPRINTS: **WRIGHT'S MEDIA** **T** | 877.652.5295 penton@wrightsmedia.com
CIRCULATION: **CUSTOMER SERVICE** **T** | 866.505.7173 **F** | 847.763.9673 microwaves&rf@halldata.com

INTERNATIONAL SALES
EUROPE: **TRACY SMITH** **T** | 913.967.1324 **F** | 913.514.6881 tracy.smith@penton.com
PAN-ASIA: **HELEN LAI** **T** | 886 2-2727 7799 helen@twoway-com.com
LIST RENTALS, CUSTOMER SERVICE—SUBSCRIPTIONS:
ONLINE MARKETING MANAGER: **SARAH NOWOWIEJSKI** **T** | (212) 204 4295
sarah.nowowiejski@penton.com

ONLINE

PRODUCT DEVELOPMENT DIRECTOR: **RYAN MALEC** ryan.malec@penton.com

DESIGN ENGINEERING & SOURCING GROUP

VICE PRESIDENT & MARKET LEADER: **BILL BAUMANN**
EXECUTIVE DIRECTOR OF CONTENT AND USER ENGAGEMENT: **NANCY K. FRIEDRICH**
GROUP DIRECTOR OF OPERATIONS: **CHRISTINA CAVANO**
GROUP DIRECTOR OF MARKETING: **JANE COOPER**

PENTON MEDIA INC.

CHIEF EXECUTIVE OFFICER: **DAVID KIESELSTEIN** david.kieselstein@penton.com
CHIEF FINANCIAL OFFICER: **NICOLA ALLAIS** nicola.allais@penton.com
SENIOR VP, DESIGN ENGINEERING GROUP: **BOB MACARTHUR** bob.macarthur@penton.com
1166 AVENUE OF THE AMERICAS, 10TH FLOOR NEW YORK, NY 10036 **T** | 212.204.4200

Penton

Electronic Design | Machine Design | Microwaves & RF | Medical Design | Source ESB | Hydraulics & Pneumatics | Global Purchasing | Distribution Resource | Power Electronics | Defense Electronics | Electronic Design Europe | Engineering TV

Keysight W1715EP SystemVue
MIMO channel builder

Keysight N9040B UXA signal analyzer
with 89600 VSA software

Keysight MIMO PXI test solution
with N7624/25B Signal Studio software for LTE-Advanced/LTE FDD/TDD and 89600 VSA software

Keysight E7515A UXM wireless test set
with E7530A/E7630A LTE-Advanced/LTE test/lab application software

Keysight Infiniium S-Series
high-definition oscilloscope
with N8807A MIPI DigRF v4 (M-PHY) protocol decode software

Keysight N5182B MXG X-Series
RF vector signal generator
with N7624/25B Signal Studio software for LTE-Advanced/LTE FDD/TDD

Keysight E6640B EXM wireless test set
with V9080/82B LTE FDD/TDD measurement applications and N7624/25B Signal Studio software for LTE-Advanced/LTE FDD/TDD

HARDWARE + SOFTWARE

The more complex your LTE-A design, the more you need help from test and measurement experts. Keysight is the only company that offers benchtop, modular and software solutions for every step of the LTE-A design process. From R&D to manufacturing, we can give you the expertise, instruments and applications you need to succeed.

- *Complete LTE-Advanced design and test lifecycle*
- *Identical software algorithms across platforms*
- *300+ software applications for the entire wireless lifecycle*

PEOPLE

We know what it takes for your designs to meet LTE-A standards. After all, Keysight engineers have played major roles in LTE-A and other wireless standards bodies, including 3GPP. Our engineers even co-authored the first book about LTE-A design and test. We also have hundreds of applications engineers. You'll find them all over the world, and their expertise is yours for the asking.

- *Representation on every key wireless standards organization globally*
- *Hundreds of applications engineers in 100 countries around the world*
- *Thousands of patents issued in Keysight's history*

KEYSIGHT
TECHNOLOGIES

Unlocking Measurement Insights

(continued from p. C1)
cooling purposes.

Of course, when an application is ready for deployment, it is also possible to replace the standard backplane with a custom backplane and I/O panel as required by a particular application, and the industrial-grade fans can be upgraded to military (MIL) grade components.

Still, this use of standard COTS chassis and components in the development phase of a program should help both in speeding development and saving on design costs. The chassis meets many MIL requirements, including MIL-STD-461F for electromagnetic interference (EMI).

According to Lynn Bamford, senior vice president and general manager for Curtiss-Wright's Defense Solutions division: "Curtiss-Wright is dedicated to reducing risk, schedule and program cost for defense and aerospace system integrators.

"With our innovative Hybricon D2D-34TLA, we've extended the benefits of D2D to demanding programs using 3U air-cooled OpenVPX modules." ■

REPORT FORECASTS VETRONICS Market

INFORMATION PROVIDER Visiongain (www.visiongain.com) has assembled a long-term report on the vehicular electronics (Vetronics) market for the next 10 years, notably for military land vehicle applications. The forecast, "Military Land Vehicle Electronics Market Forecast 2015-2025," projects healthy growth for this expected market for electronic products for communications, computers, sensors, and remote weapon stations for military land vehicles.

This is a market that has already grown considerably during U.S. ground troop deployments to Iraq and Afghanistan, although a downturn is expected in U.S. spending from 2015 onwards. However, strong investments in the market are expected from France and Australia, as both countries invest in major modernization programs in this area. The Scorpion and LAND 400 programs are cited as reasons for new ground platforms for the two countries and for their major investments in vetronics equipment. ■

THIRD MUOS SATELLITE Ready for Launch

THE U.S. Navy and contractor Lockheed Martin (www.lockheedmartin.com) both invested considerable efforts to ready the launch of the third Mobile User Objective System (MUOS) secure communications satellite. The launch of MUOS-3 from Cape Canaveral Air Force Station, Fl., aboard a United Launch Alliance Atlas V rocket, was scheduled for January 20. Lockheed Martin is under contract to deliver five MUOS satellites and the associated ground system to the Navy.

The MUOS satellites provide secure mobile satellite communications (satcom) services for warfighters. These satellites feature up-to-date electronic capabilities, providing on-demand, beyond-line-of-sight capabilities to transmit and receive prioritized voice and mission data by means of a high-speed Internet protocol-based system.

According to Iris Bombelyn, vice president of Narrowband Communications at Lockheed Martin, "The launch of MUOS-3, and the near-term certification of our fourth and final Radio Access Facility, brings us to the brink of the global coverage we anticipate for MUOS communications. This government and contractor team knows how important this capability is for our protectors in harm's way."

The MUOS satellites have been developed to replace legacy UHF systems. Each MUOS satellite carries two payloads, ensuring access to legacy UHF narrowband communication systems as well as the flexibility to support new communications capabilities. The satellites incorporate wideband code-division-multiple-access commercial technology but with a new waveform for providing security and supporting priority-based access. The MUOS system can provide more than 16 times the capacity of the legacy UHF communications system. ■

AESA RADAR "SEES" Far in Test Flight

THE F/A-18C/D Hornet fighter/attack aircraft is facing some serious upgrades, following the successful flight testing of the APG-79(V)X active electronically scanned array (AESA) radar system from Raytheon Co. (www.raytheon.com). The radar system features simultaneous air-to-air and air-to-ground capabilities along with high-resolution synthetic-aperture-radar (SAR) mapping capabilities. The AESA radar system also offers extended detection ranges compared to older radar systems.

As Mike Garcia, business development director of Tactical Airborne Systems for Raytheon's Space and Airborne Systems business, notes: "We put our latest AESA radar capability to the test and it exceeded our expectations." Garcia, a former F/A-18E/F Super Hornet pilot/instructor, adds that "Our APG-79(V)X combines the best features of our AESA portfolio to ensure low risk and give F/A-18C/D a tactical advantage for the next 15 to 20 years."

Roy Azevedo, vice president for Raytheon's Space and Airborne Systems business, explains: "Raytheon fielded the world's first operational AESA radar for fighter aircraft in 2000. Our portfolio of tactical AESA radars has now flown more than 500,000 operational hours—an industry first. We will continue to advance this technology to give our warfighters the greatest possible tactical advantage." ■

COMS METHOD Cuts NTDS Costs

THE U.S. Navy may be enjoying improved communications without suffering increased costs, as GET Engineering Corp. (www.getntds.com) launches its Virtual Naval Tactical Data System (V-NTDS) for use in place of existing NTDS setups. The new software-driven V-NTDS approach is designed to reduce development and deployment costs compared to existing NTDS method by eliminating the need for expensive adapters and cables currently used in NTDS setups. The NTDS was first developed in the 1950s and introduced to combat ships the following decade.

According to David Grundies, president and CEO of GET Engineering Corp., "We created Virtual NTDS to allow for a seamless transition of a functioning system with NTDS hardware to Ethernet communication, reducing the system's overall cost. V-NTDS provides a turnkey solution to aging NTDS applications." The new V-NTDS products require little or no modification of existing NTDS setups and eliminate the need for specialized NTDS converters.

GET Engineering Corp.'s virtual NTDS approach provides complete emulation of existing NTDS operations, with separate channels for data and external interrupts. The virtual system approach also supports a wide range of aborting conditions and termination events in the manner of the existing NTDS setups, and can perform data transactions between different NTDS setups. Using the virtual approach, an NTDS Type-A device can now communicate with other parallel types (Type B/C/H), or even with NTDS Serial data types (Type D/E). This technology has not been previously available and opens new realms for NTDS application development. ■

ELBIT SYSTEMS TO Fuel Israeli C4I Efforts

ELBIT SYSTEMS Ltd. (www.elbitsystems.com) has been awarded a number of defense contracts by the Israeli Ministry of Defense (IMOD) to supply equipment for communications systems as well as for Command, Control, Computer, Communications and Intelligence (C4I) systems. The contracts, which are scheduled to be completed over a six-year period, have an approximate total value of $117 million.

As guided by these contracts, Elbit Systems will be working on the next generation of the Digital Army Project (DAP), a program tasked with computerizing land-force operations. The DAP program is being developed to connect all field and command personnel into a central data-transfer network, enabling forces to effectively and securely exchange information between field locations and established installations. Elbit Systems will also be working on developing new communications systems as well as upgrading existing communications networks and wideband radio systems, and also provide logistic support and maintenance for these communications systems.

Elbit Systems has been a reliable supplier of advanced analog and digital communications equipment and has supplied equipment for use in electronic-warfare (EW) and signal-intelligence (SIGINT) systems, in addition to wideband radios. As Bezhalel Machlis, president and CEO of Elbit, notes: "The new contracts attest to the customer's satisfaction from our systems' past performance. Being awarded contracts for next generation DAP and communications systems, based on advanced Command and Control and communications capabilities, further strengthens our position as world leaders in this field." ■

Norsat Aids Challenging Military Communications

NORSAT INTERNATIONAL (www.norsat.com) has received an order from an unidentified military contractor for its SigmaLink AUTO and Ranger satellite-communications (satcom) product lines. These satcom systems enable the transmission of video, voice, and data communications in remote and hostile locations, at the same time providing high performance in small form factors.

The SigmaLink AUTO transportable satellites provide connectivity for mobile base camp operations and other military users in need of reliable, broadband communications with minimal setup times. The systems allow an operator to establish a communications link in less than 15 minutes using 1.8- and 2.4-m satellite antennas. The product line represents an extension of the firm's existing satellite terminal platform technology used by commercial and military customers around the world.

The Ranger is a multiple-band micro-miniature satcom terminal that also supports rapid deployment. It is a small system that provides large throughput for operations requiring reliable performance under hostile conditions. As Dr. Amiee Chan, CEO of Norsat, notes: "A key objective to our growth strategy is the introduction of new products to the market that capitalize off the base technology platform that Norsat has created. The SigmaLink AUTO and Ranger products offer new capabilities and aperture sizes to meet the evolving needs of customers that require speed, portability, and constant reliability of communications." The company expects this first order for its SigmaLink AUTO and Ranger products to ship in the first quarter of 2015. ■

Phonon to Supply SAW Radar Modules

PHONON CORP. (www.phonon.com) recently received a large order from an undisclosed prime defense contractor for pulse compression modules for a radar application. The $8-million contract is for 2015 delivery of these surface-acoustic-wave (SAW) modules for an air defense system.

The firm, based in Simsbury, Conn., was founded in 1982 and is celebrating its 30th year in operation. The company designs and supplies a variety of components and modules based on SAW technology, including filters, delay lines, and oscillators for portable, airborne, and satellite systems. The use of SAW technology in this application enables a significant saving of physical volume and weight in the airborne radar system. It has proven to provide high reliability over time and in the face of the extreme environmental conditions faced by defense electronic systems. ■

Pentagon Eyes Lockheed Martin for C-130Js

THE U.S. Pentagon recently awarded several contracts to Lockheed Martin Corp. (www.lockheedmartin.com) for various aircraft and weapon systems over the next several years. One contract is a $244 million modification contract tied to the delivery of 61 C-130J aircraft and the materials procurement for them. The C-130J aircraft are expected to be delivered no later than early 2020.

In addition, the Pentagon awarded Lockheed Martin a modification contract worth $23.8 million to supply one KC-130J weapons system trainer by Oct. 30, 2017. A third contract, valued at $8.7 million and due by November 2015, requires Lockheed Martin to support technical evaluation of the Remote Minehunting System with the Littoral Combat Ship.

Finally, as part of the latest U.S. defense budget, Lockheed Martin will receive $224 million for two additional F-35 Lightning II Joint Strike Fighter (JSF) aircraft for the U.S. Navy. This brings the total of F-35 fighter aircraft to 38 for fiscal 2015, compared to a total of 29 F-35 fighter aircraft produced and delivered in fiscal 2014. ■

JACK BROWNE | Technical Contributor

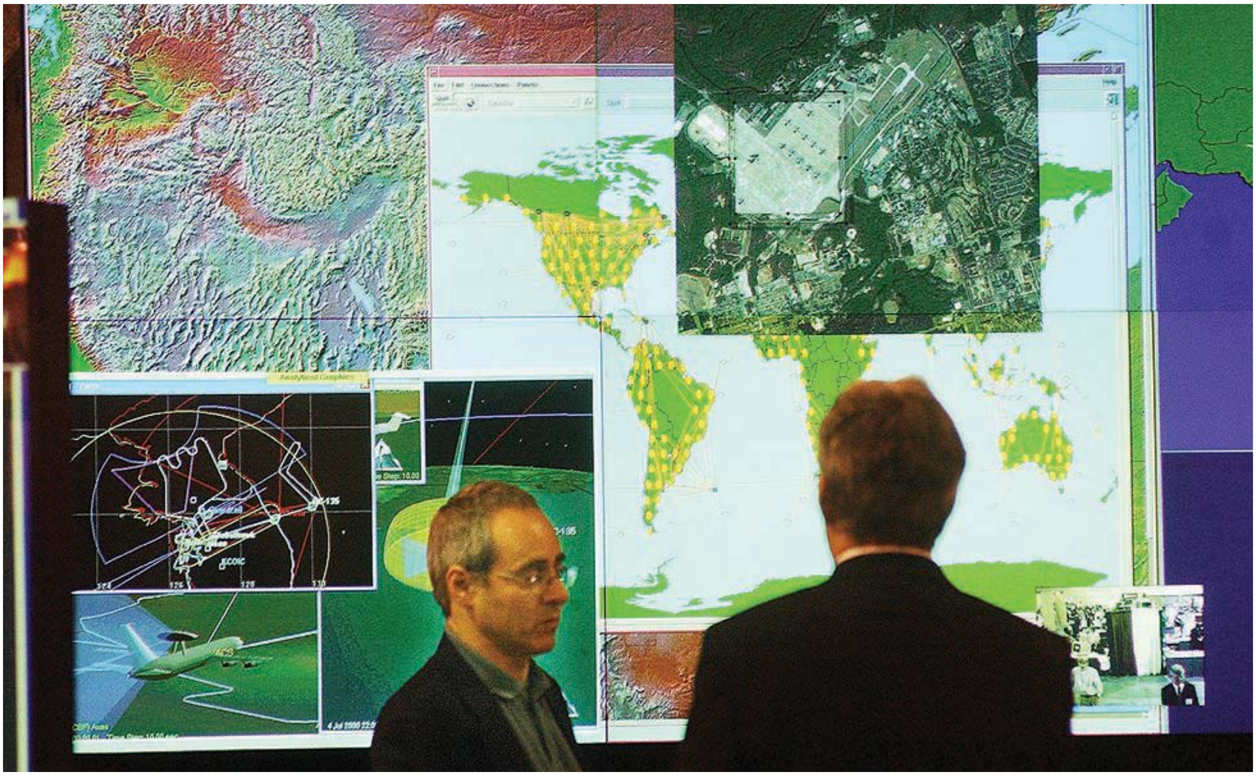

Photo courtesy of Thinkstock Images

Calming Concerns over Military Testing

Measurement challenges have long confronted the Armed Forces as they try to remain at the forefront of technology while attempting to find economical solutions at higher frequencies.

TEST EQUIPMENT and measurement solutions have assisted the technological growth of military and aerospace users since World War II, but not without concerns and challenges. Military applications have long been viewed as the backbone of the RF/microwave industry. Not since the early 1990s, with the development and growth of commercial wireless markets, has this industry benefitted from another market sector with the comparable economic size and strength as the military electronics market.

But in spite of the worldwide adoption of wireless technologies and associated electronic devices, military electronics still play a key role this industry. It is also a market that has faced many challenges over the years in terms of measurement equipment and solutions. As the industry has regularly shown, it includes individuals with the ingenuity to meet the changing needs of military and aerospace markets, as those changing needs have encouraged the development of mechanical and electrical modifications to high-frequency test equipment to keep pace with changing requirements.

Traditional measurement systems for military and aerospace systems have been based on the use of full-sized,19-in. rack-mount instruments, although military users have steadily been exploring the benefits of smaller, modular measurement systems (see p. S24). The model R&S TS6710 tester (see *photo*, facing page) from Rohde & Schwarz (www.rohde-schwarz.com) is an example of such a full-sized rack-mount test system. It was initially designed to evaluate the performance of components and devices in broadband radar systems.

The R&S TS6710 includes a vector-network-analyzer (VNA) system and associated switching and power-supply units to provide amplitude, frequency, and phase measurements using scattering parameters (S-parameters). The test system operates from 1 Hz to 24 GHz and was assembled to provide the fast measurement speeds needed to quickly test radar transmit/receive (T/R) modules over wide bandwidths and operating conditions. Its wide frequency range enables a wide range of users—even with classified radar specifications—to be able to program the system for their particular measurements.

> "Covering wide bandwidths, such as the 2 to 18 GHz typically occupied by EW and radar systems, has long been a challenge for all RF/microwave test equipment and test systems."

This test system, while offering impressive performance, is physically large; one of the challenges posed to suppliers of test equipment for military and aerospace applications is to deliver more compact equipment. As a result, modular measurement solutions will be a growing part of military test systems. Users will continue to seek more integrated test solutions, with more functions per module at lower power levels, and smaller overall test systems in modular form using industry-standard and cost-effective test software.

One benefit of a modular measurement equipment format such as VXI is that it allows more functionality within a smaller physical size than a traditional rack-mount test system. In addition, by exchanging instrument modules in a VXI chassis, functionality can be added and subtracted as needed to meet changing measurement needs of military and aerospace customers. Modular instruments from different suppliers must work together within an industry-standard modular chassis format. This has been well demonstrated for more than 25 years by the VXI modular test equipment format.

Covering wide bandwidths, such as the 2 to 18 GHz typically occupied by EW and radar systems, has long been a challenge for all RF/microwave test equipment and test systems. EW and radar systems traditionally have relied on analog RF/microwave electronic components, such as microwave mixers for frequency conversion and filters for signal selection. However, these systems are now increasingly turning to more digital components, such as analog-to-digital converters (ADCs), digital-to-analog converters (DACs), digital signal processors (DSPs), and field-programmable gate arrays (FPGAs), for inclusion in their signal-processing arsenal.

The increased use of digital components alongside of high-frequency RF/microwave components poses the challenge of how to efficiently and cost-effectively characterize the analog components, such as oscillators and mixers, and the digital components in these military and aerospace systems, especially as they work at faster clock rates, without simply adding more test instruments to a large test system.

Practical solutions are available from a number of companies that have developed broadband vector signal generators (VSGs) and vector signal analyzers (VSAs) capable of generating and analyzing in-phase (I) and quadrature (Q) signal components that can be used for evaluating the performance of both analog and digital components at clock rates to 6 GHz and higher. These VSG/VSA-based systems are available in traditional rack-mount formats, as well as in compact modular instrument formats, such as VXI and PXI.

To enable analog measurements, as well as testing of digital components within some military systems, the test systems must also be equipped with appropriate digital test equipment. Examples of this include a logic analyzer, digital storage oscilloscope (DSO), and digital signal source to provide stimuli for the digital components.

In terms of physical size, when such instruments are added to a measurement system in VXI or PXI format, they may occupy only a matter of a few slots within one instrument chassis, compared to significant portions of a full-sized 19-in. rack-mount enclosure. For military users challenged with meeting physical size requirements, the modular measurement formats offer some obvious advantages compared to traditional rack-mount systems.

The full-sized, rack-mount R&S TS6710 test system from Rohde & Schwarz (www.rohde-schwarz.com) was designed for use from 1 Hz to 24 GHz to perform high-speed testing of radar modules without being tied to a classified frequency range.

Some of the challenges facing those tasked with performing military measurements are related to newer developments in military and aerospace markets, such as the projected increased use of sensors for military applications. U.S. Army leadership is predicting a greater use of sensors (within clothing, in vehicles, and throughout military equipment) as a means of collecting environmental data and even location data on individual soldiers. By doing so, computers and software can be used to track personnel and program the battlefield.

The large number of sensors brings with it a major concern in finding ways to maintain the operation of these sensors. Because the sensors will be mounted in portable, movable applications, the implied solution for testing the sensors is a portable test system with the versatility to handle an array of different sensors and their parameters.

Changing technologies will always pose new measurement challenges for military system integrators, such as the growing use of software-defined radios (SDRs) for military communications applications. SDRs can readily change their scope of waveform usage by means of programming and software, without the need of hardware modifications. But testing SDR-based equipment requires something of a departure from conventional test solutions. Mathematical software—like Mathcad from Parametric Technology Corp. (www.ptc.com) and MATLAB from MathWorks (www.mathworks.com)—can be employed to assist in the testing.

Some military and aerospace test challenges have been ongoing, such as meeting new measurement requirements at lower costs and providing proper thermal management for different test systems. Cost control has been handled largely through the use of commercial-off-the-shelf (COTS) test hardware and software whenever available as well as the use of cost-effective test modules and modular test chassis that enable multiple measurement functions to be handled through the use of a single chassis rather than a full-sized rack-mount system.

For thermal management and ensuring that measurement accuracy is maintained over wide operating temperature ranges, once again, the use of modular measurement formats can simplify meeting some of the challenges. This is true especially in applications such as airborne systems, where size, weight, and power (SWaP) may be concerns. Effectively dissipating heat in full-sized systems can require significant amounts of thermal gasketing and absorbing materials, with fewer materials (in terms of weight, size, and cost) required in the smaller modular measurement systems.

Equipment manufacturers needing assistance on optimizing the thermal design of their system or subsystem may seek the expertise of service-oriented firms such as Thermacore (www.thermacore.com) and their European branch, Thermacore Europe (www.thermacore-europe.com). The firm can perform thermal analysis on a design and suggest a customized solution to optimize the thermal performance of the design. The company also offers qualification testing, such as for thermal shock, thermal cycling, shock, and vibration to fully prepare the system or equipment for withstanding the effects of a wide operating temperature range. Mercury Systems (www.mrcy.com) offers thermal expertise with experience in designing its OpenVPX modular systems, to create modular measurement solutions that can be fortified for wide operating temperature ranges.

Adding thermal-management materials to test solutions for effective dissipation of heat—either generated by the equipment itself or by high-power test input signals—requires careful selection of materials based on the expected operating environment. For example, for test systems onboard aircraft, thermal-management materials should be as light in weight as possible. Thermal-management materials for naval-based systems must be capable of handling corrosive fluids (e.g., salt water).

AVOIDING OBSOLESCENCE

One of the major concerns for test equipment intended for military and aerospace applications is obsolescence—that newer test equipment must be capable of providing measurements not only on newer systems and their components, but also on legacy systems and their components. Obsolescence was a major concern in the adoption of modular PXI instrumentation technology by Marvin Test Solutions (www.marvintest.com) in its MTS-3060 test system. The use of instrument modules simplified the challenge of enhancing the test system to meet the newer measurement needs brought on by numerous upgrades to the avionics and armament systems in modern fighter aircraft, including the F35 and the A-10. The MTS-3060 test system was upgraded to support testing of AIM-20 aircraft systems with new AMRAAM test capability.

Modular instrument approaches enable fairly straightforward equipment upgrades and performance modifications as measurement requirements change. The compatibility of modular test-instrument formats such as PXI and VXI effectively allows for an upgrade with the change of a card, regardless of the manufacturer. The large number of suppliers for VXI and the growing number of suppliers for PXI ensure that a steady flow of instrument products will be available for these formats, to minimize the threat of obsolescence for any one instrument. These and other test-equipment modular formats, such as AXIe, have shown that they are capable of performance levels comparable to the best full-sized, rack-mount instruments.

In terms of measurements themselves, developers of test equipment for military and aerospace applications have long been challenged with maintaining low phase noise, harmonic levels, and spurious levels in signal sources, and achieving high sensitivity and wide dynamic range in analyzers—usually for the widest-possible frequency ranges.

Measurements that have always posed challenges for radar developers include the capture of multiple simultaneous signals and the capture of closely spaced RF/microwave signals, especially within communications bandwidths. Of growing concern will be the effects of passive intermodulation (PIM) signal distortion on different military/aerospace systems, and how to measure PIM levels without adding specialized equipment. mw

JACK BROWNE | Technical Contributor

Software Teams with Test Gear FOR SIMULATIONS

The combination of simulation software and measurement hardware can provide invaluable feedback when designing and upgrading a wide range of military systems.

SIMULATION IS a vital part of military electronics systems, especially with the growing complexity of these systems. It has long been used to investigate the possible behavior of different systems and their components under different conditions, such as changes in temperature, humidity, shock, and vibration. Simulation methods work hand-in-hand with test equipment and measurement techniques—typically with measurements providing feedback to a simulator on how well an actual electronic system performs under different conditions compared to the virtual or modeled version of that system in software.

Combining test and simulation functions can help drive the design and development of different military systems, including electronic-warfare (EW), electronic-countermeasures (ECM), and radar systems. For that reason, it is not surprising to find that many companies that are developers of simulation software are also suppliers of test and measurement gear or designers of custom test solutions.

The Visual System Simulator for RADAR from AWR Corp. (www.awrcorp.com) can provide full behavioral modeling of different types of radar systems, as well as three-dimensional modeling of the antennas that are part of those systems. It can create models by means of manipulating software code or by working with data from actual measurements.

The simulator models continuous wave (CW) radars, pulsed radars, and pulsed frequency-modulated (FM) chirp radars. It can show the many effects of changes in a radar system because of the environment and how it affects system performance, such as how the height of a radar system above the ground impacts the line of sight for that system, or how noise levels change performance.

The VSS simulation software leverages a large library of system and antenna simulation models, including clutter and phased-array antenna models. The simulator provides quick links to other useful software programs, such as LabVIEW from National Instruments (www.ni.com), the parent company of AWR Corp. In working with such measurement programs, the VSS simulation software provides the synergism needed to integrate measurements into the simulations, creating a two-way arrangement that allows measurements to improve simulation models and simulations to enhance hardware designs and prototypes. Using LabVIEW as an example, the VSS simulation software is compatible with any and all measurement instruments it supports.

The R&S SMW200A vector signal generator series covers a total frequency range of 100 kHz to 20 GHz with fast switching speed and low noise needed to produce simulated signals.

Another major test equipment supplier with strong support for signal simulation is Keysight Technologies (www.keysight.com) and its Signal Studio software. The software can model and modify a wide range of different EW and radar signals and work with rack-mount and modular test instruments, such as the firm's new lines of arbitrary waveform generators (AWGs; see p. S1), to generate CW and pulsed signals as needed for testing. The company offers free-of-charge 30-day trial use of the software for interested parties to explore its many capabilities.

The Signal Studio software allows users to call waveforms from a stored collection or, alternately, to define a waveform by tuning the different parameters to create a specific CW or pulsed signal with precise characteristics. The software employs a Windows-based graphical user interface (GUI) to speed an operator through waveform creation, also providing pop-up screens to show the waveform as it is being created and modified.

Once a signal is defined, it can be used in a higher-level simulation—such as within the company's SystemVue system-level simulation—to predict the effects of the simulation waveform on different systems and their components. The waveform file can also be sent to a variety of hardware test instruments offered by Keysight, among them lines of vector signal generators (VSGs) both in traditional rack-mount and emerging modular instrument card formats. The PSG line of VSGs, for example, can produce output waveforms to 44 GHz for defense and aerospace testing.

This signal simulation software provides a great deal of flexibility by offering different operating modes: specifically, the waveform playback and real-time modes. The former permits a user to select from two levels of functionality to control their operating functionality. The latter includes closed-loop control of modifications to signals during signal generation, so that users can instantly see the effects of changes to a waveform's programming. These different program choices within the software are designed to allow a user to select the level of control needed for an application so that the software can be used cost- and time-effectively.

The Signal Studio software provides extensive pulse creation functions, allowing an operator to quickly build a library of pulses from measured data or defined characteristics. Custom pulse patterns can be created with 80-dB on/off ratios and advanced modulation formats, with such things as frequency, phase, and power offsets defined on a pulse-by-pulse basis. In addition to extensive signal library models for commercial cellular and wireless signals, Signal Studio features library models of different radar signals, multiple-satellite signals for GPS and a wide range of signals for Global Navigation Satellite System applications.

The Simulink simulator from MathWorks (www.mathworks.com), although technically a “block-diagram” system-level simulation, is often used to generate and model different waveforms and video signals for commercial and military systems. Using mathematical modeling methods, including the firm’s MATLAB mathematical software, the simulator has been used to evaluate the impact of modeled waveforms on system performance.

The waveforms created by these software tools will be limited in the real world to the hardware test instruments used to generate those waveforms. As the signal sources story (see p. S1) explains, high-frequency signals can be generated by a number of different technologies, from analog circuits to arbitrary waveform generators (AWGs) and direct-digital synthesizer (DDS) signal generators. The performance parameters vary widely among the difference signal sources.

Typically, simulation software compatible with a certain type of hardware signal source will include programmability limits for the performance levels of the hardware—not permitting the creation of waveform files with parameters, such as frequency switching speed, that exceed the limits of the hardware. Still with the high-speed signal sources currently available from Keysight, National Instruments, and other test-and-measurement equipment suppliers, simulation software can be readily teamed with available hardware signal sources to create most waveforms needed for simulating and testing military and aerospace systems.

The R&S SMW200A series of VSGs from Rohde & Schwarz (www.rohde-schwarz.com), for example, includes models covering a total frequency range of 100 kHz to 20 GHz with typical frequency switching speed of 0.6 ms. It offers the performance levels needed to match to any signal simulator on the market for EW and radar testing. These VSGs can

YIG BAND REJECT FILTERS

Omniyig Model No.	Frequency Range (GHz)	Ins. Loss (dB)	Bandwidth at 40 dB (MHz)
M107RX	8.0 - 18.0	1.5	20
M104RX	4.0 - 18.0	2.0	8
M105RX	2.0 - 8.0	1.5	10

MIL-SPEC and High Reliability!
Integrated with Analog and 12 Bit Digital Drivers.
MANY other Multioctave designs available.

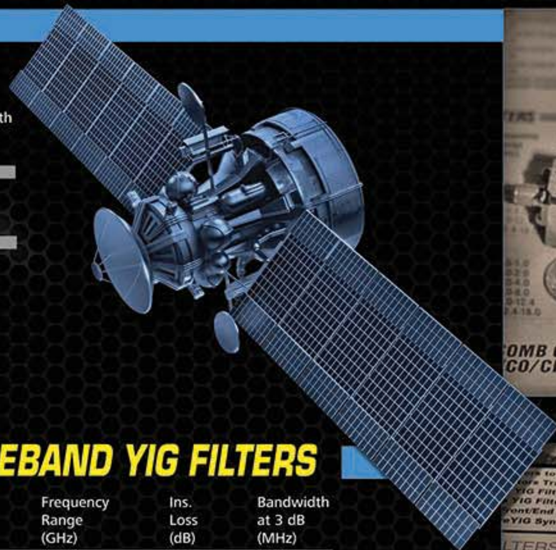

WIDEBAND YIG FILTERS

Omniyig Model No.	Frequency Range (GHz)	Ins. Loss (dB)	Bandwidth at 3 dB (MHz)
4-STAGE			
M3064	6.0 - 18.0	6.5	500 min
M2997	6.0 - 18.0	6.0	400 min
M3513	8.0 - 18.0	6.5	500 min

Industry-leading bandwidths in multi-octave, YIG units providing the widest 3dB bandwidth available!

STANDARD DETECTORS

Omniyig Model No.	Frequency Range (GHz)	k Factor	TSS (dBm)
Zero-Bias Schottky			
ODZ0004A	0.1 - 18.0	1200	-52
ODZ0328A	2.0 - 18.0	1200	-52
ODZ0441A	6.0 - 26.0	1000	-51

STANDARD LIMITERS

Omniyig Model No.	Frequency Range (GHz)	Insertion Loss (dB)	Leakage Power (dBm)
Pin			
OLP2645A	8.0 - 18.0	2.0	+19
OLP2726A	2.0 - 18.0	1.2	+19
PL473	0.5 - 12.0	1.8	+19
OLP2652	2.0 - 18.0	2.5	+20
Schottky Turn-on			
SL048	2.0 - 26.0	2.5	+14
OLD2635A	4.0 - 18.0	2.5	+14
OLD2733A	0.4 - 18.0	2.5	+14

Leakage Power Measured at P(in) = +30 dBm

STANDARD COMB GENERATORS

Omniyig Model No.	Input Frequency (MHz)	Output Frequency (GHz)	Output Power (dBm)
OHG10118	100	0.1 - 18.0	-40
OHG20218	20	0.2 - 18.0	-35
OHG51026	500	0.5 - 18.0	-28
OHG81026	1000	1.0 - 18.0	-18

Let Omniyig help with any special Limiter or Detector requirements you may have - Zero Bias Schottky Detectors, Limiter-Detectors, Comb Generators and a broad line of YIG-tuned Filters, Oscillators and Multipliers.

OMNIYIG INC.

3350 Scott Blvd, Bldg 66 • Santa Clara, CA 95054
408.988.0843 [T] • 408.727.1373 [F]
Omniyig@ix.netcom.com • www.OMNIYIG.com

be supplied with an optional second signal path, and standard models include an in-phase/quadrature (I/Q) modulator with a modulation bandwidth as wide as 2 GHz for generation of complex modulated waveforms.

Each R&S SMW200A VSG supports pulse modulation with on/off ratios of better than 80 dB and rise/fall times of less than 10 ns. The phase noise is typically −139 dBc/Hz offset 20 kHz from a 1-GHz carrier. The generator includes a large graphical display screen *(see figure on p. S18)* to simplify operation and is housed in a traditional 19-in. rack-mount enclosure.

Similarly, the fast-switching model MG37020A signal generator from Anritsu Co. (www.anritsu.com) is contained within a 19-in. rack-mount enclosure and includes a large display screen, and also offers the performance needed for creating most EW and radar signals. It covers 10 MHz to 20 GHz with 100-µs typical frequency switching speed, and is characterized by high signal amplitude and low phase noise.

An important part of blending the capabilities of computer simulation and measurement hardware is support for the control interfaces that can help tie the software and hardware together. The Bus-Tools-1553 (BTP-1553) software from GE Fanuc Intelligent Platforms (www.defense.ge-ip.com) is an integrated, Windows-based application solution for MIL-STD-1553 test, analysis, and simulation. It can work over a wide range of interfaces, including PCI, PCI Express, CompactPCI, PMC, VME, VXI, and Universal Serial Bus (USB) to control instruments and related hardware as part of the test and simulation process for evaluating MIL-STD-1553/1760 networks.

The software provides a straightforward GUI and can work with single- and multiple-function circuit boards, controlling multiple boards simultaneously as needed. The simulation software can inject and detect errors in a system for flexible simulation, and can record and readily display data during tests and simulations. BT-1553 includes a Selective Data Watch feature that allows a user to select individual data words as search parameters from any bus message.

When assistance is needed in developing simulations and test solutions for different systems, a number of firms specialize in offering professional services. Dynetics (www.dynetics.com), for example, can perform full testing and evaluation of EW threat weapon systems to develop detailed waveform descriptions of those systems for simulation and testing.

Dynetics' high-fidelity models and simulations of threat weapon systems, including models of radars, jammers, seekers, and radar warning receivers, support all phases of EW equipment development from concept of operations, through design and development, to test and evaluation. The firm's systems simulations are used in a number of different hardware-in-the-loop (HWIL) test facilities throughout the U.S.

The company manufactures specialized test equipment as needed in support of its system simulation efforts. Its integrated threat aircraft weapon system models have been used in the development of a wide range of systems, including aircraft combat simulation systems, identify-friend-or-foe systems, and fire control systems.

Dynetics supports the development of NGES, the Next Generation Electronic Warfare Integrated Reprogramming Database (EWIRDB) System. NGES, an open architecture database for representing radar threat systems as models, significantly improves the dissemination of threat RF waveform descriptions. The NGES tools developed by Dynetics allow interactive analysis and visualization of threat RF waveforms and interface of these waveforms into RF simulators for testing of EW equipment.

EW Simulation Technology Ltd. (www.ewst.co.uk) has developed radar and ECM threat simulations since 1984 by applying the latest technologies to its hardware and software solutions. Operating as part of Herley Industries (www.herley-cti.com), the firm has supplied simulation solutions to Army, Navy, Air Force, and civilian customers around the world.

Mercury Computer Systems (www.mrcy.com) has developed a series of solutions for simulating and testing radar systems, its Radar Environmental Simulators. They provide simulations of radar signals returning from different targets, for testing a wide range of active radar sensors in different systems, such as fire-control radars, surveillance systems, and imaging and guidance systems. These simulators have also been used in testing EW and signal-intelligence systems. They build upon the company's electronic-warfare digital-radio-frequency-memory (DRFM) technology with a goal of cost savings.

By receiving and digitizing real radar systems by means of the DRFMs, digitized samples can be stored and edited as needed, with such things as targets, clutter, terrain, and weather added to the radar signal models to evaluate the performance of a radar system under different conditions.

Within the Armed Forces, many of the services conduct their own simulation and test efforts, with and without the help of industry contractors. For example, in 1996, the Air Force founded the Air Force Agency for Modeling and Simulation (www.afams.af.mil) based in Orlando, Fla., as a means of supporting simulation, education, and training.

The U.S. Army's Simulation Center (www.smdc.army.mil) is referred to as the "laboratory of laboratories" for its computer simulations of space-based and missile-defense systems. The Army maintains simulation capabilities throughout its different facilities, such as the White Sands Missile Range (www.wsmr.army.mil).

In fact, the U.S. Army Research, Development and Engineering Command Communications-Electronic Research, Development and Engineering Center is currently conducting Rapid Fielding Initiative to determine the availability and development status of technologies to support an electronic-countermeasures (ECM) technique for ECM simulation, as well as for radar ECM studies. de

JACK BROWNE | Technical Contributor

Sizing Up Modular Measurement Solutions

Modular test equipment is winning more and more users away from traditional, full-sized rack-mount measurement gear with its compact size and flexibility.

MODULAR MEASUREMENT equipment and its associated software are gaining ground, even as the number of different modular formats grows and users have more options for different applications. Test equipment for different types of analog, digital, and RF/microwave measurements can constitute a major investment for users—even military and aerospace users—to such a degree that modular test instrumentation has gained a great deal of favor from them over the past decade.

Modular measurement equipment offers tremendous flexibility and testing capabilities, with the potential to pack a great many different test functions within a small equipment space. Unfortunately, no single modular measurement has ever won over the electronics field, and end-users now have a choice of numerous modular instrumentation formats (including AXIe, PXIe, and VXI test equipment).

The VXI modular measurement format is the oldest modular instrumentation platform, and easily the most widely used of the different formats, with many major instrument suppliers offering some forms of VXI modular instruments or chassis. The organization behind the VXI format and standards, the VXIbus Consortium (www.vxibus.org), was formed in 1987 with the goal of creating a universal instrument-on-a-card standard that would allow instruments from any number of different vendors to work together.

1. This VXI chassis illustrates the close spacing of modules and small instrument size possible even when realizing multiple measurement functions. [Photo courtesy of Alimar Technology (www.alimartech.com).]

The VXI specification supported by the IEEE, IEEE 1155, was adopted in 1993. The VXI plug&play Systems Alliance (www.ivifoundation.org) formed later that same year to pursue higher-level VXI instrumentation developments and advances in software to control the hardware. The VXI specification is based on the Versa Module Europa (VME) or VMEbus bus architecture.

The goals for the VXI modular format are still to produce instrument cards that will plug into any standard VXI chassis *(Fig. 1)* and enable instrument cards from any one supplier to work with instrument cards from any other supplier. A VXI system can be controlled by means of a remote general-purpose computer using a general-purpose interface bus (GPIB) or a Multisystem eXtension Interface (MXI) bus interface. In many cases, computers are embedded into a VXI chassis for direct control of the instrument modules.

The VXI format allows a test system that might have formerly occupied a floor-standing 19-in. rack-mount enclosure to fit within the slots within a single VXI chassis. VXI instruments can be operated by means of many different control interfaces, including Ethernet, Firewire, GPIB, and PCI. The standard is defined to be independent of computer controller, so that its instruments and software can outlast trends in computer technologies.

It is strongly supported by most major instrumentation manufacturers, as well as some firms that specialize in VXI. One notable example of the latter is VXI Tech-

> **"No single modular measurement has ever won over the electronics field, and end-users now have a choice of numerous modular instrumentation formats (including AXIe, PXIe, and VXI test equipment)."**

nology (www.vxitech.com), in business since 1990 and now known as VTI Instrumentation Corp. (www.vtiinstruments.com). In addition, firms like VXI Global Solutions (www.vxi.com) specialize in providing assistance to businesses wishing to develop and manage VXI test systems for their applications.

The VXI modular instrument format is well established with military and aerospace users, as well as in many high-volume manufacturing production facilities. That being said, a number of other modular instrument functions (such as AXIe) can tackle and adopt many of the functions still provided by VXI instrument modules. A growing number of analog, digital, and RF/microwave test-and-measurement functions are becoming available in compact modular formats, causing confusion for users in search of practical modular measurement solutions and wishing to know how the different instrument module formats match up.

One of the more popular of these newer instrument module formats is the PCI eXtensions for Instrumentation, or PXI. The PXI modular instrument format, which started in 1998, builds upon the personal computer architecture of the Peripheral Component Interconnect (PCI) standards and the CompactPCI specifications for communications and control. The goals for PXI are similar to those for VXI, including high mechanical integrity and ease of installation into PXI mainframes.

However, in contrast to the somewhat confined and tightly controlled specifications of the VXI standard, PXI designers and suppliers seek to leverage developments in the general-purpose (commercial) personal-computer (PC) market, achieving cost benefits in addition to performance improvements. As with VXI, instrument modules from different manufacturers are designed to be fully interoperable, although with lower costs than VXI modules and systems.

Of course, in addition to cost, there are numerous other differences between the PXI and VXI modular formats. The number of available instruments with PXI compatibility has been steadily gaining ground compared to VXI-compatible instrument modules. PXI supporters like to point to the strong link between modern PCs and PXI, and how PXI modules can benefit from enhancements in modern PCs. But VXI supporters refer to the stability of the VXI format and its bus standards, and the large number of supported instruments for military and aerospace and large-scale production test applications.

An example of another difference is in mechanical design, such as in electromagnetic-interference (EMI) shielding. The VXI standards specify that all VXI modules must be individually shielded, enclosed in metal housings and with gasketing material where appropriate to minimize the effects of electromagnetic (EM) radiated emissions, as well as EM susceptibility between and among different modules in a VXI chassis and system. For systems where EMI may be a concern, this level of engineering provides proven results, but also raises the costs of VXI modules and systems.

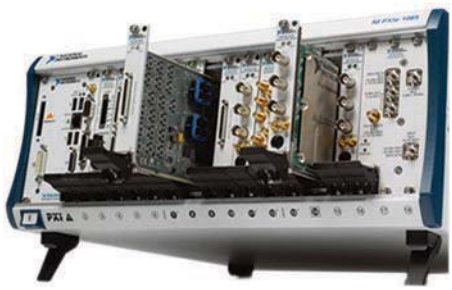

2. The PXIe modular format is home to the NI PXIe-5668R vector signal analyzer and spectrum analyzer from National Instruments, which also contains a vector signal source.

According to the PXI specifications, metal shields are not required on each PXI module. Manufacturers of PXI modules must comply with RFI/EMI regulatory emissions requirements, such as the CE specifications in Europe, but shielding can be achieved at component rather than module levels, with PXI module manufacturers applying EMI shielding around sensitive components within a module.

One mainstream supplier of test-and-measurement equipment that has supported the PXI format in a significant way is National Instruments (www.ni.com). The firm supplies PXI interface modules for a number of military and aerospace applications, including for MIL-STD-1553, ARINC 429, and AFDX buses. For avionics test system requirements, the firm collaborates with Avionics Interface Technologies (AIT; www.aviftech.com), a leading provider of avionic instrumentation and an independent division of Teradyne Defense & Aerospace (www.teradyne.com).

The PXI and PXI Express (PXIe) modular instruments feature some of the more versatile RF/microwave measurement solutions available anywhere *(Fig. 2)*, such as the NI PXIe-5668R vector signal analyzer (VSA) and spectrum analyzer. Some years ago, this PXIe instrument would have been realized as a full 19-in. rack of instruments, since it includes a vector signal generator (VSG), a VSA, and a spectrum analyzer. The system's measurement functions are coordinated through a Kintex-7 field-programmable gate array (FPGA) from

Xilinx (www.xilinx.com), with measurements programmable by means of National Instruments' popular LabVIEW test software.

The NI PXIe-5668R PXIe test solution can be supplied in versions with frequency ranges of 20 Hz to 14 GHz or 20 Hz to 26.5 GHz, with as much as 765-MHz instantaneous measurement bandwidth. It features a card-format VSG with high performance, and low phase noise of typically –129 dBc/Hz offset 10 kHz from an 800-MHz carrier. The NI PXIe-5668R operates with 12-b analog-to-digital converters (ADCs) and 12-b digital-to-analog converters (DACs) running at a sampling rate of 2 Gsamples/s.

A PXIe VSA and VSG combination is also available from Keysight Technologies (www.keysight.com) as the models M9391A PXIe VSA and M9381A PXIe VSG. The VSA is available for frequencies from 1 MHz to 3 GHz or 1 MHz to 6 GHz, typically supplied as four PXI modules: a model M9300A frequency reference, an M9301A frequency synthesizer, an M9350A frequency downconverter, and a model M9214A digitizer. The VSG also comes in versions for 1 MHz to 3 GHz and 1 MHz to 6 GHz, as well as in an arrangement with four PXI modules: the M9300A frequency reference, the M9301 synthesizer, a model M9311A digital vector modulator, and a model M9310A source output.

In the PXIe format, Marvin Test Solutions (www.marvintest.com) offers more than 20 chassis solutions in this modular configuration, to meet a wide range of physical requirements for PXIe systems. One example is the firm's GX7300 Series 20 slot, 3U PXI chassis *(Fig. 3)*. The chassis can hold as many as 19 PXIe instruments and a PXI controller and work with both PXI and Compact PCI (cPCI) 3U modules. It provides a total of 900 W power to its modules. As with many of the company's other PXI instrument chassis, the GX7300 Series incorporates forced-air cooling using a rear-mounted fan.

Yet another modular instrument format is AXIe. It is supported by the AXIe Consortium (www.axiestandard.org) and is based on the AdvancedTCA format. It was developed to aid instruments for aerospace and defense as well as in semiconductor testing and research and development. At times referred to as the "big brother to PXI," AXIe follows the programming and basic architecture of PXI with some differences. Physically, it employs horizontal configurations to minimize rack space and vertical configurations where space is not an issue. In addition, it uses larger boards than PXI to achieve higher circuit densities than PXI. It is designed to integrate easily with PXI, IXI, and LXI formats.

Although Keysight's wideband VSGs and VSAs are based on the PXIe format, the company's new high-performance model M8195A AWG employs the AXIe modular instrument format, built into a five-slot chassis. Its impressive performance levels, including bandwidth of dc to 20 GHz and sampling rates to 65 Gsamples/s, provide evidence for the measurement capabilities of the AXIe modular format, which was developed to save power and space.

3. This chassis is designed to handle a total of 20 PXIe modules, which would typically consist of a controller and as many as 19 instruments.

A number of major test instrument manufacturers have embraced the AXIe modular format, including Tektronix (www.tek.com) with its AWG70000A Series of AWGs. They operate at sample rates to 50 Gsamples/s for one channel or 25 Gsamples/s on each of two channels with 8-, 9-, or 10-b vertical resolution. These AWGs can deliver output signals to 20 GHz with spurious-free dynamic range of –80 dBc. The instruments can create complex waveforms or even sequences of waveforms and can work with files from Excel spreadsheets or mathematical programs such as MatLAB from MathWorks (www.mathworks.com) or Mathcad from Parametric Technologies Corp. (www.ptc.com) to create complex waveforms.

Tektronix's RFXpress software can also be used with the AWG70000 Series AWG for straightforward generation of radar and other waveforms for test applications. Of course, for proper operation, instruments such as AWGs that rely so heavily on digital signal generation and signal conversion must be supported by sufficient waveform memory to store the wide range of waveforms that will be used in testing.

While many instrument suppliers attempt to provide modular measurement equipment that can meet a wide range of needs and applications, some modular equipment solutions are still very focused on a very specific set of requirements, even as they benefit from the flexibility of the modular format. The T940 Digital Subsystem is one such application-specific modular instrument solution. It is a single-wide VXI module designed and manufactured by EADS North America Test and Services (www.ts.eads-na.com) as part of its Talon Instruments product line.

The T940 digital resource module (DRM) serves as the backbone of a modular VXI digital subsystem that can provide switching, analog functions, and RF/microwave measurement gear. The T940 driver/receiver daughtercard includes variable- and fixed-voltage processing for a wide range of interfaces, including transistor-transistor-logic (TTL), low-voltage-differential-signaling (LVDS), and RS-485 interfaces. The T940 DRMs are useful for a host of applications, including the testing of avionics systems, medical systems, semiconductors, and weapons systems. mw

(continued from p. C1)
starting in the digital realm and defining signals mathematically, working at 8-b resolution at a maximum sampling rate of 65 GSamples/s and achieving an instantaneous output bandwidth of DC to 20 GHz.

This small but powerful signal source can match or exceed any analog signal source in terms of pure signal performance, such as amplitude flatness, phase noise, and spurious noise, with fast pulse capabilities frequency-hopping capabilities, and standard frequency switching speed of 505 μs.

Traditionally, wideband RF/microwave signal sources have been based on analog architectures, typically using wideband tunable oscillators, such as YIG or voltage-controlled-oscillator (VCO) sources, as their primary signal generators. As digital technology has gained in performance and sophistication, however, the bandwidths and performance levels of digital RF/microwave sources have increased a great deal over the last decade, with direct-signal-synthesizer (DDSs) sources and arbitrary waveform generators (AWGs) moving higher in frequency and performance.

Of course, analog oscillators and signal sources based on these oscillators are still widely used in high-frequency military and aerospace applications. These include fixed-frequency sources such as dielectric resonator oscillators (DROs), surface-acoustic-wave (SAW) oscillators, and electronically tunable sources—the latter including voltage-controlled oscillators VCOs) and yttrium-indium-garnet (YIG) oscillators.

Each differs in spectral characteristics, such as harmonic signal levels and single-sideband (SSB) phase noise, as well as in output power, output power stability with frequency and temperature, and tuning range. Creating an embedded test signal solution for a military or aerospace system typically starts at the component level and choosing which RF/microwave oscillator technology is best suited to a particular application.

ORGANIZING OSCILLATORS

Key performance parameters that are typically compared for signal sources incorporated into military and aerospace systems include frequency range, bandwidth, frequency tuning resolution, output power, phase noise, harmonic noise, spurious noise, power consumption, size, and weight. Another parameter that is dictated by the requirements of some applications is frequency switching speed. Signal generators may be required to produce continuous-wave (CW) or pulsed signals.

At lower frequencies, a wide range of electronic systems still rely on clock oscillators for their timing and synchronization. A number of suppliers have built strong reputations for crystal oscillators employing different methods of frequency stabilization, including temperature-compensated crystal oscillators (TCXOs) and oven-controlled crystal oscillators (OCXOs). Many of these crystal oscillators are now employed in surface-mount packages, such as the different lines of military-grade TCXOs supplied by Q-TECH Corp. (www.q-tech.com).

Available with analog or digital outputs, these oscillators feature low phase noise at frequencies typically below 100 MHz. Another longtime supplier of TCXOs is Greenray Industries (www.greenrayindustries.com), with sources from 20 kHz to 1 GHz, including RoHS-compliant models.

When frequency stability is mandatory for applications such as space and avionics, Frequency Electronics Inc. (FEI) (www.freqelec.com) offers a variety of packaging options for its OCXOs. In addition, the company designs and manufactures rubidium-base atomic oscillators for precise frequencies, such as its model FE-5650A, available from 1 Hz to 20 MHz and 50.255 MHz, in a housing measuring only 3.0 × 3.0 × 1.4 in.

Vectron International (www.vectron.com) was an early adopter of microelectromechanical-systems (MEMS) technology for military-grade oscillators in its HT-MM900A Military Temperature Range MEMS Oscillator line. These ruggedized sources, which are designed to survive 50,000 g's shock, are available at frequencies from 1 to 110 MHz. They can be supplied in housings as small as 2.5 × 2.0 mm and maintain ±25 ppm frequency stability across an operating temperature range of −55 to +125°C.

Some of the older high-frequency source technologies, such as DROs, are still used as signal sources in applications like missile-guidance and point-to-point-communications systems. As an example, the DRO-1000 line of DROs from Microwave Dynamics (www.microwave-dynamics.com) can be specified with single frequencies from 10 to 50 GHz, with 100-MHz mechanical tuning range and limited electrical tuning optional. Although a DRO may not be the first choice of RF/microwave signal source when miniaturization is required, these are dependable performers capable of excellent spectral purity.

The durable DRO-1000 DROs are constructed of dielectric resonators with field-effect-transistor (FET) or bipolar-junction-transistor (BJT) amplification at microwave frequencies. They are packed into housings measuring just 2.25 × 0.93 × 0.67 in. but delivering +13 dBm output power with only ±0.5 dB output variations across frequency and temperature. These DROs are designed to perform over an operating temperature range of −55 to +105°C with low phase noise, harmonics of typically −25 dBc, and low spurious noise of typically −85 dBc. The output frequency varies only by 4 ppm/°C with temperature.

When faster frequency-switching speed is required at the module or system level, designers may reach for a VCO or DDS. Synergy Microwave Corp. (www.synergymwave.com), for example, supports wide bandwidths by means of its patented VCO technology, with single sources capable of octave tuning bandwidths, such as 2000 to 4000 MHz and 3000 to 6000 MHz. The oscillators are designed for low-power and portable applications, such as portable radios, with current consumption of typically 50 mA at +5 VDC. Model DCYS200400-5 tunes from 2000 to 4000 MHz by means of tuning voltages from 0.5 to 16.0 V.

At higher frequencies, the firm also offers low-phase-noise DROs, such as the 10-GHz model DRO100. It achieves better than –110 dBc/Hz SSB phase noise offset 10 kHz from a 10-GHz carrier. The DRO100 includes mechanical frequency tuning and is available in a surface-mount housing measuring just 0.75 × 0.75 × 0.53 in. as model SDRO100.

One of the more recent source technologies, DDS, has been gaining in frequency while maintaining its trademark fast frequency switching speed and low phase noise. A DDS incorporates a phase accumulator and lookup table with a digital-to-analog converter (DAC) at the output to generate clean analog signals. As the digital hardware has improved, the performance of available DDS sources has also improved, such as the model AD9914 DDS oscillator from Analog Devices (www.analog.com). It employs a 12-b DAC with 16-b phase tuning resolution to generate sine waves to 1.4 GHz with 190-pHz resolution.

Long specified for their low phase noise, YIG-tuned oscillators provide octave or wider tuning ranges over wide temperature ranges with excellent spectral characteristics. One supplier known for its permanent-magnet YIG oscillators, Micro Lambda Wireless (www.microlambdawireless.com), has refined its technology sufficiently to downsize YIG oscillators into small 0.5 × 0.5-in. surface-mount housings. The company refined its technology to fit permanent-magnet YIG oscillators into compact surface-mount housings. The MLSMO Series oscillators cover a total frequency range of 2 to 13 GHz with excellent spectral purity, albeit limiting frequency switching speed.

For those in need of instrumentation, Micro Lambda also produces the MLBS Series benchtop test synthesizers based on its YIG technology, with models ranging from 2 to 20 GHz. Model MLBS-2020 covers the full frequency range from 2 to 20 GHz with +10-dBm output power and 1-kHz frequency tuning resolution. The SSB phase noise is –92 dBc/Hz offset 10 kHz.

SORTING SIGNAL GENERATORS

Specifying a test signal generator is still a matter of meeting a set of minimum requirements and, for an RF/microwave source, it is usually a matter of tradeoffs among bandwidth, frequency tuning resolution, frequency switching speed, and spectral purity. As noted with the oscillators, the low phase noise of YIG-tuned oscillators generally requires a compromise in frequency tuning speed. What makes the model M8195A AWG from Keysight such a departure from traditional signal-generator choices is its rare combination of those key performance parameters without the usual tradeoffs.

Still, YIG-based signal generators have proven their worth over time in driving and testing many military and aerospace systems, and these test signal source maintain frequency, phase, and amplitude stability over time and across a wide range of environmental operating conditions, making them strong candidates for many wideband test applications not requiring fast frequency tuning speeds. Of course, some signal-generator suppliers, such as Giga-tronics (www.gigatronics.com), have refined their YIG technology to a level that coaxes the best possible switching speeds from YIG sources. Its 2500B series frequency synthesizer instruments manage to hold down phase noise while also achieving 500-µs frequency switching speed.

Signal sources based on VCOs and PLL technologies offer enhanced frequency switching speeds, typically with somewhat degraded phase noise, although designers of signal generators have developed different approaches to minimize noise. For instance, the ISB series test signal generators from FEI-Elcom Tech (www.fei-elcomtech.com) are based on a single-loop VCO frequency-synthesis architecture.

With performance suitable for radar-cross-section (RCS) measurements and W system testing, these test sources can perform frequency jumps across the full bandwidth in less than 200 µs with frequency resolution as fine as 1 Hz. The SSB phase noise is a function of carrier frequency, with typical phase noise of –105 dBc/Hz offset 10 kHz from a 2-GHz carrier, dropping to –85 dBc/Hz offset 10 kHz from a 20-GHz carrier.

Fast-tuning signal generators based on analog technologies previously reported in these pages include such models as the R&S SMA100A microwave signal generator from Rohde & Schwarz (www.rohde-schwarz.com) with an extremely broad frequency range of 100 kHz to 43.5 GHz. It achieves low phase noise of typically –102 dBc/Hz offset 10 kHz from a 10-GHz carrier, although frequency switching speed is in the range of 1.3 ms. With somewhat faster tuning, the MG37020A series of signal generators from Anritsu Co. (www.anritsu.com) covers 10 MHz to 20 GHz with 100 µs switching speed, with typical phase noise of –86 dBc/Hz offset 10 kHz from a 20-GHz carrier.

For fast frequency switching speeds in signal generators rivaling the performance of AWGs, a growing number of high-frequency signal sources employ DDS technology. The model NI PXI-565x from National Instruments tunes from 500 kHz to 6.6 GHz with the switching speed capable of a full frequency sweep in less than 2 ms for high-speed production testing. The source fits within a single PXIe module and is compatible with the firm's PXIe vector signal analyzer (VSA) for creating a modular test solution (see p. S24).

A line of fast-switching modular frequency synthesizers from Wide Band Systems (www.widebandsystems.com) serves EW applications with a 2-to-18-GHz frequency range and 5-µs frequency switching speed. Although somewhat larger, in a traditional 19-in.-rack-mount format, the model UFS-18 frequency synthesizer from FEI-Elcom Tech (www.fei-elcomtech.com) is also well suited for EW applications with a frequency range of 300 MHz to 18 GHz. It builds upon an almost-forgotten technology, direct-analog frequency synthesis (coupled with DDS technology), but its performance is noteworthy. It boasts remarkable full-band frequency-switching speed of 250 ns that is still unmatched by other wideband microwave test signal sources, regardless of technology. de

Compact Antenna Receives GPS Signals

THE ETHERHELIXGPS is reported to be the world's smallest standalone, right-hand-circularly-polarized (RHCP) Global-Positioning-System (GPS) antenna. The compact antenna measures just 35 mm in length and 15 mm in diameter, or about 27% smaller than other available GPS antennas on the market, without suffering in performance for its small size. The miniature GPS antenna is well suited for mission-critical products, including in military radios and public safety equipment. The EtherHelixGPS antenna can be tuned for a number of different satellite-communications (satcom) frequencies, as well as for right-handed circular polarization (RHCP) and left-handed circular polarization (LHCP). The RoHS-compliant antenna, which weighs just 11.8 g, is based on the firm's patented Isolated Magnetic Dipole (IMD) technology, providing high performance in a small size.

ETHERTRONICS, INC.
5501 Oberlin Dr., Ste. 100, San Diego, CA 92121;
(858) 550-3820, FAX: (858) 550-3821, www.ethertronics.com

Testers Check Radios to 3 GHz

THE ATS family of testers includes desktop and portable test instruments for analog and digital radio testing through 3 GHz. The testers are programmed via the TestEZ automated test environment, allowing users to create measurement programs by means of a simple graphical user interface (GUI). The ATS3000A is the desktop test system that loads an impressive collection of instruments within a single rack-mountable package. It includes a signal generator with frequency range of 1 to 2700 MHz and 1-Hz resolution; an RF power meter with frequency range of 1 to 2700 MHz; audio function generators and analyzers; a two-channel oscilloscope; a 10-MHz reference oscillator; and a digital multimeter with range of 1 mV to 600 V. Additional battery-operated versions of the tester are available for in-field use.

ASTRONICS TEST SYSTEMS
4 Goodyear, Irvine, CA 92618; (800) 722-2528,
(949) 859-8999, FAX: (949) 859-7139, www.astronics.com

COTS Supplies Reach 2000 W

THE TERA series of AC-DC power supplies includes three classes of 700-, 1200-, and 2000-W units designed for use across wide temperature ranges in hostile environments. The power supplies are sealed in a heat-conducting potting material that allows operation across temperatures from –50 to +85°C. The supplies, which are well suited for space-critical applications requiring reliable, shock-resistant units, offer 100-to-242-VAC universal input ports, power factor correction (PFC), galvanic isolation, high efficiency, and a full complement of protective functions. They are compliant with EN55022 Class-A conditions (Class B with filter). The power supplies are designed for ease of series/parallel connections and are priced for commercial-off-the-shelf (COTS) applications in military and aerospace systems.

SCHAEFER, INC.
45 South St., Hopkinton, MA 01748; (508) 435-6400, FAX: (508) 435-6401,
e-mail: sales@schaeferpower.com, www.schaeferpower.com

Integrated Bias Network Powers 2 to 18 GHz

MODEL MABT-011000 is a monolithic, surface-mount integrated bias network from MACOM Technology Solutions and supplied by Richardson RFPD that can power active circuits from 2 to 18 GHz. Based on the firm's patented heterolithic microwave-integrated-circuit (HMIC) process, which enables the formation of viaholes through silicon semiconductor materials by embedding them in low-loss glass, the process can also form high-quality-factor (high-Q) inductors and metal-insulator-metal (MIM) capacitors. The bias network can be used to supply DC bias to PIN diode control circuits and can support DC current to 60 mA and DC voltage to +50 VDC. Over its specified bandwidth, the bias network achieves less than 0.3-dB insertion loss and RF-to-DC isolation of better than 34 dB.

RICHARDSON RFPD
950 South Batavia Ave., Ste. 100,
Geneva, IL 60134; (630) 262-6800
www.richardsonrfpd.com

Low-Noise Amplifier Links Military Radios

MODEL SKY67103-396LF is a high-linearity, low-noise amplifier (LNA) designed for applications from 0.5 to 4.0 GHz, including for sensitive military radios. The amplifier provides 16.5 dB gain at 3.6 GHz with noise figure of 0.7 dB at 3.6 GHz. It achieves better than 17.5-dB return loss at 3.6 GHz with an input third-order-intercept point (IIP3) of +17.8 dBm at 3.6 GHz. The amplifier, which is supplied in a compact dual-flat-no-lead (DFN) housing measuring 2.0 × 2.0 × 0.75 mm, runs on supply voltages of +3 to +5 VDC and supply currents from 30 to 100 mA.

SKYWORKS SOLUTIONS, INC.
20 Sylvan Rd., Woburn, MA 01801;
(781) 376-3000, FAX: (781) 376-3100,
e-mail: sales@skyworksinc.com,
www.skyworksinc.com

Chip Inductors Gain QPL Status

THE MLRF0603 and MLRF0805 lines of RF surface-mount chip inductors have achieved qualification to the military's MIL-PRF-83446 specification. These wire-wound coil, ceramic core chip inductors employ tin/lead terminations for processes where reflow soldering is used. They have earned Qualified Product List (QPL) status for this Department

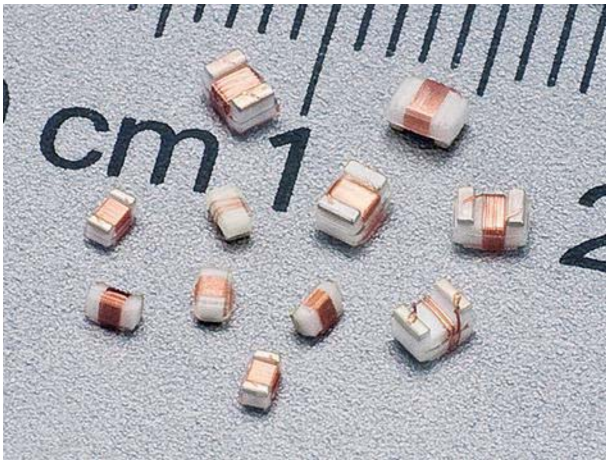

of Defense (DoD) specification. These tin/lead-terminated QPL inductors offer a time-saving, solder-friendly solution for reflow-solder applications in circuits for military, aerospace, and defense systems, including in high-reliabilty (hi-rel) designs. The MLRF0603 line includes inductors with values from 1.8 to 270.0 nH QPL-approved to MIL-PRF-83446/36B. The self-resonant frequencies (SRFs) for these components range from 0.6 to 6 GHz with current ratings from 195 to 1000 mA and minimum quality factors (Q's) from 16 to 40. The MLRF0805 line contains inductors with values from 2.2 to 2200 nH with minimum Q's of 15 to 65, SRFs from 0.040 to 6 GHz, and current ratings from 140 to 1000 mA.

GOWANDA ELECTRONICS

P.O. Box 111, Gowanda, NY 14070;
(716) 532-2234, www.gowanda.com

ADVERTISERS INDEX

USB Switch Matrix Commands DC to 18 GHz

MODEL USB-2SPDT-A18 is a broadband switch matrix capable of channeling signals from DC to 18 GHz with low loss. It contains a pair of electromechanical single-pole, double-throw (SPDT) absorptive fail-safe switches capable of 25-ms typical switching speed. The switches, which are in a break-before-make configuration, are powered by +24 VDC. Typical insertion loss is a mere 0.2 dB, with high isolation of 85 dB between ports. The switch, which handles as much as 10 W power across the full frequency range, is ideal for a wide range

of test-and-measurement applications. It is designed for more than 100 million switching operations. The switch is supplied with a compact disc (CD) containing programming software, in a metal housing measuring 4.5 × 6.0 × 2.25 in. with female SMA connectors, a DC socket, and a Universal-Serial-Bus (USB) Type-B port for remote control. The switches can be controlled separately or together, and can be operated remotely using the supplied graphical user interface (GUI) program or programmed by means of an included API DLL com object.

MINI-CIRCUITS

P.O. Box 350166 Brooklyn, NY 11235-0003;
(718) 934-4500, FAX: (718) 332-4661, www.minicircuits.com

Micro-Coaxial Assemblies Assist Ultrasound Systems

A line of custom fine-wire and fine-pitch diagnostic imaging assemblies have been developed for use with ultrasound analysis equipment for medical and other applications. These assemblies include coaxial cables with gauges from 40 to 50 AWG in ribbon-

ized or bundled assemblies. The cable assemblies include terminations ranging from 0.175 to 1.00 mm. In spite of the small sizes of these assemblies, they are designed for ruggedness and durability and can withstand more than 500,000 flexures at elevated temperatures. In particular, for medical applications, they can withstand the rigors of ethylene oxide gas sterilization. The capacitance specifications for the cable assemblies can be tuned to less than 12 pF/ft. with impedance similar controlled to tight tolerances.

HIGH SPEED INTERCONNECTS (HIS)

8777 North Gainey Center, 136, Scottsdale, AZ 85258;
(480) 998-2540, www.highspeedint.com